The Role of Phytocyanins in Secondary Cell Wall Assembly and their Potential Uses in Biofuel Production

A thesis submitted to the University of Manchester for the degree of MPhil in the Faculty of Life Sciences

2013

Angelo Gabriel Peralta

Table of Contents

1 Introduction

2 Methods

3 Results

4 Discussion

5 Conclusions, Limitations and Future Perspectives

Abstract

Lignocellulosic material is an important feedstock for second generation biofuels. Most of the sugar is in the form of cellulose that is embedded in a matrix of hemicelluloses and lignin and because of this, the hydrolysis of cellulose is hindered. Lignin, while benefitting the plant by providing essential structural support and helping prevent pathogen attack, also hinders cellulose digestibility and confers a need for pretreatment of biomass prior to saccharification. A key understanding of lignin polymerisation and synthesis would lead to manipulation of cell walls better amenable to saccharification for biofuel production. It has been proposed that phytocyanins- copper containing redox enzymes may function in the lignification of plant secondary cell walls. To investigate whether phytocyanins are involved in lignifying tissues, a reverse genetics approach using T-DNA inserts and artificial microRNA silencing was used to generate mutants. These were screened for evidence of defects in secondary cell wall deposition. Collapsed xylem vessels were observed in an RNAi line indicative of a cell wall defect. Expression data suggests that in this line two additional phytocyanin genes as well as the initial target gene are downregulated. Subcellular localisation, through GFP-tagging and fluorescence microscopy also revealed their localisation in the cell wall. Metabolic analysis by FTIR spectroscopy also demonstrated that phytocyanin mutants have a similar biochemical profile as other known lignin deficient mutants. However phytocyanins display a significant degree of functional redundancy as multiple gene knockdowns were needed to elicit an observable phenotype. With the putative role of phytocyanins established, manipulation of these enzymes could be used to generate less recalcitrant biomass sources that require less pretreatment and exhibit increased saccharification efficiency to produce more economically viable biofuels.

Declaration

No portion of the work referred to in this thesis has been submitted in support of an application for another degree or qualification of this or any other university or other institute of learning.

Note on Copyright

The author of this thesis (including any appendices and/or schedules to this thesis) owns certain copyright or related rights in it (the “Copyright”) and s/he has given The University of Manchester certain rights to use such Copyright, including for administrative purposes.

Copies of this thesis, either in full or in extracts and whether in hard or electronic copy, may be made **only** in accordance with the Copyright, Designs and Patents Act 1988 (as amended) and regulations issued under it or, where appropriate, in accordance with licensing agreements which the University has from time to time. This page must form part of any such copies made.

The ownership of certain Copyright, patents, designs, trade marks and other intellectual property (the “Intellectual Property”) and any reproductions of copyright works in the thesis, for example graphs and tables (“Reproductions”), which may be described in this thesis, may not be owned by the author and may be owned by third parties. Such Intellectual Property and Reproductions cannot and must not be made available for use without the prior written permission of the owner(s) of the relevant Intellectual Property and/or Reproductions.

Further information on the conditions under which disclosure, publication and commercialisation of this thesis, the Copyright and any Intellectual Property and/or Reproductions described in it may take place is available in the University IP Policy (see http://www.campus.manchester.ac.uk/medialibrary/policies/intellectual-property.pdf), in any relevant Thesis restriction declarations deposited in the University Library, The University Library’s regulations (see http://www.manchester.ac.uk/library/aboutus/regulations) and in The University’s policy on presentation of Theses

Acknowledgements

I’d like to express my utmost gratitude to Simon and all the members of the Turner lab.

Thanks to my friends and family for their support.

I’d also like to thank Peter March for assistance in confocal microscopy and Andrew Dean and Beth Dyson for help with FTIR analysis.

Abbreviations:

ABC	ATP binding cassette
AtBCB	Arabidopsis thaliana blue copper binding protein
ATP	Adenosine triphosphate
Bp	base pairs
cDNA	Complementary deoxyribonucleic acid
Col	Columbia
DEPC	Diethylpyrocarbonate
dH_2O	distilled water
dsRNA	Double stranded ribonucleic acids
ENOD	Early nodulin
ER	Endoplasmic Reticulum
FLA	Fasciclin-like arabinogalactan
FTIR	Fourier transform infrared
G	Guaiacyl
GFP	Green flourescent protein
GPI	Glycosylphosphatidylinositol
H	Hydroxycinnamyl
Hyp	Hydroxyproline
mRNA	Messenger ribonucleic acid
MS	Murashige and Skoog
NADPH	Nicotinamide adenine dinucleotide phosphate H+
PCR	Polymerase chain reaction
RNA	Ribonucleic acid
rpm	Rotations per minute
RT	Room temperature
S	Syringyl
T-DNA	Transfer DNA
v/v	volume/volume
w/v	weight/volume
WT	Wild type
Ω	ohm

List of Figures

Chapter 1

Chapter 2

Chapter 3

List of Tables

Chapter 1

Chapter 2

Chapter 3

Chapter 1: Introduction

1.1 Climate Change and Anthropogenic CO_2 Emissions

Over the last century, and more prononoucedly within the last decade, the earth has experienced an overall warming due to anthropogenic inputs of greenhouse gases such as CO_2. Between the years 1990-1999 and 2000-2004, the increase in yearly CO_2 tripled with a growth rate from 1.1% y^{-1} to >3% y^{-1} (Raupach et al., 2007). Recent emission measurements paint a grim picture. In 2009, 30.8 billion tons of CO_2 was emitted- making it one of the highest outputs in human history (Friedlingstein et al., 2010). Most of these emissions are due to the dependence on fossil fuel use for energy. As a result, there is a widespread incentive to discover alternative sources that are renewable and carbon neutral. One source that has received much attention is lignocellulosic biofuel. This is because using biomass for biofuel is currently more cost-effective than energy from wind and solar sources. Additionally, plant biomass i.e. lignocellulose from non-arable crops and agricultural residue conversion to liquid fuels are compatible with existing transportation technologies and do not compete with food crop sources such as corn, sugar cane and soybean (Carroll and Somerville, 2009).

1.2 Lignin Modifications to Improve Cellulosic Saccharification for Bioethanol Production

Due to the changes in climate and exhaustion of fossil fuel resources there has been a trend towards searching for alternative fuels. One such sustainable alternative is lignocellulosic biomass obtained from plant secondary cell walls. Extracted sugars could be converted into biofuel such as bioethanol. However an important barrier to the saccharification process of these polymers is the presence of lignin. Lignin polymers function biologically as barriers against pathogenic attack and cell wall perturbation and therefore are recalcitrant to anthropogenic uses such as biofuel production as well. In order to reduce recalcitrance for more efficient enzymatic saccharifications of cellulose and hemicellulose from the secondary cell wall, a clear understanding of the factors defining recalcitrance is needed. Aside from the extent of lignified secondary cell walls, the monolignol subunit content determines the degree of recalcitrance as well.

However attractive lignocellulosic sources may be, several hurdles must be overcome before they can be efficiently used for biofuel production. One such hurdle is lignin removal. Lignin is a major component in plant secondary cell walls and has a profound inhibitory effect on enzymatic hydrolysis of cellulose (e.g. Chen and Dixon, 2007). Therefore, a key understanding of plant secondary cell wall development, particularly lignification may provide new genetic modifications that will help to tackle lignocellulosic recalcitrance and increase biomass fuel production efficiency.

1.3 Plant Cell Walls

Terrestrial plants contain structures that perform various functions in order to cope with their sessile nature. Some noted functions of cell walls in plants are: imparting mechanical strength, regulating turgor pressure, allowing transpiration and serving as a physical barrier. Because of the numerous functions plant cell walls play, much of the assimilated carbon from photosynthesis is directed to forming cell wall polysaccharides. Plant cell walls are diverse in both appearance and composition. For example, cortical parenchyma is often thin and lack distinguishing features. On the other hand, xylem tracheary elements possess much thicker cell walls that may be deposited in distinctive patterns (Taiz and Zeiger, 2010).

1.3.1 Plant Primary Cell Walls

Plant cell walls are categorised into two major forms: primary and secondary walls. Primary walls are generally uniform in architecture, thin and occur in a newly established wall of a dividing plant cell. Primary walls can resist tensile forces from turgor pressure but are extensible enough to allow cell expansion an essential part of plant growth. Lastly, primary cell walls are able to integrate new wall polymers into the growing wall (Albersheim et al., 2011; Fry, Frankova and Chormova, 2011; Hamant and Traas, 2009; Cosgrove, 2005). Primary cell walls in plants are usually composed of ~ 25% cellulose, 25% hemicellulose, 35% pectins and 1-8% structural proteins. This however is not definitive for all plant tissues: grass coleoptiles contain 60-70% hemicellulose, 20-25% cellulose and 10% pectin. Cereal endosperm walls can contain up to 85% hemicellulose (Tazi and Zeiger, 2010). Plant primary walls therefore display a lot of diversity amongst species and cell types..

1.3.2 Plant Secondary Cell Walls

Once the primary plant cell wall has reached a certain stage of differentiation in which cell wall expansion has ceased, the cell retains the capacity to add layers of cell wall material at the plasma membrane. This process is designated as the secondary cell wall formation (Albersheim et al., 2011). Cellulose microfibrils in secondary cell walls orient themselves in a helical formation along the cell axis (microfibril angle) (Figure 1.1) (Barnett and Bonham, 2004). It should be noted that microfibril angles are important delineating factors in determining plant cell wall structure. Low microfibril angles relative to the cells axis allow cellulose to compact more easily, providing stiffness which prevents trees from buckling under compressive forces. In contrast, high microfibril angles tend to elicit flexibility when plants encounter wind and snow (Mellerowicz and Sundberg, 2008).

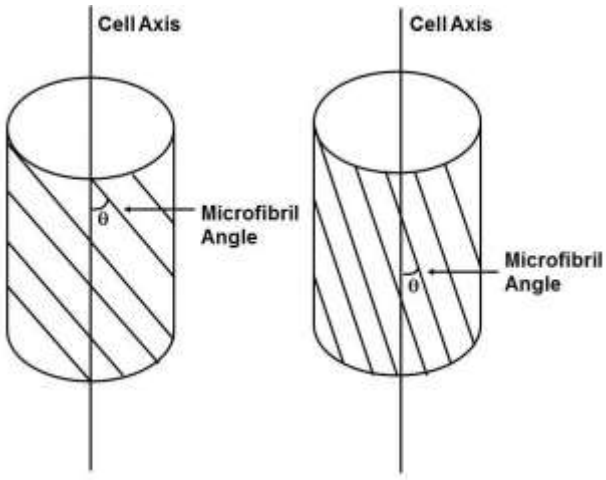

Figure 1.1: Helical arrangement of cellulose microfibrils. This pattern of deposition forms an angle relative to the cell axis. Low microfibril angles (right) provided stiffness, while large microfibril angles confer flexibility

Additionally, plant secondary cell walls also make up the major constituents of tracheary elements and fibres in wood. These confer mechanical strength, hydrophobicity to prevent water loss and barriers against pathogenic and pest attacks in woody plants. Up to 56 billion tons of CO_2 are fixed by plants every year and incorporated into the secondary cell wall [(Field et al., 1998)]. Secondary cell wall deposition occurs in specialised cells such as tracheary elemens, fibres and sclereids where it helps the

plant withstand negative pressure generated during plant transpiration and contributes to mechanical stability (Zhong and Ye, 2009). The importance of secondary cell walls has been shown from deformation of vessels that are not resistant to compressive forces as first shown in Turner and Somerville (1997), and pendent inflorescence stems (Zhong and Ye, 2009).

1.3.3 Secondary Cell Wall Biosynthesis and Composition

The most abundant elements of secondary cell walls found in plants are cellulose, hemicellulose and lignin, which form a composite materal that bestows strength and maintain plant structure. These polymers occur in different proportions depending on the plant species. Poplar can contain 48% cellulose, 27% hemicellulose and 21% lignin, while pinewood is composed of 41% cellulose, 27% hemicellulose and 29% lignin (Timell, 1982). These polymers are also varying in the plant itself. One such example is tension and compression wood, which has high cellulose and low lignin, and high lignin compared to cellulose respectively (Al-Haddad et al., 2013).

1.3.3.1 Cellulose

Cellulose, a linear chain of β-1, 4-linked D-glucose, is the major load bearing components in secondary cell walls (Figure 1.2). These polymers are organised into microfibrils via intra and intermolecular forces as well as Van der Waals forces (Van Acker et al., 2013). Cellulose is synthesised in the plasma membrane by large multi-meric protein complexes resembling a hexameric rosette structures (Brown, 1996). The model therefore proposed that each rosette or cellulose synthase complex, with its six globular complexes and six subunits per complex forms 36 individual glucan chains to form a cellulose microfibril (Cosgrove, 2005; Somerville, 2006). In *Arabidopsis thaliana*, cellulose synthase complexes are formed by specific CesA subunits. These subunits are what form the rosette like structures and are needed for catalytic synthesis of cellulose polymers. CesA4, CesA7 and CesA8 subunits are found in rosettes that form secondary walls (Taylor et al., 2003).

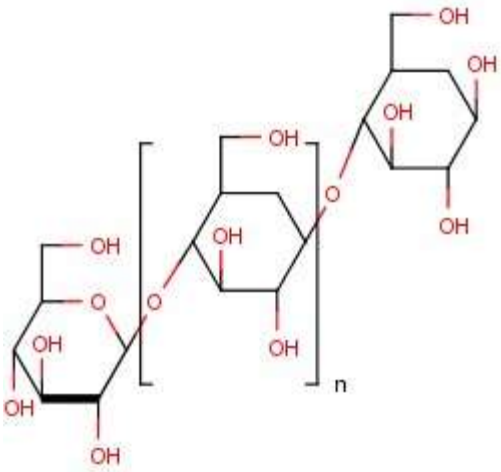

Figure 1.2: Cellulose structure. Adapted from Berg, Tymoczko, and Stryer (2002)

1.3.3.2 Hemicellulose

Hemicelluloses in secondary cell walls in angiosperms are comprised of xylan and glucomannan that are made in the Golgi apparatus and transported via vesicles to the cell walls. They function as cross linkers of cellulose microfibrils in secondary cell walls and also provide the framework for other secondary cell wall components to adhere to. Different species of plants contain varying ratios of the hemicellulose monomers: in angiosperms, they are predominantly made of xylan; as seen in poplar with a 24% xylan and 3% glucomannan while gymnosperm hemicellulose is primarily composed of glucomannan [particularly galactoglucomannan] with pine wood containing 18% galactoglucomannan and 9% xylan (Zhong and Ye, 2009). Xylan is composed b-1, 4-linked xylosyl residues in a linear chain. The xylosyl residues are substituted by other sugar residues such as, α-1, 2-linked 4-O-methylglucuronic acid, α-1, 3-linked arabinose residues and α-1, 2-linked glucuronic acid residues via glucuronyltransferases (Figure 1.3) (Lee et al., 2012a). Xylan can be acetylated as well at the C-2 and C-3 position. In addition to the xylosyl backbone, the reducing end of xylan contains a unique glycosyl sequence composed of 4-β-d-Xyl*p*-(1→4)-β-d-Xyl*p*-(1→3)-α-l-Rha*p*-(1→2)-α-d-Gal*p*A-(1→4)-d-Xyl*p* at its reducing end that is evolutionary conserved in herbaceous and woody plants (Pena et al., 2007). Glucomannan consists of linear chains containing both β-1, 4-linked mannosyl and glucosyl residues atba ratio or around 2:1. Galactoglucomannan has a similar backbone as glucomannan but contains a α-1, 6-linked galactosyl monomer added to the mannosyl residues as side chains with acetylation present. (Zhong and Ye, 2009).

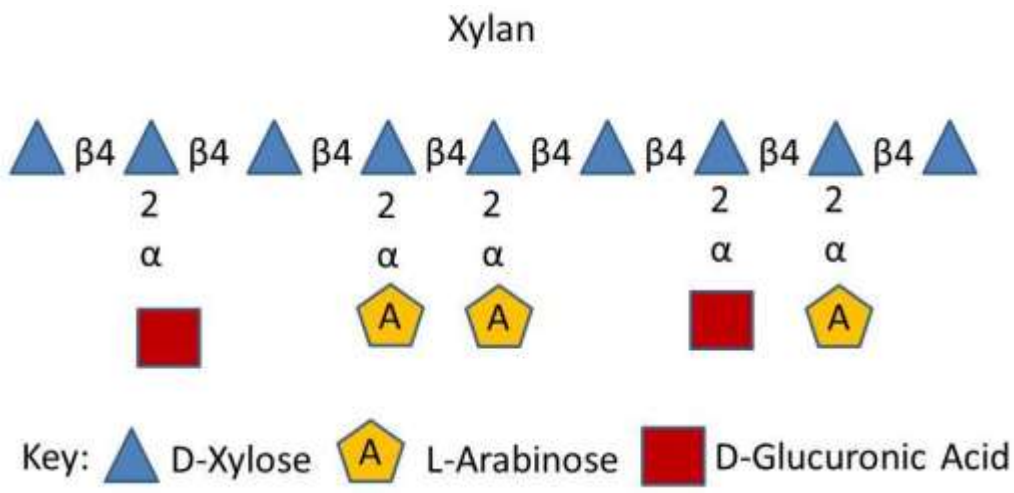

Figure 1.3: Xylan structure. Adapted from Fry, Frankova and Chormova (2011)

1.3.3.3 Lignin

Lignin, an aromatic polymer composed of 4-hydroxyphenylpropanoids is responsible for imparting rigidity to secondary walls and is part of the response to biotic and abiotic stresses i.e. wounding, pathogen attack and cell wall perturbations. coniferyl, sinapyl and *p*-coumaryl alcohol are monolignols that are the building blocks of lignin and once incorporated into the growing polymer are termed guaiacyl (G), syringyl (S) and *p*-hydroxyphenyl (H) units respectively (Figure 1.4). These units are synthesised in the cytosol from phenylalanine that originates from the shikimate pathway and then undergo further modification to produce the hydroxyphenylpropanoids (Boerjan, Ralph and Baucher, 2003; Vanholme et al., 2010; Liu, 2012). Once synthesised, they are deposited into the layers of the secondary cell wall after carbohydrate deposition. Lignin accumulation first occurs at the corners of the middle lamella and at the primary cell wall when S1 formation has been initiated. Lignification then proceeds at the S2 layer once the polysaccharide matrix has been formed. Finally, when much of the cellulose and hemicellulose has been deposited into the inner (S3) layer, lignin concentrates in this layer where it attaches to hemicellulose. Subunits of lignin are also incorporated in a coordinate manner (Boerjan, Ralph and Baucher, 2003). Typically H units are deposited, then G units and finally S units (Terashima et al., 1993). Lignin subunits may vary amongst different plant species. Secondary cell walls in angiosperms contain guaiacyl and syringyl lignin, while gymnosperms are composed of primarily G lignin. Moreover, lignin differs in cell

types of a plant species as well; in *Arabidopsis*, secondary wall vessels are predominantly lignified with G units whereas its fibres are composed of G and S units (Vanholme et al., 2010).

Figure 1.4: Lignin Subunits. Adapted from Vanholme et al., (2010).

1.4 Lignin Biosynthesis and the Phenylpropanoid Pathway

In the phenylpropanoid pathway, subsequent deamination, hydroxylation, methylation, and two successive reductions form monolignol polymers for incorporation to the plant secondary cell wall (Figure 1.5). The enzymes: phenylalanine ammonia lyase , cytochrome P450-dependent monooxygenases (Cinnamate 4-hydroxlase, *p*-coumarate 3-hydroxylase and Ferulate 5-hydroxylase), methyltransferases (Caffeoyl CoA *O*-methyl transferase and Caffeic acid O-methyl transferase), and the oxidoreductases (Cinnamoyl CoA reductase and Cinnamyl alcohol dehydrogenase) respectively perform these chemical reactions (see Table 1.1) (Bonawitz and Chapple, 2010; Fraser and Chapple, 2011). Additionally, the ATP-dependent ligase 4CL and acyltransferase HCT are required to form pathway intermediates that serve as substrates for succeeding reactions (Bonawitz and Chapple, 2010). As shown in Figure 1.5, PAL, C4H and 4CL mediated reactions from *p*-coumaryl CoA. This substrate is an important intermediate as it can be directed to the flavonoid pathway to produce flanonoids and tannins or to monolignol synthesis. Once *p*-coumaryl CoA is dedicated to monolignol production, it can divert to three possible combinations to produce the main 4-hydroxyphenylpropanoids monomers. The stepwise order of PAL, C4H, 4CL, CCR and CAD produces *p*-coumaryl alcohol (H-lignin); the additional action of HCT, C3'H and CCoAOMT are required to form coniferyl alcohol (G-lignin), and sinapyl alcohol biosynthesis requires all the enzymes to form G-lignin and additionally F5H and COMT. Most if not all of these enzymes possess

multiple isoforms encoded by different genes that may have varying kinetic properties and distributions throughout the plant. An example of such are the PAL isoforms *PAL1-PAL4* with all four expressed in stems and also being localised at different areas during later stages of development (PAL1 in the vascular tissue and PAL2 and PAL4 in seeds) (Rohde et al., 2004; Raes et al., 2003). According to Liu (2012) there is a need for compartmentalisation of the phenyl propanoid enzymes to either sequester metabolic intermediates or physically organise the pathway to avoid phytotoxicity from aromatic intermediates produced.

Because lignification occurs alongside the biosynthesis of cellulose, hemicellulose, and other polysaccharides during secondary cell wall formation, this process requires a complex network of transcription factors (Bonawitz and Chapple, 2010). Regulatory elements and transcription factors play a role in the activation and expression of lignin biosynthesis genes, respectively (Zhong and Ye, 2009).

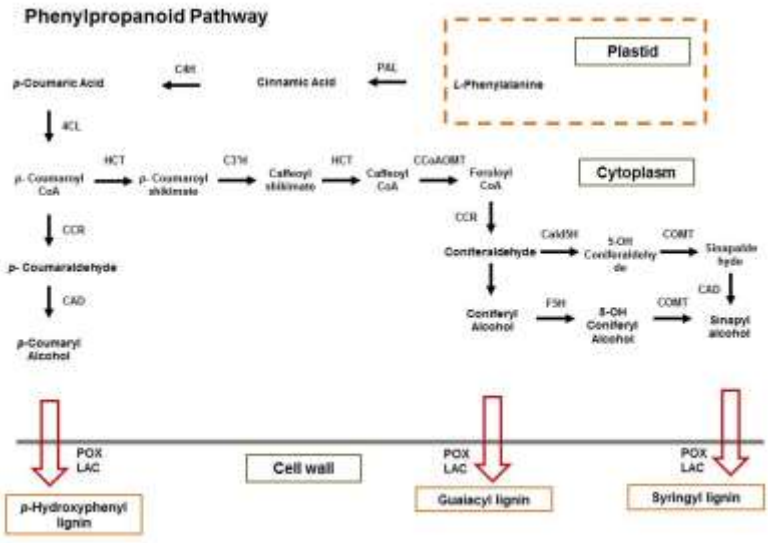

Figure 1.5: Phenylpropanoid pathway for lignin synthesis. Adapted from Liu (2012).

One such group of transcription factors discovered to drive lignin biosynthetic genes are MYB proteins (Zhong and Ye, 2009). In *Arabidopsis thaliana*, MYBs are key regulators in networks controlling development, metabolism, abiotic and biotic stress response (Dubos et al., 2010). Studies by Zhou et al (2009) revealed that MYB58 and MYB63 served as transcription activators for lignin biosynthetic genes.

MYB58 and MYB63 are specifically expressed in cells undergoing lignification and ectopic expression of lignifcation independently of cellulose and xylan production. This indicated that that MYB58 and MYB63 are necessary in the regulation of lignin biosynthesis. Further evidence supports MYB in lignification is their ability to bind to AC elements and directly activate the expression of lignin biosynthetic genes. Another MYB transcription factor, MYB85, was also discovered to activate lignin biosynthetic genes and cause ectopic lignin deposition during overexpression (Zhong et al., 2008).

Table 1.1: Lignin biosynthesis pathway genes from Arabidopsis and their AGI codes (Adapted from Fraser and Chapple, 2011)

Enzyme	AGI Codes (and Gene Names)
Phenylalanine ammonia lyase (PAL)	At2g37040 (PAL1), At3g53260 (PAL2)
Cinnamate 4-hydroxlase (C4H)	At2g30490 (REF3)
4-coumarte CoA ligase (4CL)	At1g51680 (At4CL1), At3g21240 (At4CL2)
Hydroxycinnamoyl transferase (HCT)	At5g48930
p-coumarate 3-hydroxylase (C3'H)	At2g40890 (REF8)
Caffeoyl CoA *O*-methyl transferase (CCoAOMT)	At4g34050 (CCoAOMT1)
Cinnamoyl CoA reductase (CCR)	At1g15950 (CCR1), At1g80820 (CCR2)
Ferulate 5-hydroxylase (F5H)	At4g36220 (FAH1)
Caffeic acid O-methyl transferase (COMT)	At5g54160 (COMT1/AtOMT1)
Cinnamyl alcohol dehydrogenase (CAD)	At3g19450 (CAD-C/AtCAD4/AtCAD-C), At4g34230 (CAD-D/AtCAD5/AtCAD-D)

Lastly, control of lignin biosynthesis occurs during the secondary cell wall biosynthetic program and is activated by NAC, SND1 and its homologues NST1, NST2, VND6 and VND7 (Figure 1.6). It has been shown as well that secondary cell wall thickening and lignin deposition comes to a halt in double knockouts of SND1 and NST1 (Zhong et al., 2008); supporting the idea that lignin synthesis is simultaneous turned on with cellulose and xylan by the same switches. SND1 and another MYB

transcription factor MYB46 also activate downstream genes such as MYB58 and MYB63, further indicating their roles in the transcriptional network that regulates secondary cell wall lignification (Zhou et al., 2009) (Figure 1.5).

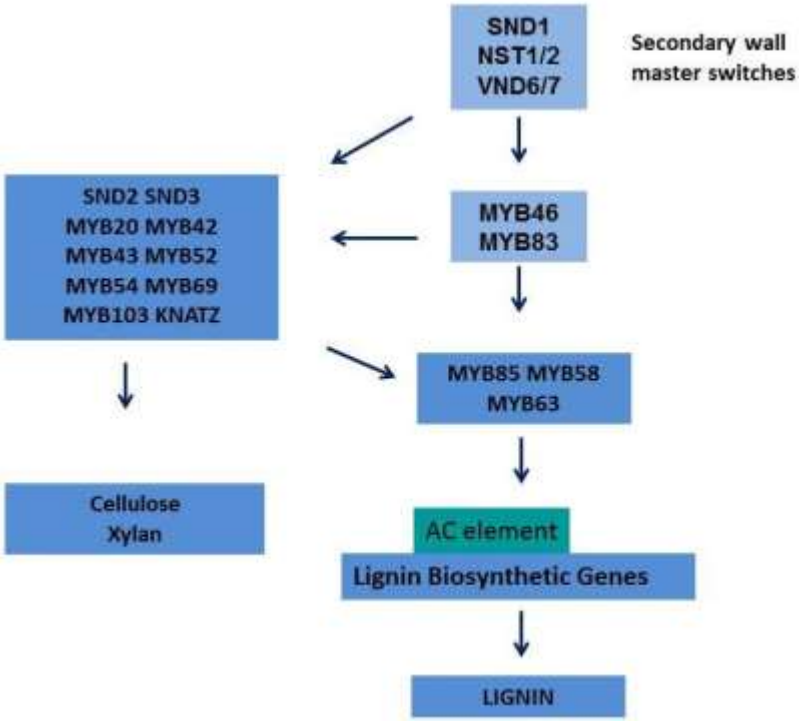

Figure 1.6: Diagram of the transcriptional network regulating secondary cell wall biosynthesis. Adapted from Zhong and Ye (2009).

1.4.1 Lignin Transport and Polymerisation

After cytosolic synthesis of the monolignols, transport across the cell membrane for cell wall cementing is needed. Prior to any transport of cytosolic monomers to the apoplast, monolignols can exist as either aglycones (non-sugar compounds) or 4-*O*-β-D-glucosides which are typically found in gymnosperms and in some angiosperms. Coniferin (coniferyl glucoside) was found at significant levels within protoplasts from the developing xylems of Jack pine (*Pinus banksiana*) and Eastern white pine (*P. strobes*) (Whetten and Sederoff 1995). The presence of this modification in gymnosperms and even some angiosperms belonging to the *Magnoliaceae* and *Oleaceae* family suggests that glucosylation functions as modifications for transport and/or storage of monolignols prior to lignin biosynthesis. It is reasonable

therefore to speculate that monolignols are sequestrated first from cytosol to vacuole to prevent phenolic toxicity and are transported from vacuole to the cell wall during lignin deposition (Liu et al., 2011).

Glucosyltransferases are responsible for the previously mentioned conversion of monolignols; deglucosylation occurs via β-glucosidases found in apoplasts (Liu, 2012). β-glucosidases play a role in releasing monolignols from their glycoconjugates for cell wall deposition in xylem tissues. However, studies in the functional characterisation of glucosyltransferases in *Arabidopsis* that showed reduction and accumulation of monolignol glucosides due to respective down-regulation and up-regulation of the transferases presented no significant alternations in lignin deposition of secondary cell walls (Vanholme et al., 2008). Additionally, studies by Miao and Liu (2010) confirmed in *Arabidopsis thaliana* that there is a polarised distribution of the different forms of monolignols and their glucosylated form. Therefore, glucosylation via glucosyltransferases is needed for vacuolar transport of monolignols.

Despite a clear understanding of glycoconjugation of monolignols, transportation of monolignols to the wall remains yet to be fully understood. Several models have been proposed (Liu, 2012). The first is exocytosis via ER-Golgi-vesicles that is similar to the mechanisms found in non-cellulosic polysaccharides (pectin and hemicellulose) (Lerouxel, 2006) and is based on studies of lignin precursors using autoradiography and immunochemistry. Feeding isotopically labelled phenylalanine, tyrosine and cinnamic acid in developing xylem resulted in incorporation into the rough ER, Golgi and plasma membrane associated vesicles (Picket-Heaps, 1967). However, Kaneda et al. (2008) fed [3H]-Phe to cambium/developing xylem tissues of lodgepole pine, while inhibiting phenylpropanoid and protein synthesis. The results showed that radioactivity in the ER-Golgi-vesicles pathway were due to proteins rather than phenylpropanoids.

Passive diffusion is another model proposed for transporting monolignols through the plasma membrane. This idea was formulated because of the observed plasticity of lignin subunit depositions i.e. its aldehyde precursors in mutants deficient in certain enzymes of the phenylpropanoid pathway. When poplar and several plant phenylpropanoid knockdown mutants were analysed, it was revealed that compounds such as 5-hydroxyconiferyl alcohol, hydroxycinnamaldehydes and hydroxycinnamic acids, as well as the

enzymatic derivatives of monolignols, such as sinapyl *p*-hydroxybenzoate, coniferyl and sinapyl *p*-coumarate, and coniferyl and sinapyl acetate were incorporated into the secondary cell wall (Boerjan et al., 2003; Morreel et al., 2004; Leple et al., 2007; Ralph et al., 2008; Lu, 2004; Del Rio, 2007 and 2008). The plasticity observed supports the idea of passive diffusion transport of monolignols. This is due to the fact that if specific transporters were needs for monolignol transporters, aldehyde and cinnamic acid precursors would not be recognised and could not cross the plasma membrane. The only explanation for such transport of lignin precursors and the resulting lignin plasticity observed is that aberrant or premature monolignols are transported by passive diffusion. Supporting this theory are studies by Boija et al. (2007 and 2008) using *in vitro* partitioning experiments by using immobilized liposomes or lipid bilayer discs as the model membranes. Once lignin precursors were added to the liposomes or lipid bilayer discs, they easily partitioned into the artificial membrane phase confirming that lignin precursors can pass through the membrane by passive diffusion which explains the lignification plasticity during secondary cell wall development.

Lastly, ABC transporters have been proposed to traffic monolignols from the cytoplasmic side to the apoplastic region (Liu, 2012). Recent studies have not only demonstrated the roles of ABC transporters in monolignol transport empirically, but have resolved questions of passive diffusion, glucosylation and vacuolar compartmentalisation of monolignols. Since ATP and multidrug and toxic compound extrusion (MATE) transporters have a role in the transport phenolic compounds (Kazaki, 2005), Miao and Liu (2010) investigated the role of ABC transporters isolated from plasma and vacuolar membranes of *Arabidopsis* rosette leaves and roots of poplar. Their results showed that monolignol transport is ABC dependent by either blocking the transporter by inhibitors or omitting ATP. They showed that these transporters are substrate specific: plasma membrane and vacuolar ABC transporter only allow aglycones or 4-*O*-glucosides to pass respectively. Also, rates of transfer of monolignols from one interphase to another behaved in a Michaelis-Menten fashion, confirming their transport to be protein mediated rather than passively diffused. All these results indicate that lignin transport is a selective and highly ordered process in plants and as indicated by the specific deposition of its monolignols in different tissues (Liu, 2012).

Once transport and deposition in the cell wall occurs, monolignols undergo dehydrogenation to produce radicals that are stabilised via resonance structures (Figure 1.7). Subsequently, the radicalised phenols then couple to form a dimer with a covalent bond between the monomers (Vanholme et al., 2010). This coupling happens in a combinatorial fashion and depends mostly on the chemical nature of each of the monomers and on cell wall conditions (Ralph et al., 2010). To form a successive polymer chain, the dimer needs to be dehydrogenated then a phenolic radical can add itself to the growing polymer (also known as endwise coupling). Monolignols combine generally at their β positions, limiting dimerization to β- β, β-*O*-4 and β-5 structures (Vanholme et al., 2010). On the other hand dimerizations with no β positions involved are substrate dependent. For example, S/G dimerization is rare while G-units are more common due to their stable 5-5 linkages (Wagner et al., 2009). During this coupling in either dimerization or polymerisation, two radicals are consumed from the contribution of each electron to form a single bond- thus named termination reaction (Vanholme et al., 2010). This method of polymerisation persists till the formation of a chain with an average length of 13 to 20 units (Stewart et al., 2009).

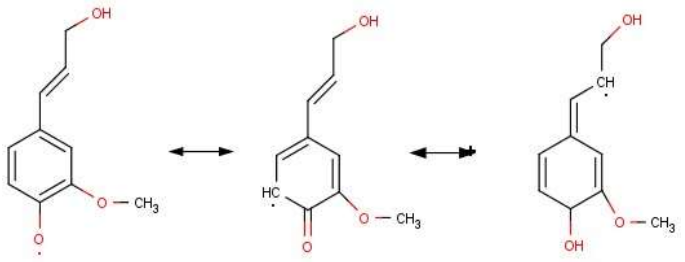

Figure 1.7: Resonance forms of dehydrogenated coniferyl alcohol with unpaired electron "localised" (Adapted from Vanholme et al., 2010)

Monolignol polymerisation uses peroxidases and or laccases, enzymes that belong to large gene families with overlapping activities (McCaig et al., 2005). Laccases and Peroxidases however, differ in substrates during their redox activities using hydrogen peroxide and oxygen respectively (Wang, 2013). These enzymes differ in activation during plant development as well: laccases are said to polymerise monolignols into oligolignols during early stages of lignification; on the other hand, cell wall peroxidases are generated during late stage xylem formation or during abiotic stresses (Sterjiades et al., 1993).

1.4.2 Random Coupling and Protein-Mediated Model of Lignification

It is generally accepted that such lignin polymerisation occurs in a combinatorial fashion, dictated by the availability of subunits (G, S and H) within a cell wall region. Dehydrogenation polymers (DHP) to produce synthetic lignin have been employed to support the combinatorial mechanism of lignification. The Zulauf (bulk method) and Zutropf (dropwise method) of adding monolignols have different effects on bonding propensity, the latter produced near *in vivo* bonding patterns as compared to the former (Hatfield and Vermerris, 2001). It provided clear evidence that only the rate of transfer of monolignols is needed to produce lignification patterns seen *in vivo*. Whilst at the start of polymerisation, dimerization needs to occur. The stereospecific formation of a pinoresinol dimer from β-β bonding of monolignols may cause the random coupling mechanism to come into question (Ralph et al., 2008b). However as noted by the review of Ralph et al., (2008b), even though such dimerization cannot occur in a random fashion, what causes dimerization are: relative energies of the transition states and pH, solvent polarity, temperature etc. and any change of these states will cause alterations in dimerization. Therefore, lignin polymerisation occurs in a "combinatorial" rather than random manner. Additional evidence to support the combinatorial mechanism is the plasticity of dehydroxyphenylpropanoid monomers incorporated into the secondary wall. Down-regulation of cinnamyl alcohol dehydrogenase results in the incorporation of coniferyl and sinapyl aldehydes to substitute the missing alcohols normally present in wild type plants (Kim et al., 2000). The evidence of the racemic nature of lignin structures from the favoured β coupling and the chiral carbon formation in the β carbon of monolignols also support the random coupling mechanisms of lignin monomers; lignins lack any demonstrable optical activity (Ralph et al., 1999; Ralph et al., 2008b). Lastly, transgenic Poplar overexpressing *F5H* resulted in a lignin composition of up to 97.5% S unit composition. Bonding patterns and chain structures of lignin are altered; proving that there is no evidence of gatekeeping under proteinaceous control (Stewart et al., 2009).

Nonetheless, an alternative pathway of protein-mediated lignification, via dirigent proteins, has been proposed. The main drive for the proliferation of this hypothesis is the idea that lignin formation, due to its integral functions for plant viability, should not be left to the vagaries of the available constituents and the environment of the apoplast (Davin et al., 1997). Dirigent proteins are responsible for the stereo-specific

structures of compounds. One such example is a dirigent protein found in *Forsythia intermedia* stems that possess high levels of (+) pinoresinol generated from two coniferyl alcohol monomers. This lignan demonstrated optical activity and displays partiality for both monomer usage and its enantiomer. Recent advances have also provided insight into the protein mediated hypothesis of lignin polymerisation. In *Arabidopsis*, a (-) pinoresinol was reported by Kim et al., (2012) based on the observation that pinoresinol reductase homologs (AtPrR1 and AtPrR2) from Arabidopsis root tissues preferentially converted (-) pinoresinol to (-) lariciresinol over its (+) antipode. This was done using in vitro studies by adding lariciresinol in the presence of AtPrR2, resulting in enatiomeric excess of the (-) antipode. In a loss-of-function study, the double T-DNA mutant (*atprr1-1 atprr2*) accumulated (-) pinoresinol and no lariciresinol was observed. Thus, it was deduced that there seems to be a stereoselective preferential formation of (-) pinoresinol from its coniferyl alcohol substrates. It was then confirmed that AtDIR6 is a (-)-pinoresinol-forming dirigent protein, whose physiological role was further confirmed using overexpression, GUS expression patterns and RNAi strategies *in vivo*. Additionally Hosmani et al. (2013) showed that a dirigent domain containing protein, ESB1 can direct stereospecific coupling of monolignols to form the lignan pinoresinol in the presence of peroxidases *in vitro* (Hosmani et al., 2013). Because the production of a monolignol dimer such as pinoresinol serves as initiation of lignin polymerisation it might be ascertained that the discovery of these proteins provides *in vivo* evidence of dirigent proteins participating in lignification by producing lignans or as mentioned, serve as initation sites for lignin polymerisation.

Recent studies by Hosmani et al. (2013) provided evidence that ESB1 is also responsible for the correct pattern of lignification in the Casparian strip of *A. thaliana*. Loss of function mutants in this protein results in a complete loss of well-organised Casparian strip structure but still retain lignin-like material of similar make up to wild-type Casparian strips and xylem lignin. *ESB1* also results in the disrupted polymerisation of monolignols activated by NAPDH oxidases due to perceived irregularly deposited lignins in the Casparian strip.

Additional experiments also theorise a role dirigent proteins play in determining template directed monolignol biosynthesis. In template directed polymerisation as suggested by Chen and Sarkanen (2003

and 2010), lignin chains cannot be displaced and are highly restricted from their locus. Therefore the preserved lignin may occur via direct template polymerisation: each daughter strand is topologically complementary to its parent chain. Such a process requires a double stranded template that forms a rigid complex. As coupling of a new monolignol and the template strand commences, the radical from the template strand is immobilised adjacently to the radical of the growing daughter chain. A new covalent bond is formed and creates a complementary substructure similar to the parental double strand (Figure 1.8). As a monolignol radical couples to the end of a growing lignin chain, the new substructure formed tends to associate in a head-to-tail fashion with the corresponding dimeric motif in the proximal template strand. However, this process leads to puckering and the dimeric substructures from the parental strand would be untenable. To compensate for this, a replication fork is caused by the dissociation of the proximal strand now attached to the new growing lignin chain from the distal chain (Figure 1.8).

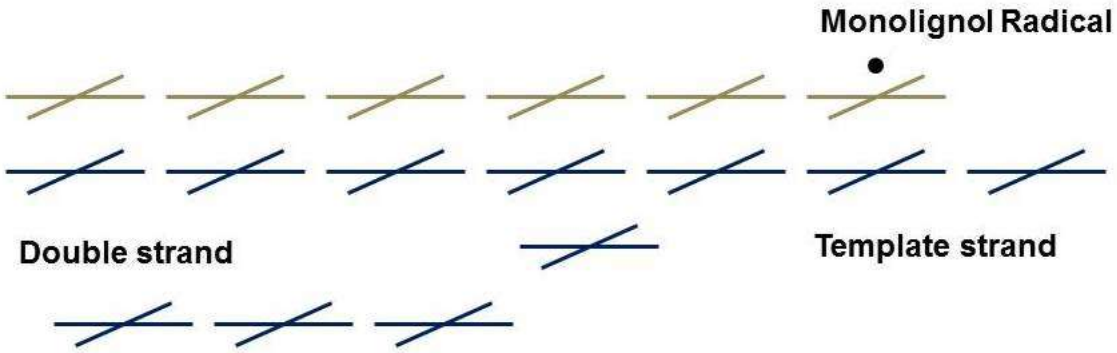

Figure 1.8: Template strand polymerisation of Lignin. Adapted from Chen and Sarkanen (2003).

With that in mind, the lignin chain could be synthesised to completion in an endwise manner before growth of the subsequent layer can begin in the reverse direction. If such a mechanism were to occur, the recruitment of pinoresinol lignan may provide a moiety that has already been covalently linked into a macromolecular lignin chain. It will wait for the growing chain of monomers above the template strand and when the last monomer residue is beside the lignan, 5-*O*-4 coupling can link the pinoresinol molecule to the polymer chain. Another pinoresinol molecule will then combine with the new daughter lignin chain and biosynthesis of the next lignin strand in the layer above can begin in the reverse direction. The

mechanism parallels brick layerings in an anti-parallel manner (See Figure 1.9) (Chen and Sarkanen, 2003).

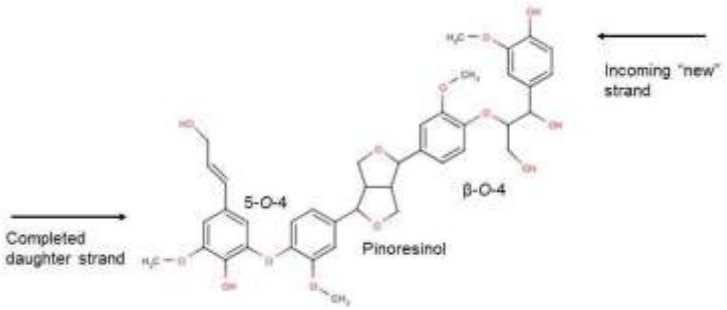

Figure 1.9: Pinoresinol lignan serving as a linker for growing template mechanism of lignification. Arrows indicate direction of polymerisation.

1.5 Phytocyanins: members of the cupredoxin superfamily

One factor that could contribute to overall lignin polymerisation and structure are a family of cupredoxins called phytocyanins. Members of the cupredoxins are blue copper proteins containing a single blue copper binding domain similar to those that serve as an electron shuttle in various energy conversion systems (Nersissian and Shipp, 2002; Gough and Chothia, 2004). In terms of structure, cupredoxins exhibit a β-sheet sandwich structure that is conserved amongst this family. Its composition is made up of seven or eight parallel and antiparallel strands, a variable α-helix region at one side with its copper moiety at the top (Gough and Chothia, 2004; Nersissian et al., 1998). Cupredoxins are typically freely diffusible proteins; plastocyanins for example, are diffusible electron transfer proteins in the lumen of thylakoid membranes of PhotoSystem I. Nersissian and Shipp (2002) reported that during redox reactions between cupredoxins and its partners a transient complex will form and subsequently dissociate once the electron transfer has lapsed indicative of an inner sphere electron transfer.

1.5.1 Phytocyanin Domains

Phytocyanins are part of a family of plant cupredoxins and are divided into subfamilies including: Stellacyanins, Uclacyanins, Plantacyanins (Nersissian et al., 1998) (Figure 1.10). Sequence homologues for these proteins have not been found in other organisms; phytocyanins are therefore plant-specific

proteins. Phytocyanins are chimeric proteins (excluding plantacyanins) that coalesced from structurally and functionally discreet domains. Their N-terminal domains are derived from cupredoxins due to their distinct type one/blue configuration (single Cu ion bound to the protein molecule) (Nerssisian et al., 1998). Due to their chimeric nature, different domains were identified amongst the subfamilies of phytocyanins. These four domains are responsible for the structural and biochemical properties, cellular localization and putative biological functions of phytocyanins. The N-terminal domain, present in all phytocyanin subfamilies is the classical ER-targeting signal sequence without any KDEL or HDEL retention signals, making them destined towards the secretory pathway (Nerssisian et al., 1998). Domain II is the copper binding domain which classifies phytocyanins as cupredoxins [with the exception of ENODs]. It is also said to bear Asn-X-Thr/Ser sequences that serve as potential N-linked glycosylation sites and further supporting traffic through the ER secretory pathway.

Domain III resembles plant-cell wall glycoproteins and is related to arabinogalactan proteins (Nersissian et al., 1998, 2001). Moreover, the abundance of Ala, Pro(Hyp), Ser, Thr and Gly in phytocyanins is also comparable with arabinogalactan proteins with these five residues accounting for more than 70% of their total residues (Nersissian et al., 1998). Kieliszewski and Lamport (1994) and Nersissian et al., (1998) also reported that cucumber stellacyanins and *Arabidopsis* uclacyanin 3 bear palindromic sequences that allow their integration and self-assembly into the plant cell wall. Domain IV possesses characteristics of glycosyl-phosphatidyl Inositol (GPI) anchoring signals. GPI-linked proteins are likely to be anchored to the exterior leaflet of the cell membrane. This C-terminus signal sequence is composed of hydrophobic amino acids that remain in the ER membrane. During post-translational modification, the hydrophobic end is subsequently cleaved off and replaced by the GPI-anchor via enzymatic action of GPI transaminidase. This moiety contains a conserved core of ethanolamine phosphate with an amide linkage to the carboxyl terminus of the protein, followed by three mannose residues, glucosamine and phosphatidylinositol (Mayor and Riezman, 2004).

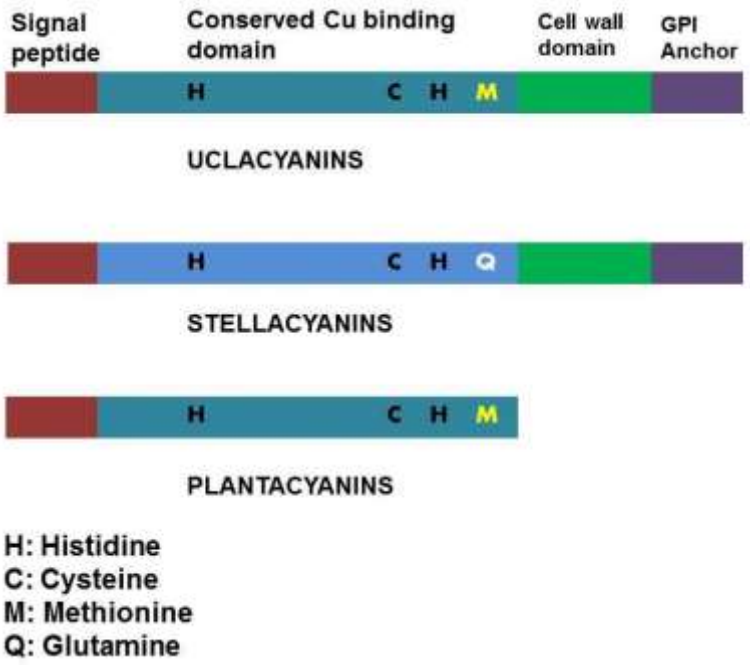

Figure 1.10: Phytocyanin subdomains. Adapted from Nersissian et al. (2001).

1.5.2 Phytocyanin Structure

In terms of structure, phytocyanins resemble the cupredoxin Greek key β-barrel topology of two α-helices and eight β-strands; strands 1, 2, 4 and 6 organizing the first β-sheet and strands 3, 5, 7 and 8 forming the second. In the first β-sheet, strand 2 bonds to strand 4 via one hydrogen bond. The remaining sheets have interactions similar to the prototypical β-sheets found in other cupredoxins. The second β-sheet is disordered and exhibits a significant degree of torsional strain. The asymmetrical nature of the two sheets results in a β-barrel topology where it is more flattened and more exposed on one side as compared to other cupredoxins. This feature allows the copper moiety with its two histidine, one cysteine and one glutamine/methionine ligands to be more solvent exposed at the top end of the β-barrel. Its degree of exposure allows the two histidines to be completely solvent exposed as compared to only one histindine in other cupredoxins. A more solvent exposed site is proposed to make the copper site more accessible allowing redox reactions with small molecular weight compounds rather than protein electron mediators. Phytocyanins are also documented to form a disulphide bridge at two sites: the first cysteine, located between a small α-helix and the second cysteine is positioned subsequent to the His94 ligand of the

copper binding site. This cysteine bond stabilises the overall phytocyanin and- is only found in phytocyanin and early nodulin proteins. (Nersissian et al., 1998)

In the copper binding domain of phytocyanins, there is also some variability in redox properties exhibited in comparison to cupredoxins and within its subfamilies. Phytocyanins generally exhibit a perturbed blue copper site as compared to the classical blue copper sites found in plastocyanins. Perturbed copper sites have shorter ligand moiety bonding lengths. This copper binding site feature could be a plausible reason for the generation of a distorted tetrahedral geometry found in phytocyanins and stabilised by a disulphide bridge. The perturbation may also affect its structural changes during oxidation and reduction as phytocyanins also exhibit a more acute compaction and relaxation in these respective states. This creates a relatively large movement and indicates that they do not follow entatic state concepts (Nersissian et al., 1998). A feature, unique to phytocyanins results in outer sphere electron transfer, making them unable to participate in long-range electron transfer and more suited for low molecular compounds. This juxtaposes plastocyanin's inner sphere electron transfer which results in an acquiescence to transient complexes being formed. The variability between subfamilies, such as that observed in the axial ligands of uclacyanin and plantacyanin copper binding site also produce changes in redox properties. Uclacyanins contain methionine residue whilst stellacyanins, have a glutamine residue. The single residue change in the copper site can reduce redox potential by almost a half as seen in Table 1.2.

Table 1.2: Redox potential differences observed in phytocyanin subfamilies and their corresponding amino acid change in the metal-binding site. Adapted from Nersissian et al. (1998)

Phytocyanin Subfamily	Amino Acid Composition of metal-binding site	Redox Potential (mV)
Stellacyanin	2 His, 1 Cys, 1 Gln	180 -280
Uclacyanin	2 His, 1 Cys, 1 Met	320

1.5.3 Phytocyanins and Their Putative Role in Lignification

The structural and biochemical properties of phytocyanins have provided an understanding to the putative roles of phytocyanins in secondary cell walls. However, what seems to be equivocal is in what aspect of secondary cell wall formation they are active in. Insight into phytocyanin's role in secondary cell walls has

been suggested by the following studies that their plausible functions are primary defence or lignification. According to Van Gysel et al. (2003), an AtBCB gene encodes a cupredoxin-like that may play roles in electron transfer reactions in the cell membrane region of *Arabidopsis*. This protein has 86% amino acid similarities with horseradish umecyanin (belonging to the subfamily stellacyanin). Umecyanins were found to be bound to peroxidases; because of this Van Driessche et al. (1995) proposed that peroxidases with bounded umecyanins function together in root cell membranes. Thus, because AtBCB has sequence similarities with horseradish umecyanin, it may play equivalent roles. Drew and Gatehouse (1994) also reported blue copper binding proteins being connected to lignification in the pea pod's endocarp through mRNA expression studies. Lastly phytocyanin related sequences were found from cDNA isolated from differentiating xylem in loblolly pines (Allona et al., 1998). Phytocyanins due to their copper binding domains could be responsible for lignin metabolism in the cell wall.

Because much of the genetics and biosynthetic pathways of lignin and its precursors are widely characterised (Bonawitz and Chapple, 2010) and with the recent discoveries of alternative pathways in monolignol production such as the CSE mutants by Vanholme et al. (2013); it begs to question what roles do phytocyanins play in lignification? Non-enzymatic polymerisation of monolignols using transition metals by Landucci (1995) may rationalise a similar mechanism for the phytocyanins' involvement in lignin polymerisation. Their data showed that one-electron transition metal oxidants such as copper (II) acetate and magnesium (III) acetate polymerised monolignols to oligolignols with similar bonding patterns of monolignols (β-*O*-4, β-5 and β-β) found in *in planta* lignin. Additionally, based on 13C- NMR spectroscopy these biomimetic compounds displayed a more accurate representation of natural lignin compared to peroxidase mediated polymerisation. Because the copper in cupric (II) acetate and the copper moiety in phytocyanins have similar oxidation states, phytocyanins may polymerise monolignols in a similar fashion.

Phytocyanins may also act as dirigent proteins for lignan biosynthesis. Recently studies on a dirigent protein found in *A. thaliana* called AtDIR6 revealed AtDIR6 possessed an anti-parallel β-barrel like structure, a disulphide bridge and N-linked glycosylation sites (Pickel et al., 2012). These structural

features are reminiscent of phytocyanin structures and may therefore invoke similar functions to AtDIR6 as well. However there is conflicting evidence towards this because dirigent proteins do not possess oxidative capacity by themselves (Kazenwadel, 2013).

Lastly, arabinogalactan proteins are known for mediating an interphase between the plant plasma membrane and its cell wall; they also initiate secondary walls formation through the intercalation of monolignols or its intermediates and serve as nucleation sites for such monomers (Albersheim et al., 2001). Lignification is also affected by and correlated with Golgi secreted glycine rich proteins during lignin initiation (Albersheim et al., 2011; Burlat et al., 2001). Incidentally, certain phytocyanins have glycine rich regions near their c-terminal (AGP) domain which would be consistent with a role in cell wall architecture via lignin interactions (AGI, 2000).

1.6 Arabidopsis as a Model Plant

Arabidopsis thaliana, a small annual plant of the mustard family (Brassicaceae) has become the model organism for modern plant biology. First promoted by Friedrich Laibach in 1943 it soon became well-established for plant genetics, molecular biology and development (Koornneef and Meinke, 2010). Arabidopsis contains many attributes suited for molecular studies. Firstly, Arabidopsis size is very small. When grown at low density, its leaf rosette has a maximum diameter of four to six centimetres and its inflorescence stem reaches 30 to 40 cm in height. The compactness of *Arabidopsis* allows large numbers of plants in a small indoor growth chamber, negating the need for field plots. It produces thousands of seeds and is small enough to grow on petri dishes allowing evaluation of specific nutritional requirements or antibiotic resistance of transgenic lines (Koornneef and Meinke, 2010).

Arabidopsis also has a short generation time, will flower within a month and produce seeds in two. Additionally, generation time can be shortened by two weeks when grown under continuous light conditions (Koornneef and Meinke, 2010). Self-fertility and large numbers of progeny allow maintenance of genetic stocks and analyses of inheritance. The small genome (125 megabase pairs) and number of chromosomes (n =5) decreases labour and effort to clone and mutate genes and streamlines genetic

mapping respectively. The complete sequence of *Arabidopsis thaliana* ushered in the era of its genomics study and drives to determine the function of its 28000 genes in its genome (AGI, 2000).

Transformation of *A. thaliana* is fast and simple for introducing genes into the genome by floral dipping (Clough and Bent, 1998). This method has yet to be performed efficiently in other species. From this method, insertional mutations (mutations where a foreign segment of DNA is inserted in the middle of a gene, causing the loss of function of the gene product) in almost all *Arabidopsis* genes have been created and identified. This resource allows functional analysis of any gene (Alonso et al., 2003).

In terms of cell wall research, *Arabidopsis* allowed identification and functional characterisation of genes important in plant cell-wall biosynthesis. Numerous studies on *A. thaliana* have provided key insight into the involvement of CESA proteins in cellulose synthesis such as *radial swelling 1* (*rsw1*) mutant. *RSW1* displayed decreased cellulose content and loss of rosette structures thereby providing evidence of a link between CESA proteins, cellulose synthesis and rosette formation. Arabidopsis has also been employed to study CESA complexes *in vivo* by live cell imaging of fluorescently-tagged CESA subunits and studying their movement in the plasma membrane relative to the cytoskeleton and it's delivery to the membrane (Liepman et al., 2010).

Due to recent surge in interest in using plant cell wall material as a potential source of biofuels, xylan research has garnered much interest. This major component of many woody secondary cell walls is a potential source of sugar for saccharification. But due to its pentose composition and cross linkage with lignin via ferulic and *p*-coumaric acid, microogranisms such as *S. cerevisiae* and *Zymomonas* mobilis do not possess enzymes that ferment pentose sugars and the cross-linkages of xylan and lignin make it less accessible for cellulose hydrolysing enzymes. Therefore, understanding and manipulation of xylan biosynthesis is an important area for lignocellulosic biofuel research. The Arabidopsis genome sequence has significantly contributed to recent advances in our understanding of xylan biosynthesis, most notably by facilitating the use of genome-wide expression data. Co-expression analysis, using marker genes for secondary cell-wall biosynthesis, identified six glycosyltransferases (IRX7, IRX8, IRX9, IRX10, IRX14 and PARVUS) with a role in xylan biosynthesis (Brown et al., 2005, 2007, 2009; Persson et al., 2005, 2007;

Zhong et al., 2005; Pena et al., 2007; Wu et al., 2009). A mutation in any one of these sequences results in a reduction in 1, 4-β xylan content (Liepman et al., 2012).

Arabidopsis has also provided insight into GPI-anchoring. Little is known about GPI-anchoring in plants, but because Arabidopsis contains genes homologous to numerous animal and yeast genes responsible for GPI anchor synthesis, putative functions can be assigned based on known animal or yeast homologues. Mutations in these genes have been reported to cause severe deficiencies in plants. For instance, mutations in *seth1* and *seth2* in Arabidopsis, which are homologues of the GPI–transamidase complex involved in the transfer of D-GlcNAc to phosphatidylinositol, specifically blocked pollen germination and tube growth (Lalanne et al., 2004).

Arabidopsis has proven to play an important role in the identification of genes and functional analysis of proteins involved in plant cell-wall biosynthesis. In addition, application of these insights allows biotechnological applications such as the engineering of plant cell-wall biomass for biofuel uses.

1.7 Elucidation of Gene Function via Mutagenesis

In order to determine gene function it is possible to study the phenotype of plant with mutations in a given gene and compare it with wild-type (Brown et al., 2005). Elucidation of gene function using mutagenesis is done in two ways: forward genetics and reverse genetics. Forward genetics is the process of discovering a gene by unsystematic mutation followed by a screen of mutants for an observable phenotype. On the other hand, reverse genetics is a more systematic approach of mutation, inhibition or deletion of a specific gene that is hypothesised to have a certain function and is confirmed by a resulting phenotype (Bonawitz and Chapple, 2010).

1.8 Reverse Genetics as a Tool to Study Gene Function

Currently there are excellent tools for the *Arabidopsis* researcher. Reverse genetics progresses from genotype to phenotype using several gene manipulation techniques. Different consortia generated collections of insertion mutants, which are either screened for a knockout in a gene of interest by PCR or by comparing flanking sequences in the insertion with a sequence of the gene of interest. The

Arabidopsis Biological Resource Center, the Nottingham Arabidopsis Stock Centre (NASC), the Salk Institute, the Flanking Sequence Tags (FST) Project at Versailles (see link) and the Torrey Mesa Research Institute (TMRI, see link) all maintain insertion databases so that known insertions in a gene of interest can be easily searched (Page and Grossniklaus, 2002). Mutations in genes of interest are then identified from PCR screening of pooled mutant populations. Therefore, the use of reverse genetic approaches to study genes of interest with unknown function is a convenient yet powerful tool (Sessions et al., 2002).

1.9 Artificial microRNA (amiRNA) for the Identification of Gene Function

To generate mutants in genes without available T-DNA inserts, artificial microRNAs (amiRNA) provide a practical alternative. Artificial microRNAs are analogous to naturally occurring microRNAs (miRNAs) in terms of structure and mode of action. These short RNAs (~19 to 24 nucleotides in length) are produced from fold back precursors from transcribed imperfect inverted repeats in the genome. These precursors are processed by specific RNases like DICER-LIKE1 and then interact with specific double stranded RNA (dsRNA) binding protein, HYL1. The single stranded 21 nucleotide RNAs are then incorporated into the silencing complex [usually with the argonaut4 protein (AGO4)] and subsequently mRNA degradation occurs. Whilst animal miRNAs are flexible in terms of complementarity to its target for translational arrest, plant miRNAs need to possess very few mismatches (0-5) to trigger transcriptional cleavage and its degradation of mRNAs. Because amiRNAs were reported to silence endogenous and reporter genes comparable to natural miRNAs, they provide an effective gene silencing tool. Silencing is further specified when controlled by an inducible promoter as e.g shown by amiR-lfy-1 with *LFY* promoters which resulted in *lfy* (regulator of floral identity) mutants (Schwab et al., 2006; Ossowski et al., 2008).

amiRNAs exploit the endogenous miRNA precursors that direct gene silencing. amiRNAs can silence genes similar and produce phenotypes of plants with mutations in the respective genes. In fact, >90% of T1 amiRNA silenced plants display defects, with a fraction of the population resembling null mutants. In an example reported by Weigel et al. (1992), amiR-lfy-1 overexpression led to floral defects similar to typical *lfy* null mutants. Other amiRNA constructs showed effects indicative of weak and intermediate *lfy*

alleles. Since natural miRNAs silence multiple targets, derived amiRNAs should produce the same result. In most cases, the phenotypes of amiRNA overexpressers implied targeting of multiple genes *in vivo* (Schwab et al., 2006). amiRNA silencing of genes involved in trichome development displayed congruent phenotypes of *try* and *cpc* double mutants that resulted in highly clustered trichomes on leaf base (Schellmann et al. 2002). Short interfering RNAs (siRNA) not only cleave and destroy selected targets, but can also become primers for RNA-dependent RNA polymerases. These extend the local RNA double strands and produce templates for secondary siRNAs by Dicer action. The unrelated secondary siRNAs can affect other genes not targeted by the original siRNA (Schwabb et al., 2006). This supports the idea that amiRNA specificity is akin to that of natural miRNAs.

Since amiRNA possesses similar properties to endogenous miRNAs, and their reported efficacy, the construction of amiRNAs from the Web MicroRNA Designer (WMD) would allow synthesised amiRNAs for effective gene silencing. Streamlined input of data is possible through the use of gene identifiers (e.g. Atg22480, Os01g24680) in the “Design” tool. Allele-specific silencing is also possible. Because not all genome sequences and annotations are available, WMD can exploit EST collections as well (Ossowski et al., 2008).

The Design of amiRNAs using WMD applies an optimisation of small RNAs for maximal effectiveness, and from that, selection of the candidate with highest specificity for the target gene. Optimization of amiRNA sequences are shown in the flowchart (Figure 1.10) and goes as follows. In the first step, candidate 21-mer sequences are chosen from a reverse complement of the whole target transcript. Position 1 needs to contain a uracil in all cases, even though other nucleotides can be found at this position. Next, all candidates are mutated *in silico* at positions 13–15 and 17–21. The resulting mutated candidates must hybridize with the target gene and cannot contain more than two mismatches between positions 13 and 21. For amiRNAs with multiple targets allow for maximally one mismatch from amiRNA positions 2 to 12, none at the cleavage site (positions 10 and 11), and up to four mismatches between positions 13 and 21, with no more than two consecutive mismatches. In addition, acceptable amiRNA–target duplexes must have at least 70% of the free hybridization energy calculated for a perfectly complementary amiRNA, with at least -30 kcal mol^{-1} (Ossowski et al., 2008).

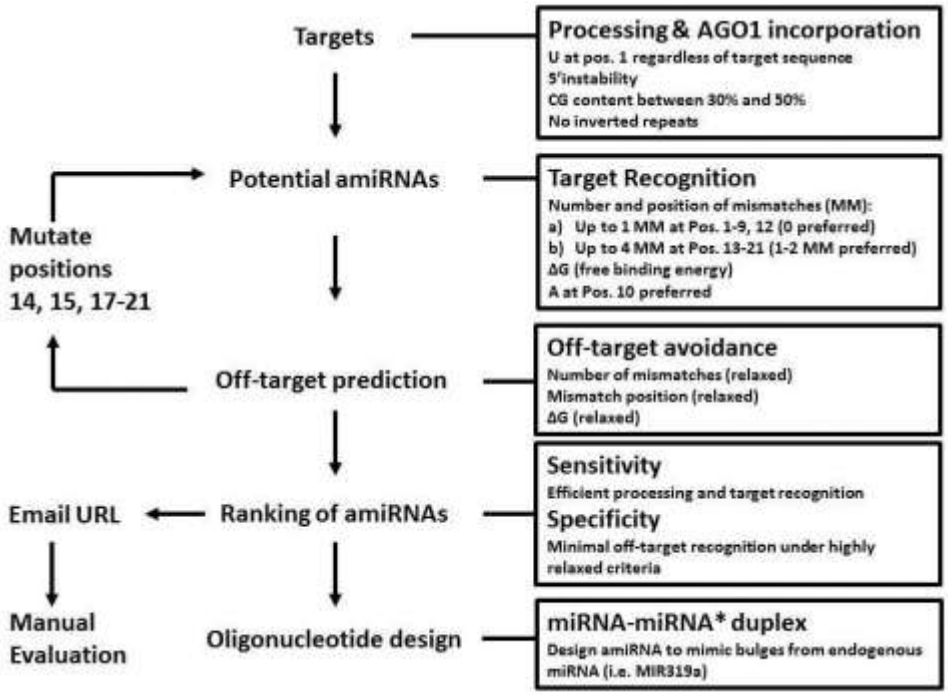

Figure 1.11: Flowchart of Web MicroRNA Designer (WMD) programme for amiRNA design. Adapted from Ossowki et al., 2008)

1.10 Identification Genes Involved in Secondary Cell Walls Using Expression Data

The emergence of oligonucleotide arrays and cDNA microarrays enabled biologists to measure expression levels of thousands of genes at the same time. A suitable application of this technology is to monitor gene expression while an organism undertakes a certain biological function (Heyer et al, 1999). The *Arabidopsis* plant makes a good candidate for such analysis due to its genome being sequenced and annotated (AGI, 2000). Using coexpression data provides a prudent method to determine gene of interest function. First, it is known that many functionally related genes are coexpressed (Eisen et al., 1998). For example, genes coding for elements of a protein complex tend to have similar expression patterns. The second reason is that in coexpressed genes, coexpression may uncover information about the genes' regulatory systems. If a single regulatory system controls two genes, it is therefore highly likely that they are coexpressed (Heyer et al., 1999). Most web-based coexpression tools calculate the relationships based on Pearson's correlation coefficient (PCC). With this, coexpression relationships can be visualised in a network form with its nodes representing genes and their connections between these nodes

signifying transcriptional coordination. These networks are then being divided based either on rank-based or value-based networks. For the former, the network is based on a certain PCC-value threshold. This method has some drawbacks in that weakly transcriptionally coexpressed genes are excluded despite their biological relevance. On the other hand, if PCC-value thresholds were slackened, this would result in excessively large networks. Rank based methods provide an alternate criterion in that the ranks of two given genes in their mutual coexpression lists determine coexpression correlation.

Coexpression data have provided a vital tool to identify new genes involved in secondary cell wall synthesis. Analysis done by Persson et al. (2005) with publicly available *Arabidopsis* microarrays to determine previously implicated genes involved in cellulose synthesis. These candidate genes were then subjected to mutant analysis and were observed to have *irx* phenotypes. Moreover, Brown et al. (2005) also used coexpression analysis to show secondary cellulose synthase subunits (CesAs) show similar expression patterns and that lignin and xylan synthesis genes are also coordinated during expression of CesAs. Thus, in silico coexpression analysis provide a useful tool to identify new genes in a multicomponent process such as secondary cell wall synthesis. Therefore the identification of phytocyanins involved in this process using similar approaches would be able to at least narrow down candidate genes for reverse genetics and streamline mutagenic analysis of these proteins.

GeneCAT (http://genecat.mpg.de/525/genecat.html) is an online tool that allows various coexpression analyses from their database. GeneCAT can generate graphs of expression values of genes of interest across available microarrays which permit coexpression analysis in a specific tissue. It can also cluster genes based on similarity of their expression profiles and visualise them using a dendogram. Lastly, it can measure similarities between a lists of genes co-expressed with a bait gene in comparison to the lists of genes co-expressed with target genes. This tool can be used to compare co-expression environments of genes within an organism (Schmid et al., 2005).

Another tool for studying gene function via knockdown approaches would be to discern their sequence homology. This ability, to precisely predict gene function from its sequence is a vital challenge in biological research. This has become important in the genomics age where numerous gene sequences

are generated without any accompanying experimental data. Most functional prediction relies on the characterisation, identification and quantification of similar sequences between the gene of interest and any other information available from related sequences. Because the sequence of the gene of interest is the major factor in determining function, sequence similarity therefore implies similarity of function. This assumption is typically valid. However, sequence similarity does not always result in the same functions; it is also common that groups of genes with similar sequences have different functions. Therefore, the identification of sequence similarity is not necessarily enough to appropriate a predicted function to an uncharacterised gene (Eisen, 1998).

Phytozome is a programme for plant genome and gene family data and analysis. Phytozome allows a view of plant genes at sequence levels, gene structure, gene family, and genome organization. It gives access to annotated plant gene families, to examine plant genes in genomic context, assigns putative function to uncharacterised genes and provides access to plant genomics data sets consisting of complete genomes, related (e.g. homologous) sequences and alignments, gene functional information and gene families (Goodstein et al., 2012).

1.11 Aim and Objectives

At the start of this study, phytocyanin function and localisation remained speculative. Therefore, the aim of this thesis is to identify the putative function of phytocyanins in secondary cell walls. *Arabidopsis thaliana* will be used as an experimental system. To begin with we will identifiy phytocyanin genes and their homologues that are coexpressed during secondary cell wall deposition. Then the use of T-DNA

insertions and amiRNA synthesis will identify mutants in these coexpressed genes. Multiple mutants will also be generated to test if functional redundancy occurs and if they have a discernible cell wall phenotype based on xylem morphology and histochemistry. Attempts to determine phytocyanin localisation will be done by GFP tagging and visualised under fluorescence microscopy. Lastly characterisation of any cell wall defects using FTIR by comparing phytocyanin mutants with other cell wall mutants of known function.

Chapter 2: Methods

2.1 Plant Material and Growth Conditions

Arabidopsis thaliana ecotype Columbia (Col) was used for the experiments. For a detail of knockout mutants see Table 2.1. Seeds were sterilised in 10% NaOCl (>8% free Cl), 0.1% Triton-X100 for 5

minutes and subsequently washed with sterile de-ionised H_2O (dH_2O) six times for 1 minute. Following sterilisation, the seeds were placed on plates containing ½ MS (Murashige and Skoog) media with vitamin B5 and 1.0% (w/v) agar and sealed with micropore tape. Seeds were stratified for 2 days in the dark at 4°C. Plates were placed vertically in growth cabinets (Sanyo MLR) at 20°C with a light intensity of 140 µmol $m^{-2}s^{-1}$ for 7 days. Seedlings were then potted in a mixture of compost:vermiculite:perlite (3:1:1) and grown under continuous light (120-150 µmol $m^{-2}s^{-1}$) in a growth cabinet (Percival, Ohio, USA) at 22°C. Inflorescences stems were harvested once they had reached 7 ±0.5 inches, the flowers were removed, and saved for DNA extraction and the stems were divided into 3 equal sections for RNA extraction.. For FTIR analysis (Table 2.2), plants were grown similar as above with some modification. Once the seedlings were potted, they were grown under short days (8 hour light and 16 hour darkness) for 6 weeks and switched to long day conditions (16 hour light and 8 hour darkness) to synchronise flowering. A pool of 5-7 10 cm stems and 3 biological replicates were used. Samples were freeze dried (Christ, Osterode, Germany) for 2 days and milled by rapid shaking with 3 ball-bearings for 1.5 hours using a Tissuelyser (Qiagen, Crawley, UK).

2.2 Plant Crossing

Plant crosses were performed as as follow). A single plant was surveyed for early flowers present. Then under a dissecting microscope and using a watchmaker's forceps, flowers were opened and the petals and stamen removed, leaving only the stigma. Using a flower chosen from a different line that has bright yellow pollen, .a stamen was removed with the watchmaker's forceps and lightly brushed on to the chosen stigma a couple of times.

2.3 DNA Extraction

Plant DNA extraction was performed according to Lukowitz et al. (1996) with modifications as described: Inflorescence flowers were placed in 1.5ml Eppendorf tubes, frozen with a ball mill and homogenised using a TissueLyser (Qiagen, Crawley, UK). 400 µl of DNA extraction buffer (140mM d-Sorbitol, 220mM Tris-HCl pH 8.0, 22mM EDTA pH 8.0, 0.8% (w/v) CTAB, 1.0% (w/v) n-lauroyl sarcosine and 400 µl

chloroform was then added. The Eppendorf was vortexed and centrifuged at 13,000 rpm for 5 minutes. Avoiding the interface, the upper aqueous was then transferred to a new Eppendorf. An equal volume of isopropanol was added, vortexed quickly and incubated at room temperature (RT) for 10 min. The sample was centrifuged at 13,000 rpm for 15 min. After removing the supernatant, the pellet was washed with 200 µl 70% EtOH. The DNA pellet was dissolved in 1X TE pH 8.0 buffer, and stored at -20°C until required.

2.4 PCR Screening of T-DNA Insertion Mutants

For genes selected for study, the SIGnal database (Alonso et al., 2003) was used to select lines that contain T-DNA insertions most likely to cause loss of gene function. Lines were obtained from NASC (Nottingham University, UK) and ABRC (Ohio State University, Columbus, OH) (Alonso et al., 2003) (Table 2.1) (Figure 2.1).

Table 2.1: List of single mutants in this study

Gene Accession No.	Mutant Identification	T-DNA Insertion Site
At1g22480	SAIL_381_C11	Intron
At5g20230	SALKseq_60215	Exon
At1g72230	SALK_083847	5'-UTR
	SALK_201823	Exon
At5g07475	SAIL_582_G03	Exon
At3g27200	SALK_053270	Exon

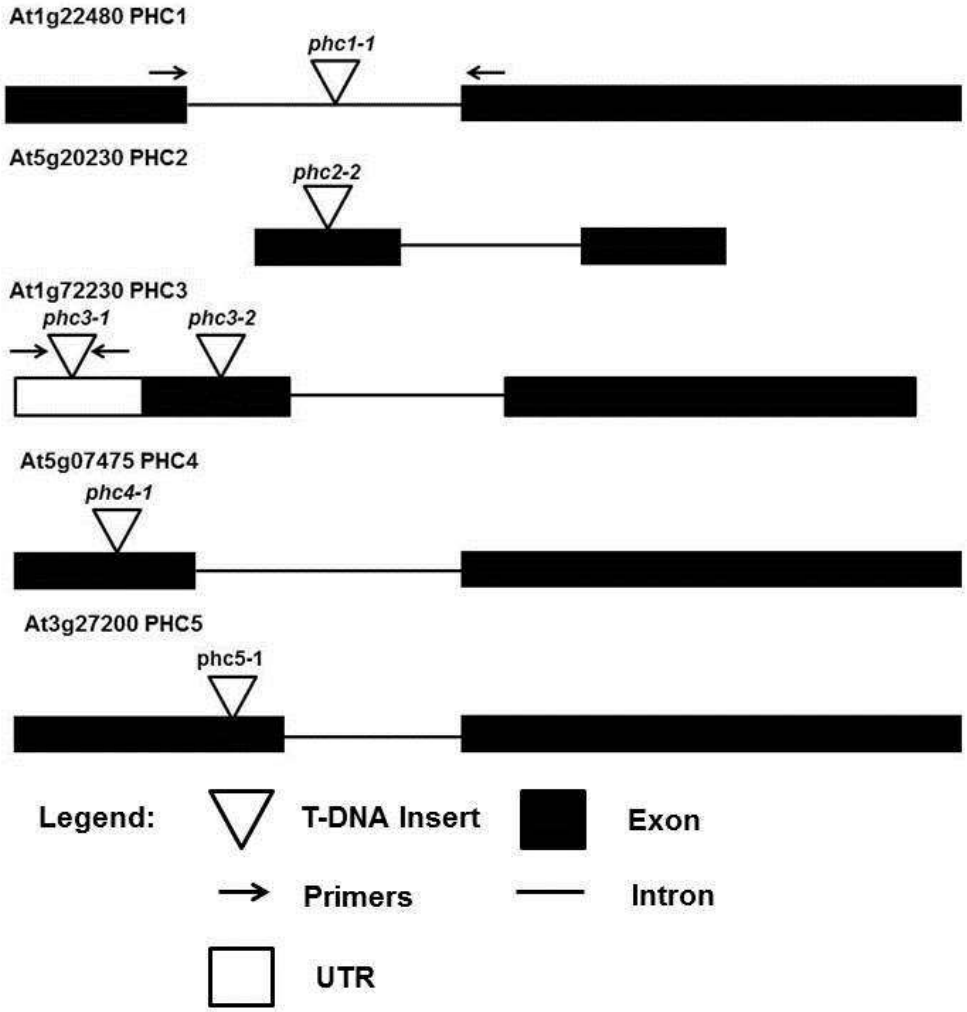

Figure 2.1: Schematic of T-DNA inserts in candidate phytocyanin genes.

Mutant lines were checked for T-DNA insertions using flanking primers produced by the SIGnal T-DNA Verification Primer Design webpage (http://signal.salk.edu/tdnaprimers.2.html) (Table 2.2) and a left border primer either ATT TTG CCG ATT TCG GAA for SALK lines or GCC TTT TCA GAA ATG GAT AAA TAG CCT TGC TTC for SAIL lines (Alonso et al., 2003).

Table 2.2: T-DNA inserts and left border primer sequences

Gene Accession No.	T-DNA Insertion	Forward Primer (5'→3')	Reverse Primer (5'→3')
At1g22480	SAIL_381_c11	TTC AAA TGG ACG GCT TAG ATG	TCG ACT AAA TCA ACA CAC CCC
At5g20230	SALKseq_60215	CAT TAC CCA AAA AGT AAT TAG TCA CG	GTT GCA CCA GCA GCA ACT AC
At1g72230	SALK_083847	AAT GCC GAA GAC AAA TCA ATG	ATT GTT CGT TTG CAA GCA AAG
	SALK_201823	AAA GGA GAA ACC TCC AAT TGG	GTC ACT TTC GCT CAC TTC GTC

The PCR amplification procedure is as follows: a 20 µl reaction of 3 µl DNA (~10ng DNA), 50pmol oligo-nucleotide primers (Eurofins MWG, Ebersberg, Germany), in 1x PCR buffer (67 mM Tris-HCl pH 8.8, 16mM $(NH_4)_2SO_4$ with 0.01% stabiliser), 2.5mM $MgCl_2$, 1 u *Thermus aquaticus* DNA polymerase (Bioline Reagents Ltd, UK) and 0.125mM each of dGTP, dCTP, dATP and dTTP (Bioline Reagents Ltd, UK). PCR was performed using either a MJ research PTC-200 (MJ Research Inc, USA) or Biorad Thermocycler C1000 (Biorad, USA). PCR programme as follows: 94°C for 5 minutes; 34 cycles of 94°C, 15 seconds; 55°C, 30 seconds; and 72°C for 1 minute; with a final extension of 72°C; 5 minutes and an 8°C hold.

2.5 RNA Extraction

Total RNA was extracted from stem material that had been stored at -80°C using the Trizol® (Life Technologies) method. Up to 100 mg plant material was ground in a mortar and pestle with a crushed cover slip to facilitate homogeneity during grinding. The homogenous solution was placed in a 2.0 ml Eppendorf tube on ice, and vortexed for a few seconds. 400 µl of chloroform was added, vortexed and centrifuged at 4°C, 11,000 rpm for 15 minutes. The aqueous phase was collected and equal volumes of isopropanol were added. The samples were then vortexed and incubated at room temperature for 10 minutes and subsequently centrifuged at 11,000 rpm for 15 minutes at 4°C. The supernatant was

removed and 700 µl of 70% EtOH in 30% DEPC water was added and inverted several time. The sample was again centrifuged at 4°C, 11,000 rpm for 5 minutes, the EtOH was discarded and the pellet left to air dry on ice for 10 minutes. 30 µl of DEPC-H_2O was then added and the samples were frozen at -80°C prior to first strand synthesis. RNA samples were quantified using a Nanodrop spectrophotometer (ND-1000, Labtech).

2.6 First Strand Synthesis

First strand synthesis was based in accordance to the manufacturer's instruction and some minor modifications (Peter Etchells, personal communication). A volume equivalent to 4 µg of RNA was added to 8 µl of RT-PCR buffer (Bioline Reagents Ltd, UK) and 4 µl of RQ1 DNAase I (Promega) and DEPC-H_2O to a final volume of 40 µl. The sample was then incubated at 37°C for 60 minutes. Afterwards, 4 µl of DNAase stop solution (Promega) was added and incubated at 65°C for 10 min. 10 µl was aliquoted from the DNAase treated preparations, placed on ice and 0.5 µg/µl oligo dT primer, 0.125mM each of dGTP, dCTP, dATP and dTTP (Bioline Reagents Ltd, UK) and DEPC-H2O was added to a final volume of 14 µl. The preparations were then subjected to denaturation at 65°C for 5 minutes and chilled on ice. Once chilled, of 1 µl of RNAsin (Promega) and 1 µl Bioscript™ Moloney Murine Leukaemia Virus (MMLV) reverse transcriptase (Bioline Reagents Ltd, UK) were added and the sample made up to a final volume of 20 µl. First strand synthesis was performed at 37°C, for 50 min and 70°C for 10min using a Thermocycler C1000 (Biorad) to maintain the temperature. cDNA was kept at -20°C until needed.

2.7 Real Time PCR (RT-PCR) for Phytocyanin Transcript Abundance in T-DNA Insertion Lines and amiRNA Lines

Real-time PCR (RT-PCR) was performed using Thermocycler C1000 (Biorad). Primers (Table 2.3 and 2.4) were designed using Primer3 (http://bioinfo.ut.ee/primer3-0.4.0/). PCR programme used as follows: 94°C, 3 min; 34 cycles of 94°C, 30s; 55°C, 30s; 72°C, 1min; final extension at 72°C, 5 min and on hold at 8°C. PCR reactions were performed in a volume of 20 µl containing 1 µl cDNA, 10 µl 2X Biomix™ Red (Bioline Reagents Ltd, UK), 50 pmol oligo-nucleotide primers (Eurofins MWG, Ebersber, Germany), 0.125mM each of dGTP, dCTP, dATP and dATP and. The cDNA was standardised using primers for the housekeeping gene ACT8 (Table 2.3).

Table 2.3: Primer sequences of RT-PCR for transcript abundance of T-DNA insertion lines.

Name	Gene	Forward Primer (5'→3')	Reverse Primer (5'→3')
PHC1-1	At1g22480	ACC GAC TAC ACT CCG CTC AC	TCG TGA GAG CTA TGG TCG TG
PHC3-1	At1g72230	CCC ATT CTT ACG GTG TAG CAA	GCA GGT GCA AAC ACA TTG AA
ACT8	At1g49240	GCC ATC CAA GCT GTT CTC TC	ACC CTC GTA GAT TGG CAC AG

Table 2.4: Primer sequences of RT-PCR for transcript abundance of amiRNA overexpressor lines

Name	Gene	Forward Primer (5'→3')	Reverse Primer (5'→3')
PHC1	At1g22480	ACC GAC TAC ACT CCG CTC AC	GTA GCA ACC AAA GCC CGT AA
PHC2	At5g20230	CGT TTC TTG TTT TGG TTT TC	CAA ATG CAG CTT CTG ATA CA
PHC3	At1g72230	GTT GGC TAC CGG AAA GTC CT	TCA CAA CCA AAG CAT CCA AC

2.8 amiRNA Design

amiRNA design was employed by the Web MicroRNA Designer tool (Schwab et al., 2006). The sequences are shown in Table 2.5. (Eurofins MWG, Ebersberg, Germany). The amiRNA sequences were introduced into the miR319a precursor via site-directed mutagenesis. Using plasmid pRS300 that contains the amiRNA precursor as a template, overlapping PCR was performed with the primers depicted in Table 2.6. For reactions 1,2 and 3, (Table 2.6) (Schwab, 2005) separate PCR reactions in a volume of 50 µl containing 1x AccuBuffer (60 mM Tris-HCl, 6 mM $(NH_4)_2SO_4$, 10mM $MgSO_4$) (Bioline Reagents Ltd, UK), 50 pmol oligo-nucleotide primers (Eurofins MWG, Ebersber, Germany), 0.125mM each of dGTP, dCTP, dATP and dATP and 2.5 u high fidelity DNA polymerase. PCR programme were run at: 95°C, 2 min; for 24 cycles 95°C, 30 sec; 55°C, 30 sec (lower temp to 53°C for reaction 2); 72°C, 40 sec; a final extension at 72°C, 7 min and hold at 8°C. Reaction d consisted of the same concentrations of reagents and with a 50 µl reaction with the following programme: 95°C, 2 min; for 24 cycles 95°C, 30 sec; 55°C, 30 sec; 72°C, 1.5 min; a final extension at 72°C, 7 min and hold at 8°C.

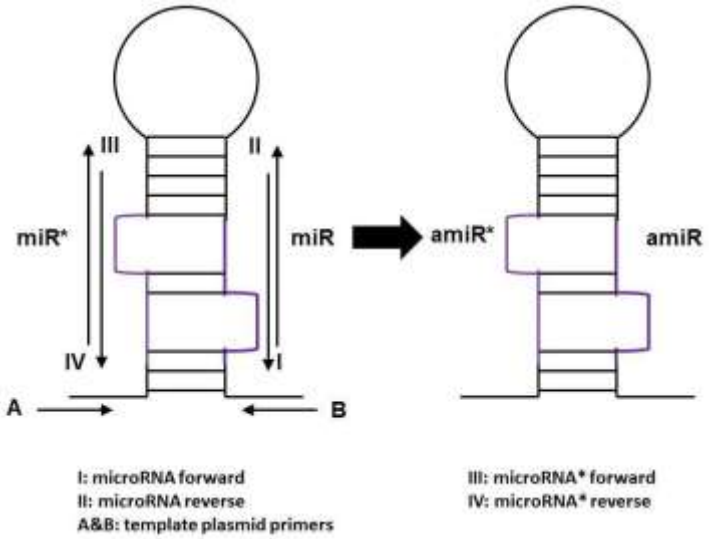

Figure 2.2: Engineering of amiRNA. This was done by performing site-directed mutagenesis on precursors of endogenous miRNAs using overlapping PCR. Oligonucleotide primers I to IV (Table 2.6) were used to replace endogenous miR and miR* regions (purple) with artificial sequences (amiR* and amiR). Primers A and B (Table 2.6) were based on template plasmid sequence. A functional amiRNA precursors is generated by combining PCR products A-IV, II-III, and I-B in a single reaction with primers A and B (Schwab et al., 2005).

Table 2.5: Primer sequences for overlapping PCR

Oligo	Sequence
I	TAAAGATAGTAAATGACCCCG
II	CGGGGTCATTTACTATCTTTA
III	CGAGGTCATTTACAATCTTTT
IV	AAAAGATTGTAAATGACCTCG
A	CTG CAA GGC GAT TAA GTT GGG TAA C
B	GCG GAT AAC AAT TTC ACA CAG GAA ACA G

Table 2.6 Primer Sequences and overlapping PCR strategy

Reaction	Forward Primer (5'→3')	Reverse Primer (5'→3')	Template
1	CTG CAA GGC GAT TAA GTT GGG TAA C	AAAAGATTGTAAATGACCTCG	pRS300
2	CGAGGTCATTTACAATCTTTT	CGGGGTCATTTACTATCTTTA	pRS301
3	TAAAGATAGTAAATGACCCCG	GCG GAT AAC AAT TTC ACA CAG GAA ACA G	pRS302
4	CTG CAA GGC GAT TAA GTT GGG TAA C	GCG GAT AAC AAT TTC ACA CAG GAA ACA G	1+2+3

2.9 Entry Clone Construction

To insert amiRNA fragment into a gateway cassette, p-ENTR dTOPO® (Life Technologies) cloning was employed. Prior to setting up the TOPO reaction, the PCR product (d) from amiRNA overlapping PCR was run on a 2% agarose gel, bands were excised and gel extracted using QIAquick Gel Extraction Kit according to manufacturer's guidelines (Qiagen). TOPO cloning was performed in a reaction consisting of 2 µl PCR product, 1 µl of salt solution, 1 µl recombinase enzyme and TOPO vector with sterile water added to a final volume of 6 µl. Reaction was incubated at room temperature overnight. Entry clone construction of GFP tagged PHC1 was done without TOPO cloning because recombinase sites were added in the artificial synthesis of the gene. The synthesised gene was amplified by PCR in a 20 µl reaction containing 1 µl synthesised gene 1x AccuBuffer™ (60 mM Tris-HCl, 6 mM $(NH_4)_2SO_4$, 10mM $MgSO_4$) (Bioline Reagents Ltd, UK), 50 pmol M13 oligo-nucleotide primers (Eurofins MWG, Ebersber, Germany), 0.125mM each of dGTP, dCTP, dATP and dATP and 2.5 u high fidelity Accuzyme™ DNA polymerase (Bioline Reagents Ltd. UK). PCR was perfomed with the following programme: 94°C, 2 min; for 34 cycles 94°C, 30 sec; 55°C, 30 sec; 72°C, 1 min; and a final extension step of 72°C, 7 min and a hold at 8°C. The PCR product was then placed into an entry clone plasmid pDONR by Gateway® recombination reaction: 1 µl of PCR fragment, vector (pDONR/zeo), BP Clonase and 2 µl of sterile water. The reagents were added into a 1.5 ml Eppendorf tube and incubated at RT overnight. For subsequent construction of entry clones with GFP at N and C termini, phc1-pDONR plasmids were digested with XbaI or SpeI, treated with shrimp alkaline phosphatase. Concomitantly, a GFP containing plasmid (RM16) was also digested with XbaI, run on 1% agarose gel and the smaller fragment was excised and gel extracted using QIAquick Gel Extraction Kit (Qiagen) according to manufacturer's guidelines. phc1 and RM16 fragments were ligated in a 10 µl reaction with 1x ligase buffer, 2 µl phc1, 6 µl RM16, and 1 µl DNA ligase. The reaction was incubated at RT for 30 min and transformed into competent *E. coli* (Agilent Technologies). XbaI and SpeI digested fragments oriented GFP at the N or C terminus during ligation respectively. Entry clones with GFP at the N or C terminus were named NGFPphc1 and phc1CGFP respectively. Restriction digest with BamHI and AvaI (Fermentas) of the entry clone was performed to check presence of insert and correct orientation (see Figure 2.3).

2.10 Transformation of Entry Clones into Competent *E. coli*

6 µl of phc1-c-pDONR, phc1-d-pDONR and phc2-1-pENTR were separately added to 70 µl of chemically competent *E. coli* DH5α *(*Agilent Technologies) into a 1.5 ml Eppendorf tubes. The solution was incubated on ice for 10 min, followed by heat shock treatment of the cells at 42°C for 1 min. The tubes were transferred on ice immediately followed by the addition of 250 µl RT Luria Bertani medium (Table 2.7) (Bertani, 2004) (Sigma Aldrich). Tubes were shaken at 150 rpm at 37°C for 1 hour and 100 µl of the transformation was spread onto Zeocin plates for phc1-c-pDONR, phc1-d-pDONR and Kanamycin plates for phc2-pENTR and incubated at 37°C overnight.

Table 2.7: Luria Bertani Broth components

Components	Concentration (g/L)
Tryptone	10.0
Yeast Extract	5.0
NaCl	5.0

2.11 Analysis of Transformants by PCR

Positive colonies were picked from the plate, cultured in Falcon 12 ml tubes with 5 ml LB medium (Table 2.8) and 50 µg/µl Zeocin or Kanamycin for pDONR and pENTR plasmid vectors. Culture PCR was subsequently performed in a 20 µl reaction consisting of 1x Biomix™ Red, 50 pmol of M13 oligonucleotides (Eurofins MWG, Ebersberg, Germany), and 1 µl of bacterial culture. PCR parameters were performed as follows: 94°C, 2 min; for 34 cycles 94°C, 30 sec; 55°C, 30 sec; 72°C, 1 min; a final extension at 72°C for 7 min and hold at 8°C. PCR reactions were visualised in 1% agarose gels. Positve colonies were selected for plasmid extraction using QIAprep Spin Miniprep Kit (Qiagen, Crawley, UK) according to manufacturer's guidelines. Once correct clones were identified, constructs were sent for sequencing (GATC Biotech AG, Konstanz, Germany).

2.12 Gateway Transformation of Entry Clone to Destination Vector

Purified PHC1:GFP and amiRNAphc2-1 entry clones from section 2.2.2 were transferred to a destination clones. PHC1:GFP was added to p3HC and pB2GW7 and amiRNAphc2-1 to p3HC using Gateway transformation (Life Technologies) using Gateway LR Clonase II Enzyme mix. The p3HC destination

clone is a 12652 bp plasmid with multiple cloning sites, site-specific recombinases, irx3 inducible promoter and antibiotic resistance for Kanamycin, Gentamycin and Hygromycin; (Gift from Manoj Kumar) and pB2GW7 is a 10882 bp plasmid with multiple cloning sites and antibiotic resistance for Spectinomycin, Gentamycin and Glufosinate (BASTA™). To perform the LR recombination reaction, 2 µl each of LR Clonase II and destination vector (p3HC), 1 µl of the entry clone and 3 µl of sterile H_2O were mixed in a 0.5 ml Eppendorf tube. The reaction was incubated at RT overnight and transformed into competent *E. coli* cells DH5α (Agilent Technologies) using Kanamycin/Gentamycin to select positive colonies (see Figure 2.3).

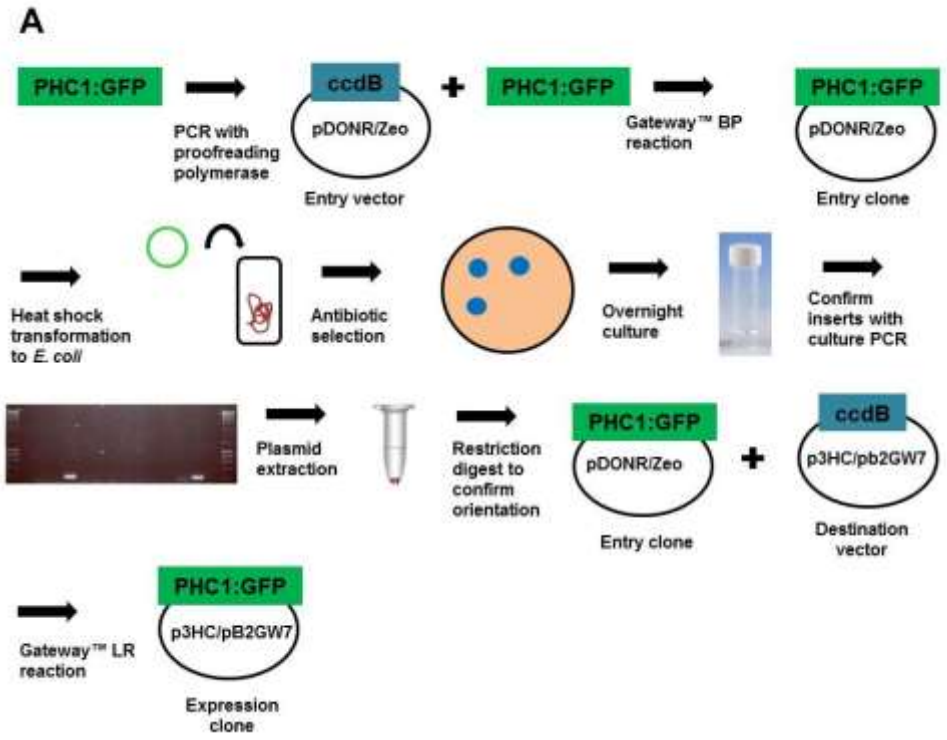

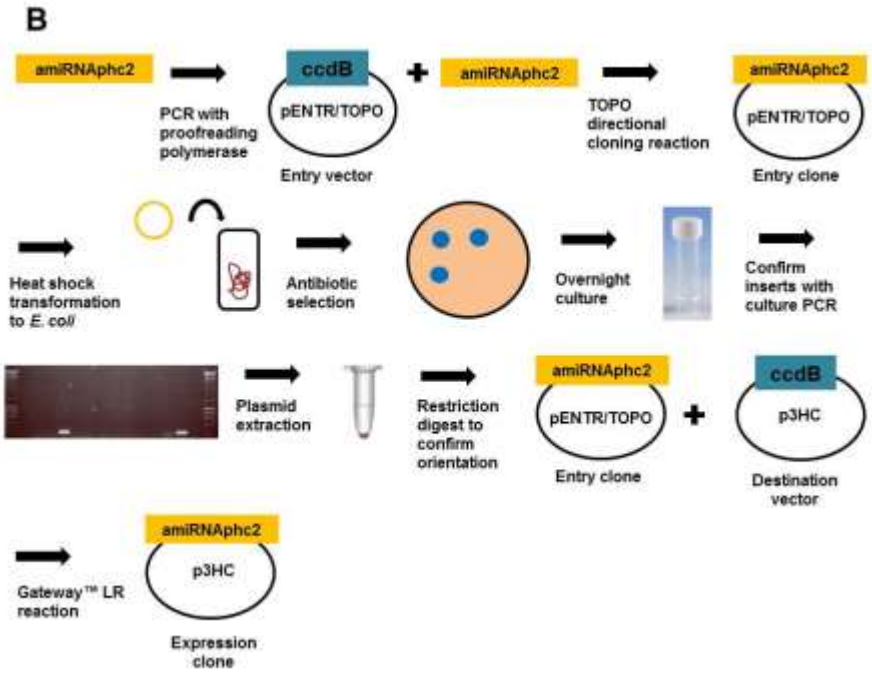

Figure 2.3: Summary of cloning method for PHC1:GFP and amiRNAphc2-1. A: PHC1:GFP cloning into expression clone using Gateway™ BP reactions to generate an entry clone and subsequent Gateway™ LR reactions to clone PHC1:GFP into p3HC and pB2GW7 vectors B) amiRNAphc2-1 cloning into expression clone using TOPO™ directional cloning and subsequent Gateway™ LR reactions to clone PHC1:GFP into p3HC vector

2.13 Transformation of Destination Vector to Electrocompetent *Agrobacterium tumefaciens*

Agrobacterium transformation was carried out according to Weigel and Glazebrook (2006) with modifications in the conditions (Peter Etchells, personal communication). 1 µl of destination vector plasmid and 50 µl electrocompetent *Agrobacterium tumefaciens* GV 3101 were placed in a pre-chilled Gene Pulser® 0.2cm electrode cuvette (Biorad) and incubated on ice for 10 minutes. The cuvette was then placed on the Gene Pulser (Biorad) and electroporated with the following conditions: capacitance, 25 µF; voltage, 2.5 kV; resistance, 600Ω; and a pulse length of 13 miliseconds. Transformed cells were then incubated in 1 ml LB broth at 30°C for 1 hour and subsequently transferred to 300 ml LB broth with 50 µg/µl Kanamycin and Gentamycin.

2.14 Plant Transformation of *Agrobacterium tumefaciens* by Floral Dipping Method

Transgenic plants were generated by by floral dipping (Clough and Bent, 1998). T1 seeds were harvested and plated on ½ MS media with Hygromycin (50 µg/µl). T1 plants positive for Hygromycin resistance were selected and used for subsequent analyses.

2.15 Histochemical Analysis

Hand hand cut cross section of stems were taken from the base of the stems when the plants reached a height of 25-30cm with and age of 4-6 weeks and stained with 0.05% toluidine blue O for 5 minutes (pH 4.5) or Mäule's stain. For the Mäule stain sections were fixed in 5% glutaraldehyde for 1 hour at RT, washed briefly in water followed by incubation in 0.5% $KMnO_4$ for 10 min, washed briefly in water, incubated in 10% HCl for 5 min, washed briefly with water and mounted in concentrated 30% NH_4OH. Sections were observed under bright field illumination using a DMR (Leica) microscope.

2.16 Fluorescence Microscopy of GFP lines

T3 selected lines were grown on ½ MS plates as described in section 2.2.1 with Hygromycin selection of a final concentration of 50 µg/µl. The roots of one week old seedlings were then visualised using a DMR microscope (Leica) with an eGFP filter and UV light source under 63x water objective and photographed with a SPOT Xplorer 4MP camera (Diagnostic Instruments).

2.17 Confocal Microscopy of GFP Lines

T4 lines exhibiting high intensity fluorescence were selected for confocal microscopy with a 63x water objective and sample preparation as described in section 4.2.5. Samples were visualised under a TCS SP5 confocal microscope (Leica) with an argon ion laser and an eGFP filter excited at 488 nm and fluorescence acquired in the range of 500–560 nm using a 63x objective.

2.18 FTIR Sample Preparation and Analysis

Deionised H_2O was added to the milled sample from section 2.1 to a final concentration of 50 µg/ µl. 5 µl of each sample was loaded on top of a silicon plate making sure the plant cell wall sample is evenly distributed and left to air dry. For FTIR analysis, a Bruker IFS28 spectrometer (Bruker Spectrospin Ltd, Coventry, UK) with a mercury-cadmium-telluride (MCT) detector was used. The spectra were collected as described by Brown (2005). The wave number range was 4000cm^{-1} to 600cm^{-1}; acquired at a rate of 20s^{-1} and a resolution of 4cm^{-1}.

FTIR data was then normalised such that the total area was equal to one. The data was then analysed with Principal Component Analysis (PCA) using Matlab 8.1 (The MathWorks Inc., Natick, USA). Principal components extrapolated were then subjected to Discriminant Functional Analysis with a priori knowledge of the replicate structure from the data set as directed.

Chapter 3: Results

3.1 Identification of Arabidopsis Phytocyanins Candidates Involved in Secondary Walls Using Coexpression and Phylogenetic Analysis

3.1.1 Phytocyanin Genes are highly coexpressed with the secondary cell wall gene IRX3

To determine whether phytocyanins have a putative role in secondary cell wall synthesis, a known secondary cell wall gene irx3 was chosen as the bait gene for co-expression analyses (Taylor et al., 1999). The AtGenExpress software plots selected genes on a graph to show raw expression values of these genes across a selection of available microarrays. Figure 3.1.1A represents all phytocyanins plotted against irx3. Due to the number of phytocyanin genes plotted, it was confusing to clearly see which genes were coexpressed against irx3. therefore, each of the phytocyanin genes was then individually plotted against irx3 for a more comprehensible visualisation of coexpression (3.1.1 B). Phytocyanin genes highly coexpressed with irx3 and that displayed a high degree of sequence homology from phylogenetic analysis software (At1g22480 and At1g72230) were given high priority for further analysis. Other genes that had moderate levels of coexpression and/or close sequence similarity with these two genes, such as At5g20230, were also selected for further study. The coexpression of At1g22480 and At1g72230 have previously been observed in other expression profiling studies on secondary cell wall deposition by Kubo et al. (2005), Ehlting et al. (2005), and Brady et al., (2007). Additionally, studies by Mutwil et al. (2008) applied the Rosetta tool from geneCAT to compare coexpression lists to determine functional conservation within these genes (Table 3.1.1) and concluded that At1g22480 and At1g72230 displayed highly coordinated transcription with irx3 during secondary cell wall biosynthesis and with several laccases genes. Similar trends were observed with expression profiles of the candidate genes in geneCAT (data not shown). At5g07475 however, had no coexpression data in any of the publicly available arrays. It was therefore chosen because it could display interesting mutant phenotypes. A summary of the candidate phytocyanin genes are their relative coexpression with irx3 are summarised in Table 3.1.2.

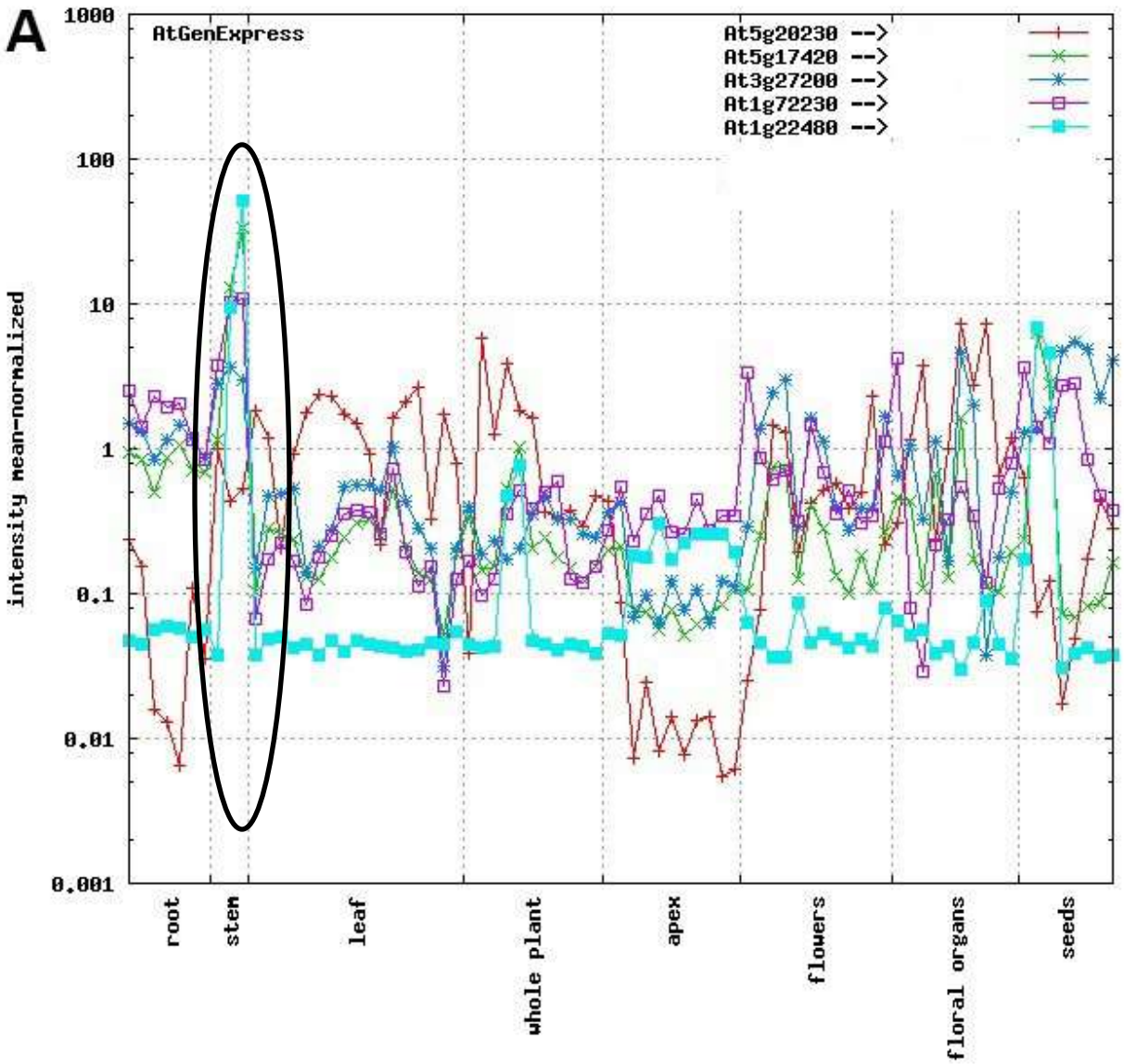
A
AtGenExpress
At5g20230 -->
At5g17420 -->
At3g27200 -->
At1g72230 -->
At1g22480 -->
intensity mean-normalized
1000
100
10
1
0.1
0.01
0.001
root
stem
leaf
whole plant
apex
flowers
floral organs
seeds

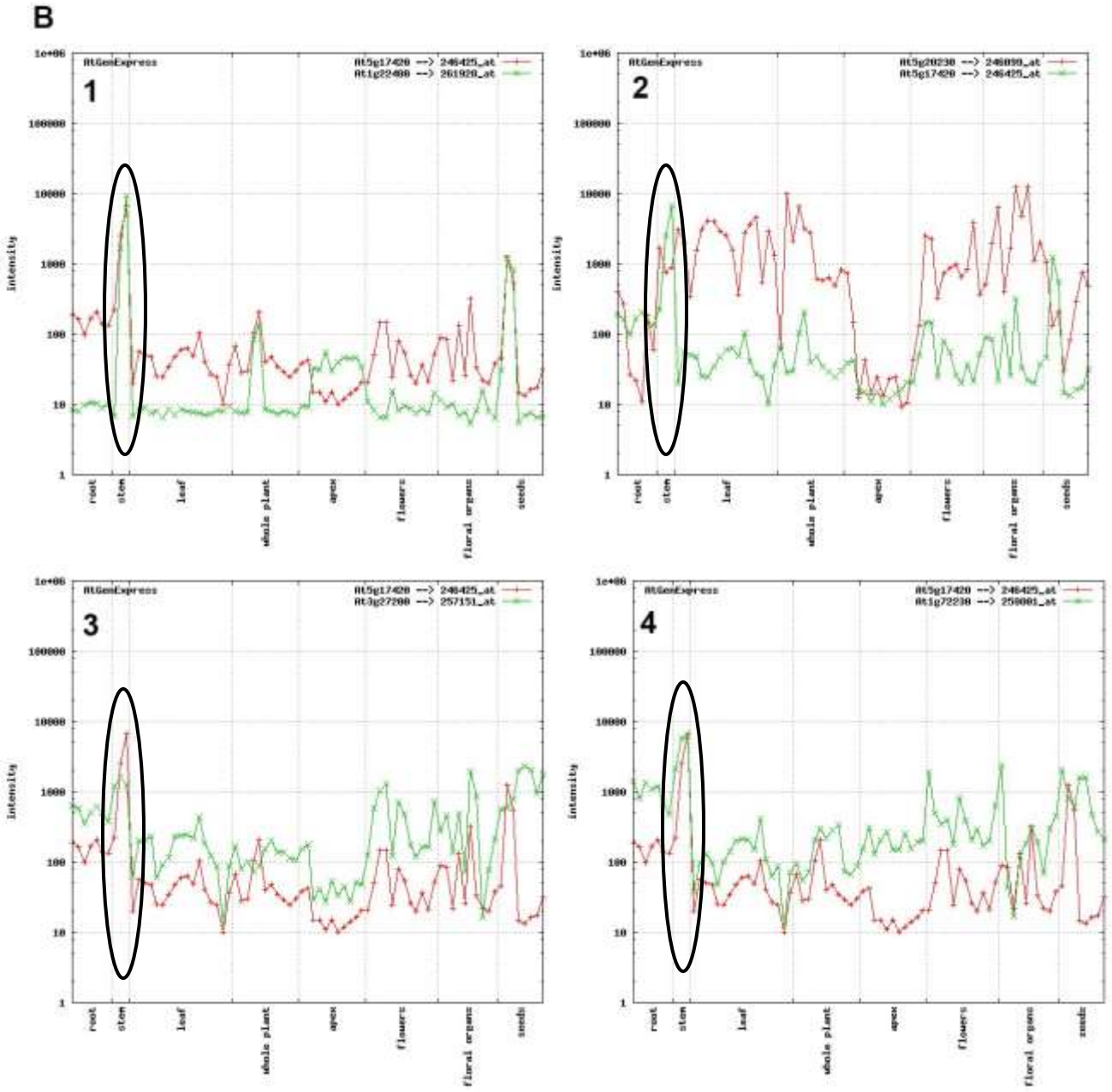

Figure 3.1.1: Coexpresion plot of AtGenExpress. A represents all phytocyanin genes plotted alongside irx3. B represents candidate phytocyanin genes (green) similar to A but plotted against irx3 (red) individually 1: At1g22480, 2: At5g20230, 3: At3g27200, 4:At1g72230. Circles represent signal intensity secondary cell wall of stem tissue. Circles depict signal intensity at secondary cell walls of stem tissues (Schmid et al., 2005).

Table 3.1.1: Rosetta analysis of coexpressed genes with IRX5. Coexpression level is at a descending order with the top corresponding to most similarly coexpressed with the target gene (Adapted from Mutwil et al., 2008). Phytocyanin genes are highlighted in yellow.

Target 1: At5g44030
At5g17420 cellulose synthase AtCesA7
At5g44030 cellulose synthase AtCesA4
At4g18780 cellulose synthase AtCesA8
At5g15630 COBRA-like 4
At3g16920 CTL2
At1g19940 glycosyl hydrolase family 9 protein
At2g28760 NAD-dependent epimerase/dehydratase
At5g59290 UDP-glucuronic acid decarboxylase (UXS3)
At5g26330 plastocyanin-like domain-containing protein
At3g27200 plastocyanin-like domain-containing protein
At1g72230 plastocyanin-like domain-containing protein
At1g22480 plastocyanin-like domain-containing protein
At3g15050 calmodulin-binding family protein
At3g42950 glycoside hydrolase family 28 protein
At1g80170 polygalacturonase, putative
At3g45870 integral membrane family protein/nodulin
At4g27435 expressed protein
At5g03260 laccase, putative
At2g38080 laccase, putative
At5g01190 similar to laccase
At5g05390 laccase, putative
At2g29130 laccase, putative
At5g60020 laccase, putative

Table 3.1.2 Summary of candidate phytocyanin genes coexpressed with irx3

Gene	Level of Co-expression With irx3
At1g22480	High
At5g20230	Moderate-Low
At1g72230	Moderate-High
At5g07475	N/A
At3g27200	Moderate

3.1.2 Phylogenetic Tree of Phytocyanins

The phylogenetic analysis provided by Phytozome (Figure 3.1.2) was used to create a cladogram based on homology of the whole protein sequence including the cupredoxin domain of the phytocyanin gene family. The genes that were selected for subsequent analysis are based on their coexpression with irx3 using AtGenExpress software (as described above) and also whether their sequences were similar deduced from the cladogram. The phylogenetic analysis using ClustalX also showed similar relationships and similar groupings of the phytocyanin genes i.e. At1g22480 with At1g72230 and both somewhat with At5g20230. At5g07475 and At3g27200 also clustered together but were distantly related to At1g22480, At1g72230 and At5g20230. The check the validity of the clustering of these genes, ClustalX another phylogenetic analysis programme was used. Similar patterns of phyotcyanin gene homology were also observed (Figure 3.1.3) even with the addition of plastocyanin (a member of the cupredoxins). Therefore, these genes possibly share similarity of function based on coexpression with irx3 and homology. Members of the phytocyanin family selected for further analysis were abbreviated as PHC for convenience (Table 3.1.3)

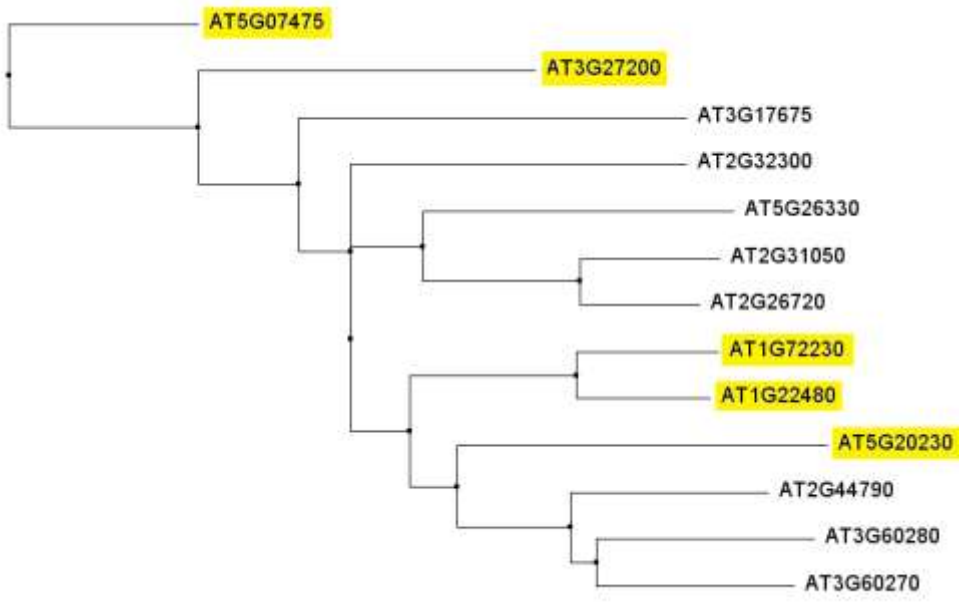

Figure 3.1.2: Phylogenetic analysis of phytocyanins using the Phytozome programme. Candidate genes are highlighted in yellow.

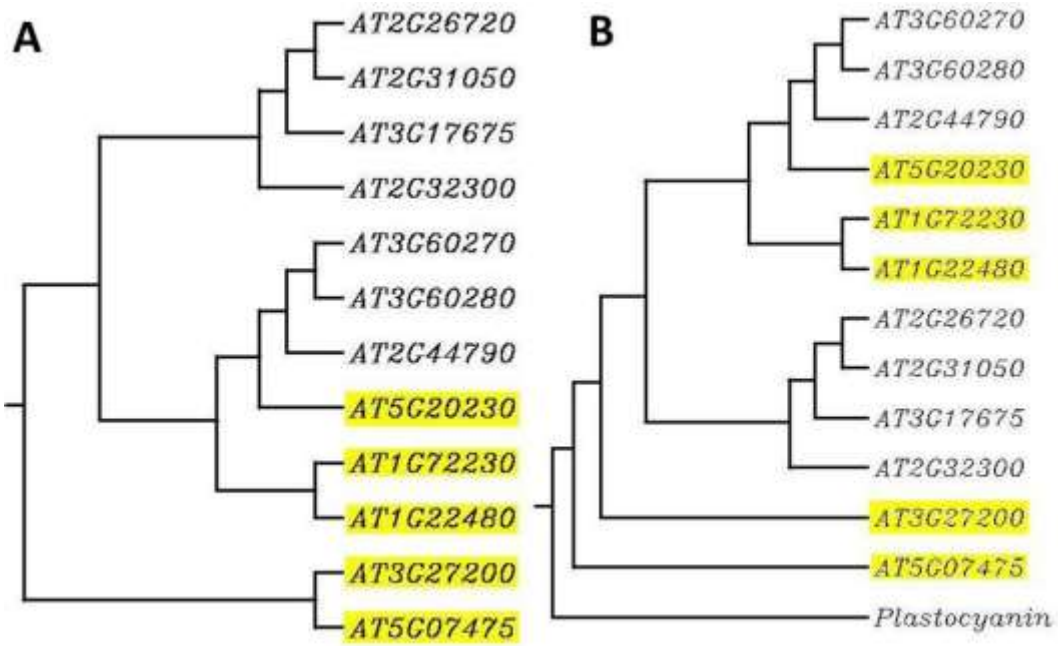

Figure 3.1.3: Phylogenetic analysis of phytocyanins using Clustal. Candidate genes are highlighted in yellow. Sequence similarities with (A) and without (B) plastocyanin comparison.

Table 3.1.3: Abbreviation of phytocyanin candidate genes

Gene	Abbreviation
At1g22480	PHC1
At5g20230	PHC2
At1g72230	PHC3
At5g07475	PHC4
At3g27200	PHC5

3.2 Molecular Characterisation of Phytocyanin T-DNA Insertions Mutants and the Production of *phc1* and *phc3* Double Mutants

3.2.1 Identification of T-DNA Insertions via the SIGnaL Database

To identify gene function using reverse genetics, T-DNA inserts were used. The SIGnaL database (http://signal.salk.edu) (Alonso et al., 2003) was employed to identify T-DNA insertion lines likely to disrupt those genes chosen for analysis. Insertions that occurred within exons early in the gene or within the first 300b of the 5' non coding region were preferentially selected. Insertions in the intron were also used when no other insertions were available (Table 3.2.1).

Table 3.2.1: Candidate phytocyanins and their T-DNA inserts used in this study

Gene Name	Gene Accession No.	T-DNA Insertion	Mutant name	Insertion position
PHC1	At1g22480	SAIL_381_C11	phc1-1	Intron
PHC2	At5g20230	SALKseq_60215	phc2-2	Exon
PHC3	At1g72230	SALK_083847	phc3-1	5'-UTR
		SALK_201823	phc3-2	Exon
PHC4	At5g07475	SAIL_582_G03	phc4-1	Exon
PHC5	At3g27200	SALK_053270	phc5-1	Exon

3.2.2 PCR Genotyping of T-DNA Insertion Lines

Plants were genotyped by PCR as described in the SIGnaL database (Alonso et al., 2003) to identify whether or not plants were homozygous, heterozygous or wild-type for a specific insertion. Primer sequences are shown in Table 2.2. Screening was done with 5-8 plants and a wild-type (WT) control using gene specific and LBb1 primers. Therefore, the genotype of the plant can be determined by the size and/or number of bands seen on an agarose gel. WT plants contain a single band at ~900bp and homozygous mutants contains smaller sized bands at ~500bp. Heterozygous plants contain both the WT and the mutant bands. Screening for single mutants revealed the presence of at least one mutant band for all lines and their seeds were collected for subsequent histochemical analysis and plant crossing (Figure 3.2.2). Homozygous lines were also verified in the double mutants generated from crossing phc1-1 with phc3-1 and phc1-1 with phc3-2; T2 lines were screened for homozygous inserts similar to PCR genotyping methods from single mutants (Figure 3.2.3).

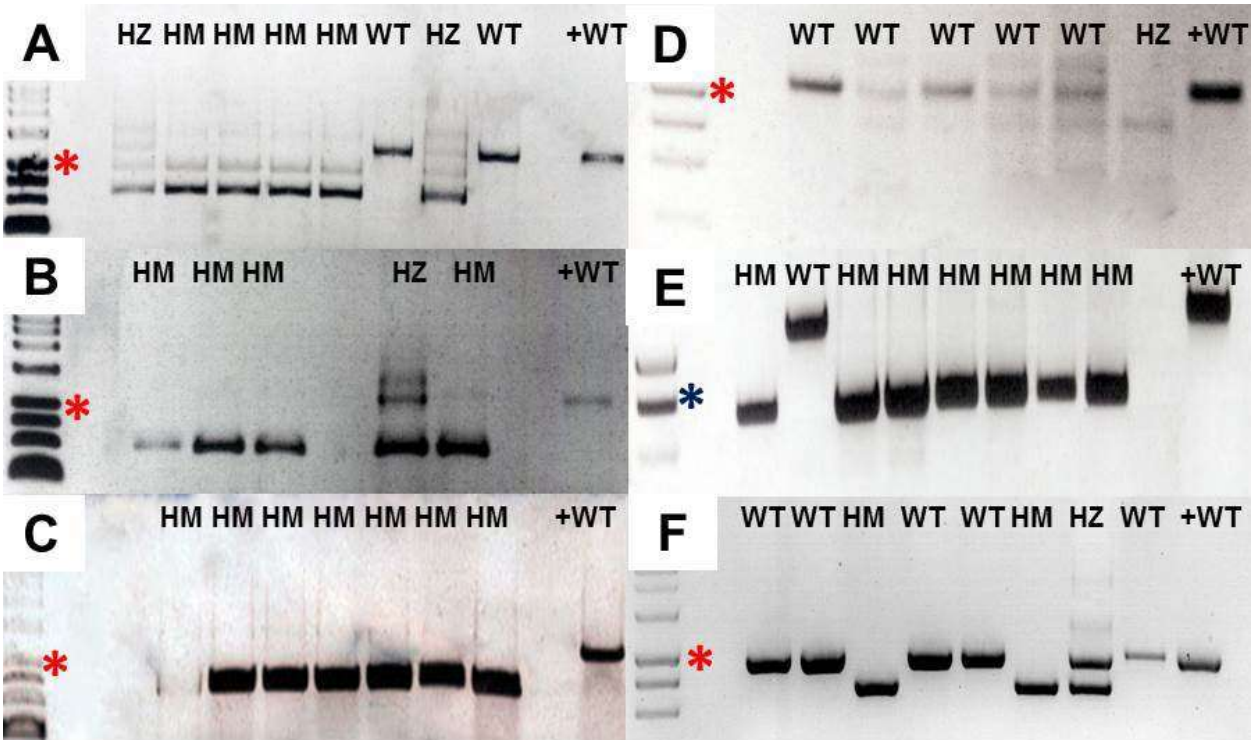

Figure 3.2.1: Agarose gel electrophoresis of PCR screening of single T-DNA insertion lines. Every well is derived from an individual plant that was genotyped with flanking and left border primers. The first lane is a DNA ladder (Hyperladder I, Bioline Reagents Ltd, UK) with red asterisks indicating 1kb band and blue asterisk indicating 600bp band. HM, HZ, WT and +C represent, homozygous mutant, heterozygous, wild type homozygous and positive control respectively. Primers used: A: SALK_083847, B: SAIL_381_C11, C: SALK_201823, D: SALK_053270, E: SAIL_582_G03, F: SALKseq_60215

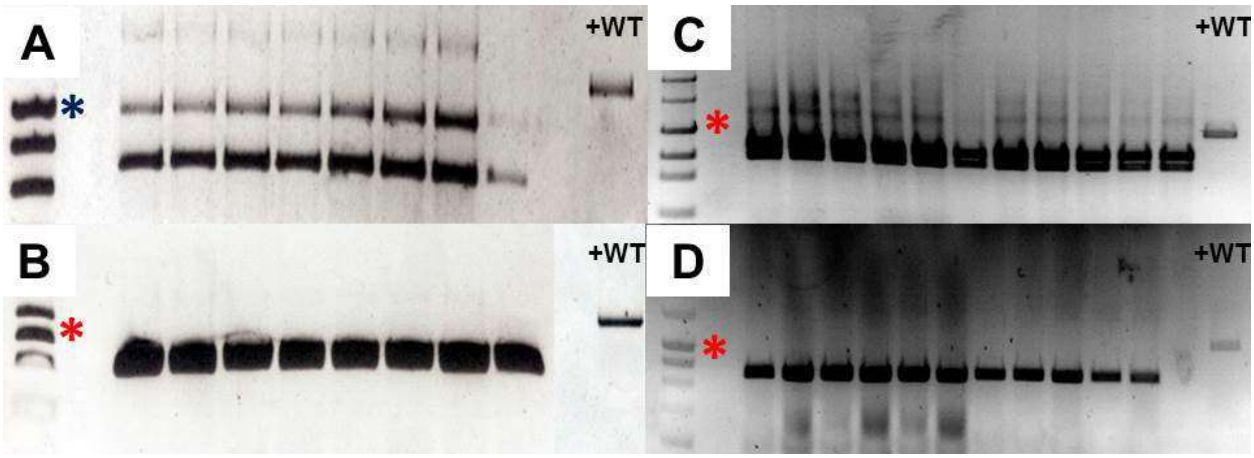

Figure 3.2.2: Agarose gel electrophoresis of PCR of double T-DNA insertion lines. Each lane is derived from a single line with every well signifying an individual plants containing SAIL_381_C11 together with either SALK_083847 or SALK_201823 that were genotyped with flanking and left border primers. The first lane is a DNA marker (Hyperladder I, Bioline Reagents Ltd, UK) with red asterisks indicating 1kb band and blue asterisk indicating 800bp band.. +WT represents WT control. Primers used were: A: SALK_083847, C: SALK_201823 B & D: SAIL_381_C11.

3.2.3 Transcript Abundance of Candidate Genes

To verify the effect of T-DNA insertion on mRNA expression of the candidate genes, real-time (RT-PCR) was performed with gene specific primers designed to be close to the T-DNA inserts in exon or 5' untranslated regions and the adjacent exons region nearest intronic inserts (Figure . RT-PCR confirmed that in the single mutant *phc3-1,* transcript levels for the phc1 gene were severely down regulated. The gene appeared to be more severely down-regulated in- the *phc1-1 phc3-1* double mutant (Figure 3.2.3). This variation could be due to lack of specificity of the primers or just error within the experiment. Both results however are consistent with severe down-regulation of the phc1 gene, but not a complete knockout. No transcript was detectable in the *phc3-1* mutant suggesting the T-insertion gives a complete knockout. For *phc2-2* and *phc3-2*, transcript abundance was not determined as their insertion positions were located at an exon. Insertions in an exon are effective in that only 1.1% shows no effects in transcript level and 0% increased transcript level. Therefore inserts at an exon empirically show a 98.9% chance of knockout/knockdown effects (Wang et al., 2008).

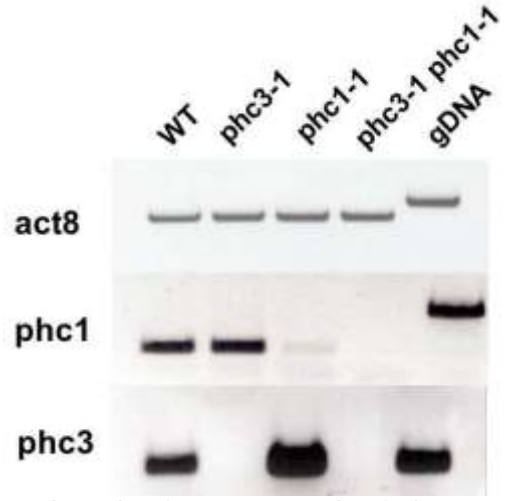

Figure 3.2.3: Agarose gel electrophoresis of RT-PCR study of phytocyanin transcript expression levels. Labelling on the tope indicated the genotypes used and the gene-specific primers used indicated on the left hand side.

3.2.4 Whole Plant Phenotype

In terms of whole plant phenotype (Figure 3.2.4), mutants displayed qualities comparable to wild type. Overall, plant morphology appeared normal and no significant alteration in leaf pigmentation or mature rosette diameter was observed. Their anatomical features and developmental processes such as

presence of inflorescences, siliques and seed formation were similar to wild-type plants. In terms of plant height, certain mutant lines appear shorter than the wild-type. However, there are certain inconsistencies. The double mutant (*phc1-1 phc3-1)* that contains a T-DNA insertion in the 5' UTR of PHC3 (phc3-1) appears considerably shorter that the WT, while the double mutant (*phc1-1 phc3-2*) with a T-DNA insert at the exon of PHC3 (*phc3-2*) appears to have a height comparable to wild-type. This meant that there is a need for further checking of plant heights with a larger sample size to determine if there is any decrease in height that is statistically significant.

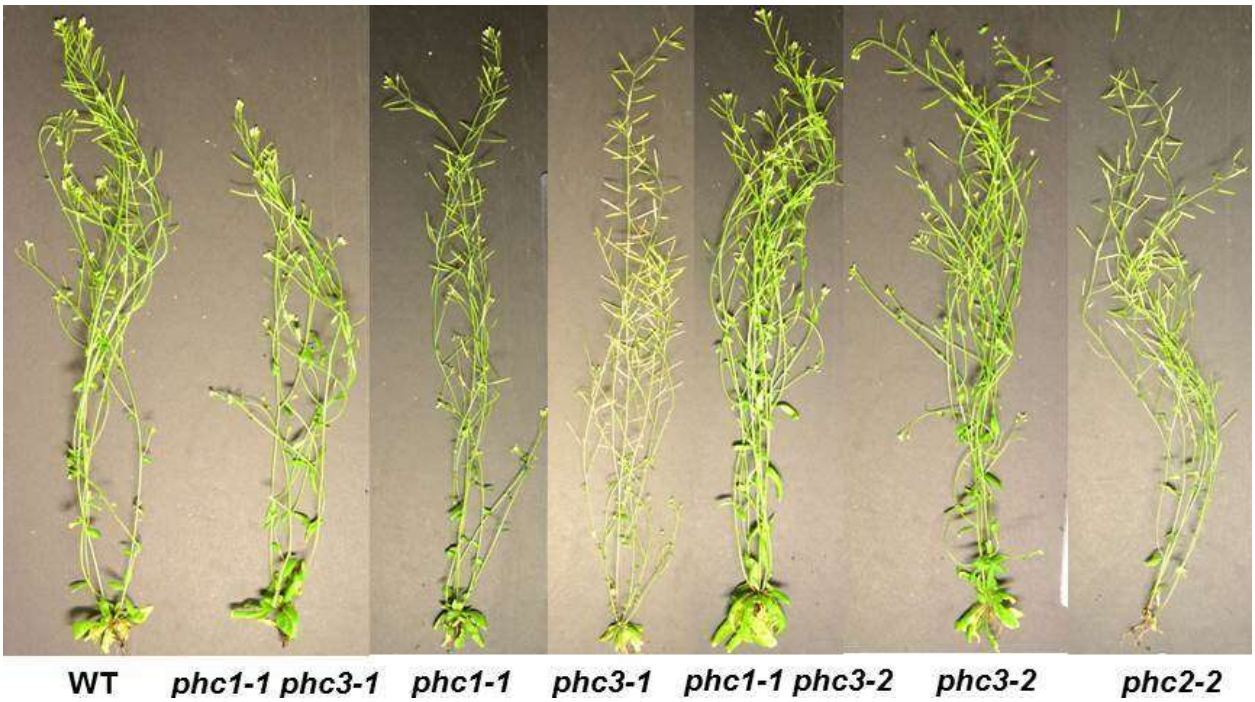

Figure 3.2.4: Whole plant phenotype of lines with insertion in phytocyanin genes. Samples are a representative of a pool of 15.

3.2.5 Xylem Phenotype

Stem histology from hand sectioning from the base of the mature *Arabidopsis* stem is used for determining stem organisation and cell morphology. This method is also applicable for identifying secondary cell wall mutants that exhibit collapsing xylem vessels as a consequence of a secondary cell wall defect caused by decreased deposition in cellulose (Turner and Somerville, 1997), lignin or xylan (Jones et al., 2001; Brown et al., 2007). The use of toluidine blue O gives excellent colour contrast in

vascular tissues to discriminate plant stem morphologies (i.e. xylem vessels and fibres, phloem, cortex and epidermis). Differential staining can also give some indication of the biochemical composition. Simple colour changes or absence of stain can confirm the presence of biochemical compounds and their composition. One such chemical is Mäule staining for lignin. Stem tissues composed primarily of S lignin appear bright red and those with a mixed S/G compositions appear dark red to brown depending on the ratio (more G lignin appear brown). Therefore, Mäule staining can provide a quick assay to determine any changes in lignin composition of phytocyanin mutants in comparison to the WT. No significant structural abnormalities or changes in biochemical composition can be observed in any of the mutants after sectioning and staining (Figure 3.2.5). Xylem vessels in all mutant lines appeared to be intact like the WT. Lignin composition also looked similar to WT such that fibres stained with Mäule's reagent appeared bright red and a tarnished brown in vessels indicative of typical lignin deposition patterns (Albersheim et al., 2011).

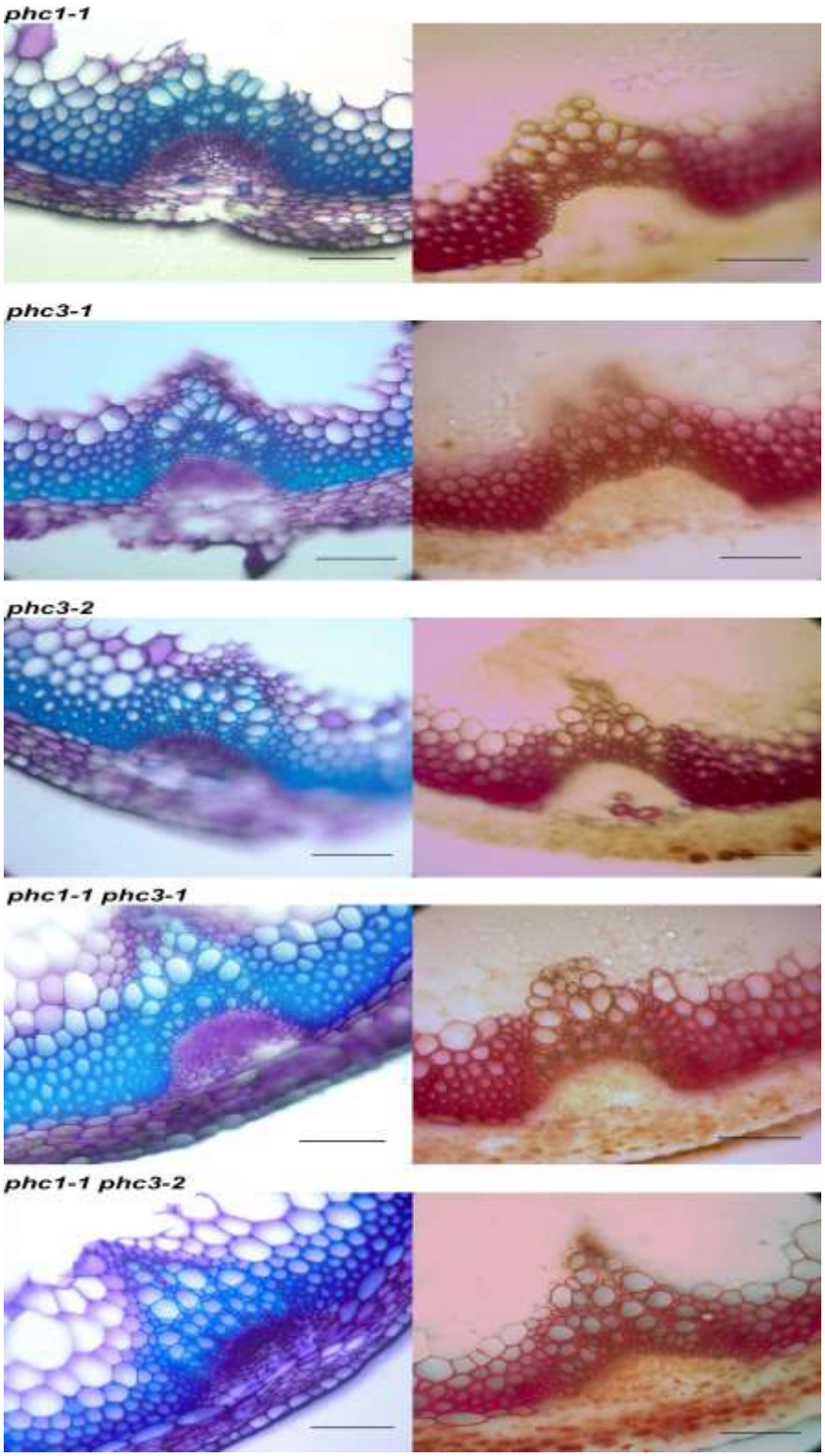

Figure 3.2.5 T-DNA inserts show no altered morphology or lignin composition. (A) Transverse Toluidine Blue-stained and (B) Mäule reagent-stained sections of vascular tissue from 8 week old inflorescence stems. Scale bars:10 µm.

3.3 Gene Silencing Effect of Artificial microRNA (amiRNA) Construct phc2-1 on WT and *phc1-1 phc3-1* Double Mutants

Artificial microRNAs (amiRNAs) are single-stranded 21mer RNAs, not found in plants but synthesised from endogenous miRNA precursors. They are designed based on parameters for plant miRNA target selection and the result is a 21mer with gene specific silencing. In *Arabidopsis*, the MIR319a miRNA precursor is used to synthesise amiRNAs by replacing the original miR319a (> the first 20 nts of the 21mer) with the artificial sequence (21mer). Similar to RNAi, amiRNAs also function in tissue-specific and inducible fashion. amiRNAs are a suitable substitute in circumstances where suitable T-DNA insertions are not available for reverse genetic studies.

The synthesised amiRNA gene was generated using overlapping PCR as mentioned in section 2.9. The constructs were then placed into entry vectors by TOPO directional cloning and were then cloned into the destination vector p3HC which is a binary vector and contains an irx3 promoter. Once the expression clone pIRX3::amiRNAphc2-1 was generated (Figure 3.3.1) it was transformed into *Arabidopsis* seedlings for subsequent analysis

3.3.1 Assessment of Transcript Abundance by Real Time PCR (RT-PCR)

Several T1 lines in which the pIRX3::amiRNAphc2-1 construct was transformed in to the wild type were screened for effective silencing of the phc2 gene. Comparing the transcript levels of several lines with a wild type control using RT-PCR showed that lines that exhibited effective silencing of phc2 were selected for further analysis (Figure 3.3.2). Figure 3.3.2 show that levels of transcripts in individual transformants vary from no perceptible change to subtle and complete silencing. Near silenced and silenced transformants from the RT-PCR analysis (Figure 3.3.2, lanes 7 and 8) were selected and their T2 progeny were chosen for histochemical analysis.

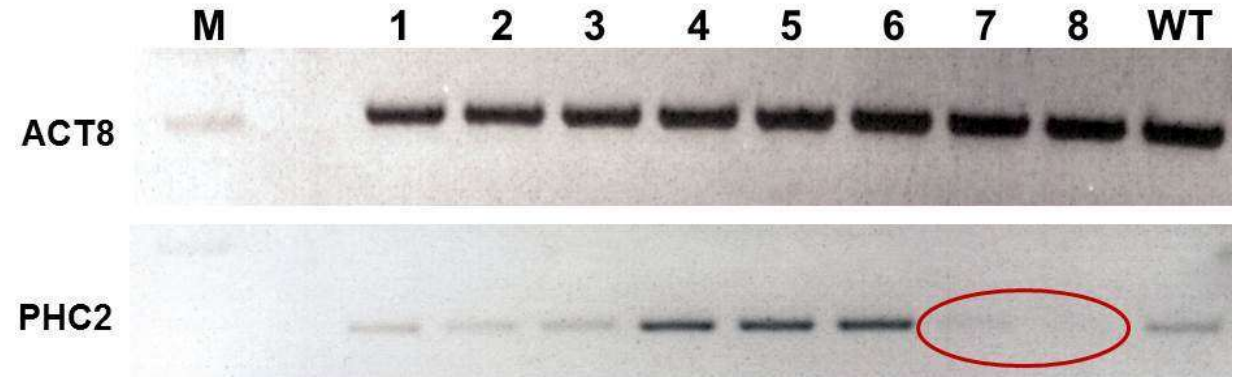

Figure 3.3.1: Analysis of gene silencing in T1 amiRNA-phc2-1 lines (WT background)with gene specific primers. Upper panel and lower panel represent RT-PCR reaction using ACT8 and PHC2 primers respectively. The red Circle depicts silenced lines picked for further analysis.

In order to probe for functional redundancy and in the interest of time, the pIRX3::amiRNAphc2-1 construct was also transformed into the phc1-1, phc3-1 double mutant and T1 lines screened for effective gene silencing of phc2. Several lines that appeared to exhibit severe down regulation of the phc gene were identified (Figure 3.3.1). Plants corresponding to lanes 3, 4 and 8 were chosen for further analysis as they showed effective gene silencing. T2 lines selected for analysis were subjected to histochemical analysis.

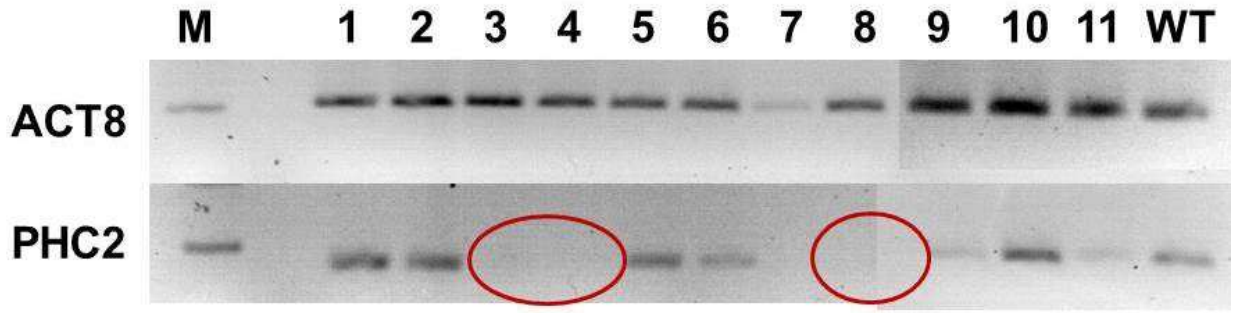

Figure 3.3.2 RT-PCR of amiRNAphc2-1 in *phc1-1 phc3-1* lines with gene specific primers for gene silencing analysis. Upper panel and lower panel represent RT-PCR reaction using ACT8 and PHC2 primers respectively. Red Circle depicts silenced lines picked for further analysis.

3.3.2 Xylem Phenotype

Cross sectioning of *Arabidopsis* stems from lines 7 & 8 for pIRX3::amiRNAphc2-1 in WT revealed mild and intermediate degrees of *irx* phenotype. Mäule staining revealed no real signal decrease in staining which may indicate unaltered lignin content. Xylem vessels however, displaying similar colouring as wild-type visually indicative of its canonical S/G ratio composition (Figure 3.3.3 B).

Selected T2 lines 3, 4 & 8 in which pIRX3::amiRNAphc2-1 was transformed into *phc1-1 phc3-1* were also subjected to histochemical analysis. Similar results were obtained to that of lines 7 & 8 pIRX3::amiRNAphc2-1 in WT; xylem vessels also appeared to exhibit the irx phenotype to a considerable degree. In the Mäule staining however, there appears to be a significant decrease in signal intensity which suggests a substantial decrease in lignin content. The decrease in signal intensity pIRX3::amiRNAphc2-1 transformed into *phc1-1 phc3-1* lines under Mäule staining may also have caused the loss of G subunit content from the reduction in brown colouring of xylem vessels observed (Figure 3.3.3 C).

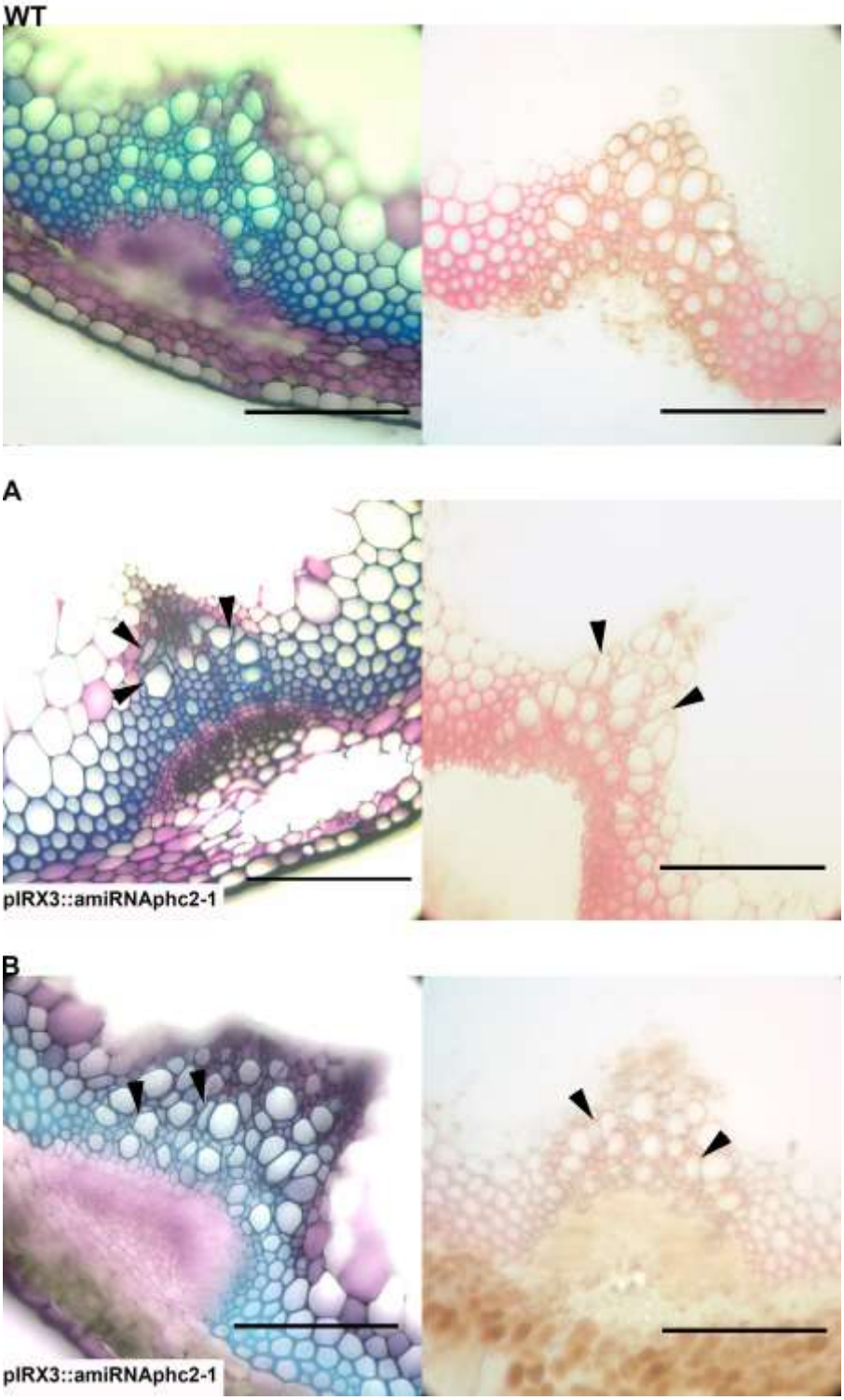

Figure 3.3.3: *amiRNAphc2-1* mutants show *irx* phenotype. Toluidine Blue-stained (left hand side) and Mäule reagent-stained (right hand side) transverse sections of vascular tissue from 8 week old inflorescence stems. (WT) Wild type control sections, (A) pIRX3:amiRNA2-1 transformed into wild-type and (B) pIRX3::amiRNA2-1 transformed into phc1-1 phc3-1 double mutant. Arrowheads indicate collapsed xylem. Scale bars: 20 µm. Sections are representative of a pool of 15 samples

3.3.3 Off Target Investigation Using Real Time PCR (RT-PCR)

Since pIRX3::amiRNA-phc2-1 transformed into wild-type produced a perceptible *irx* phenotype, it is possible the amiRNA construct generated by the WMD programme is silencing off-target genes and inadvertently creating a triple mutant instead of directly correlating *phc2-1* to the phenotype observed. To verify this, T2 plants from selected from confirmed for phc2-1 gene silencing lines were analysed using the same RT-PCR with phc1 and phc3 specific primers to evaluate off target effects of the amiRNA. Figure 3.3.4 shows that in certain lines, off target gene silencing was indeed observed. The encircled faint bands confirmed down regulation of off target genes in the amiRNA silenced line.

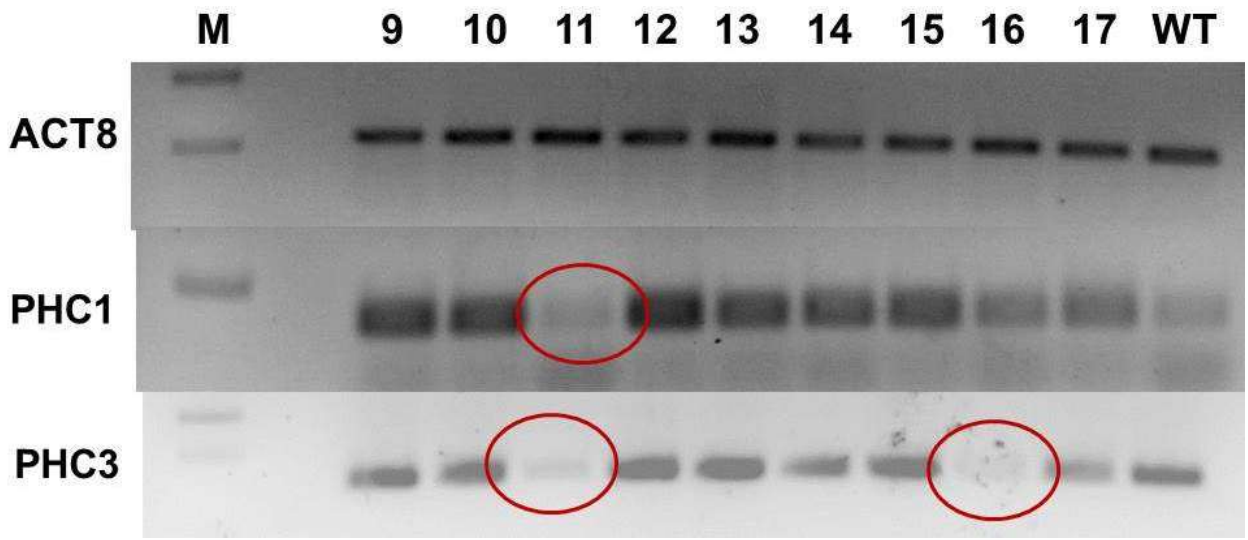

Figure 3.3.4: Off target analysis of T2 pIRX3::amiRNAphc2-1 line 8 transformed in WT by RT-PCR. Red circles depict confirmed downregulation of off target genes. Upper panel, middle panel and lower panel represent RT-PCR reaction using ACT8, PHC1, and PHC3 respectively. Regions highlighted with red circles depict lines that appear to exhibit off target downregulation.

3.3.4 Whole Plant Phenotype

Plant morphology of both WT and *phc1-1 phc3-1* amiRNA lines was comparable to wild type. No significant alteration in leaf pigmentation, mature rosette diameter, was observed. Their anatomical features and developmental processes i.e. presence of inflorescences, siliques and seed formation were similar to wild-type plants. In terms of plant height, mutant lines appeared to be shorter (Figure 3.3.5).

Figure3.3.5: Whole plant phenotype of pIRX3::amiRNAphc2-1 lines. A & C: WT control, B: pIRX3::amiRNAphc2-1 line 8 insert in WT, and C: pIRX3::amiRNAphc2-1 line 3 insert in *phc1-1 phc3-1*. Samples are representative of a pool of 15 plants.

3.3.5 Functional Analysis of New T-DNA Insert in PHC2 Gene

During the course of this project a new insert (SALKseq_60215) was identified for the PHC2 gene and is inserted in the exon. This insert was used to determine whether the phenotype observed in pirx3::amiRNAphc2-1 is due to the silencing of phc2 or off target effects from amiRNA silencing events. Homozygous lines were selected for SALKseq_60215 and designated *phc2-1*. Stems from the *phc2-1* insertion line were sectioned and subjected to the histochemical analysis as before. The sections revealed no evidence of an *irx* phenotype comparable to the amiRNA lines (figure 3.3.4). This is consistent with the observed *irx* phenotype in amiRNA lines being due to off target silencing of multiple genes and not solely from the downregulation/silencing of phc2. In terms of whole plant phenotype, *phc2-1* also exhibits no defects in plant morphology i.e. rosette diameter, anthocyanin production, inflorescence and silique formation. The T-DNA insert also displays similar stunted plant height as observed with T-DNA inserts and IRX3::phc2-1 lines 8 in the WT background and lines 3,4 and 8 in *phc1-*

1 phc3-1 transformants (Figure 3.3.5). Ultimately, better quantitative analyses with many more lines and careful measurements are needed to verify this effect.

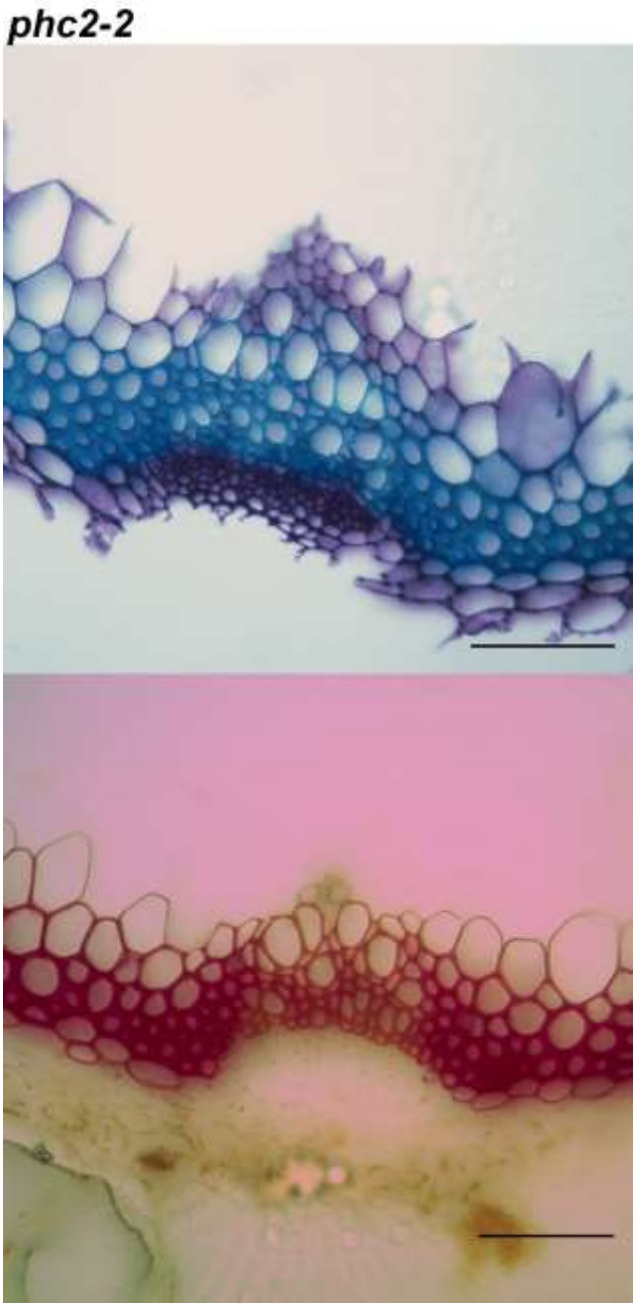

Figure 3.3.6: *phc2-2* T-DNA inserts show no xylem collapse. Transverse section 8 week old inflorescence stem. Upper panel shows Toluidine Blue-stained section and lower panel shows Mäule reagent-stained sections. Scale bar: 10 µm.

3.4 Subcellular Localisation of PHC1 in the Secondary Cell Wall Using GFP-tagging

Based on the domain structure of phytocyanins as reported by Nersissian et al. (1998, 2002), they are shuttled to the plasma membrane via the secretory pathway and are fixed in the membrane by GPI anchoring. In order to investigate whether PHC1 is localised in the secondary cell walls, particularly in the xylem vessels; both WT and *phc1-1* and *phc3-1* double mutant Arabidopsis were transformed with PHC1 fused to green fluorescent protein (GFP) at both the N and C termini using both the 35S and irx3 promoters (p35S::NGFPphc1, p35S::phc1CGFP and pIRX3::NGFPphc1, pIRX3::phc1CGFP respectively) (Figure 3.4.2). Transformants (Figure 3.4.1) were viewed using fluorescence microscopy with an eGFP filter. GFP fluorescence in spiral thickenings of xylem vessels in *Arabidopsis* seedling roots revealed that PHC1-GFP was expressed and targeted to mature secondary cell walls irrespective of N- or C-terminal tagging. There were differences in signal specificity when different promoters were used: plant transformed with 35S construct displayed ubiquitous but less intense signal. Conversely, irx3 promoted PHC1-GFP constructs in the N and C termini gave vivid and specific fluorescence at the secondary walls (Figure 3.4.3).

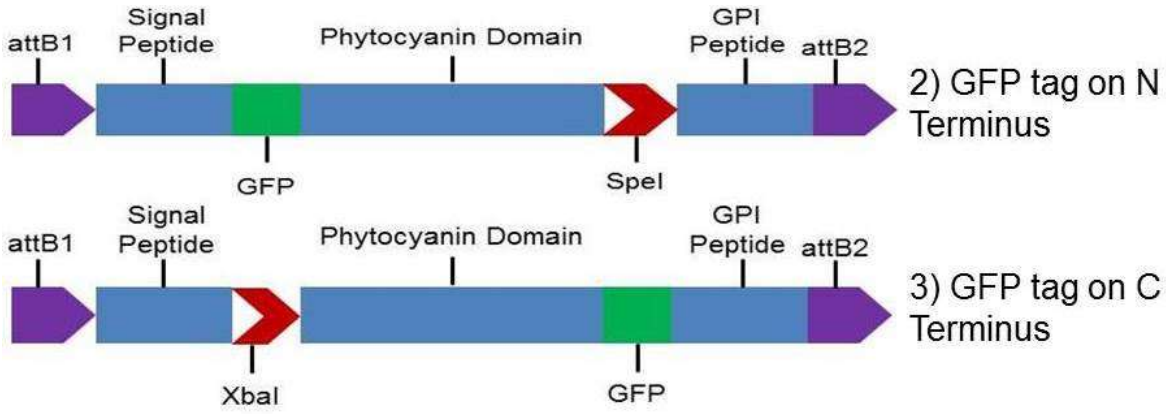

Figure 3.4.1: GFP constructs. 2 and 3 are separate constructs with GFP at either the N or C terminus.

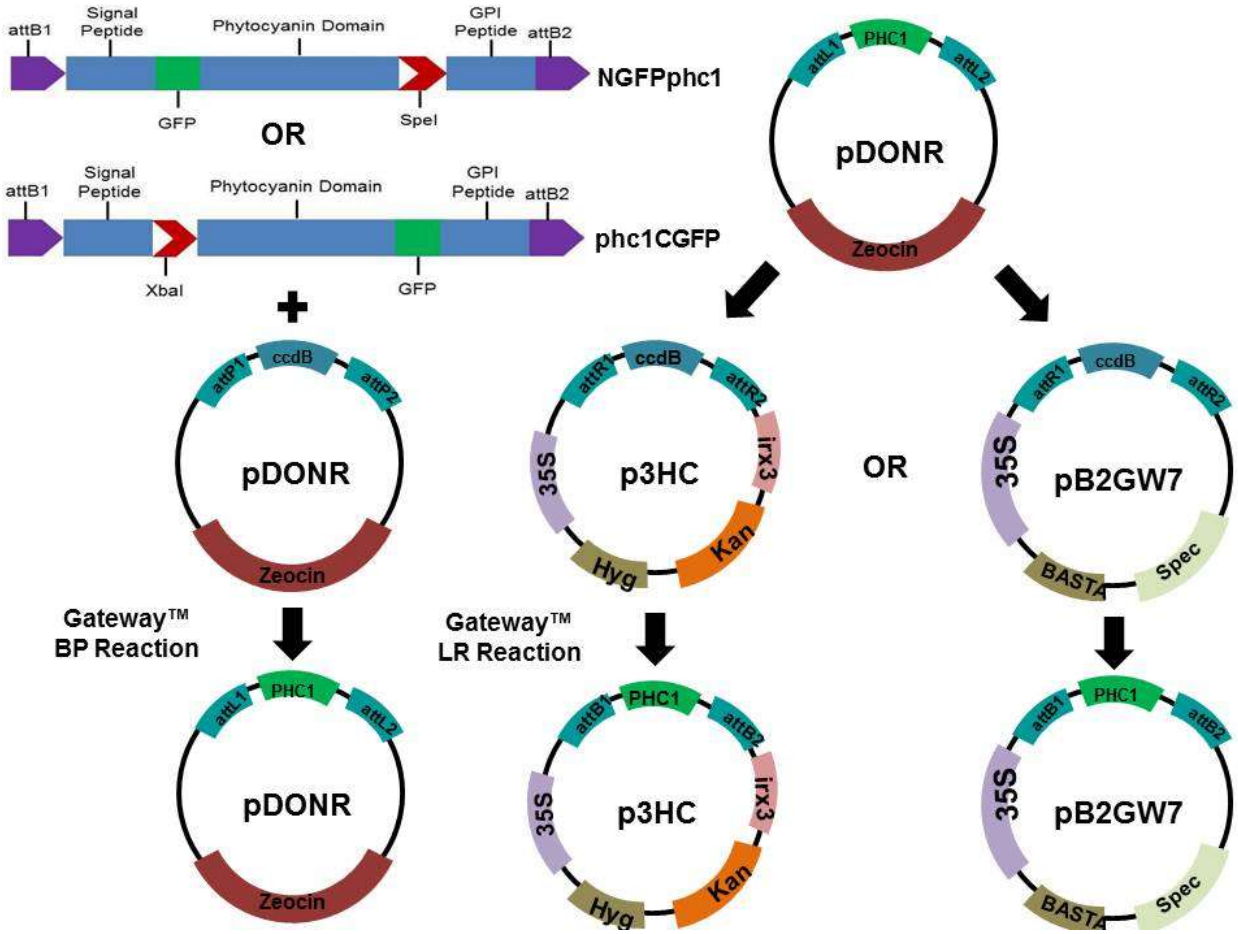

Figure 3.4.2: N & C termini PHC1GFP versions transformed into vectors. pDONR represents entry vector and were done using Gateway recombinase sites.

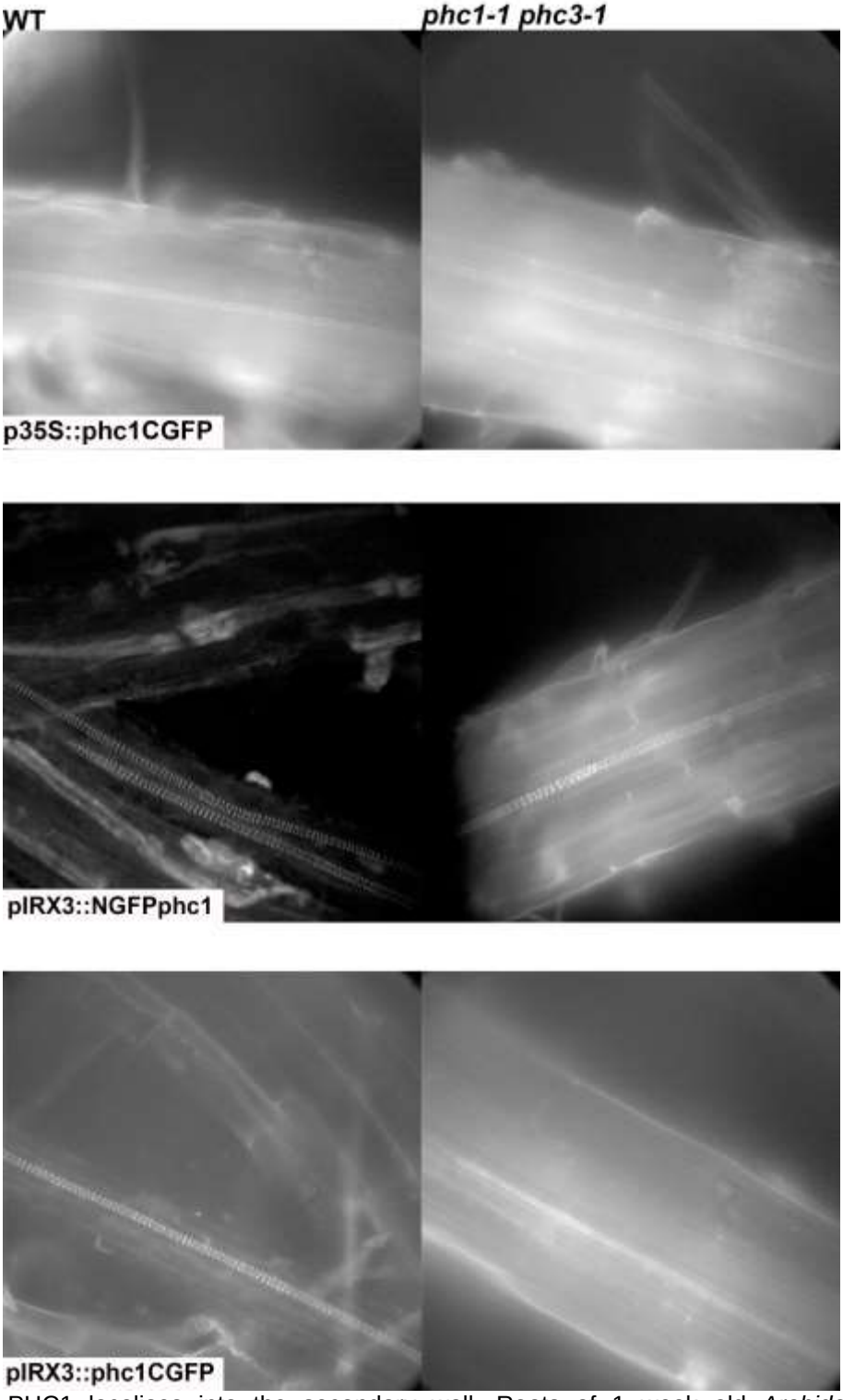

Figure 3.4.3: PHC1 localises into the secondary wall. Roots of 1 week old *Arabidopsis* seedling expressing GFP under UV transillumination with eGFP filter. Left hand side: WT transformed seedlings, right hand side: *phc1-1 phc3-1* transformed seedlings. Upper panel represents C-terminus GFP construct under 35S promoter. Middle and Lower panels represent N and C-termini GFP construct under IRX3 promoters respectively.

To validate the results of the fluorescence microscopy, an SP5 (Leica) confocal microscope was used to study GFP localisation and similar results were found (Figure 3.4.4). Signal intensity was localised to xylem spiral thickenings in *Arabidopsis* root seedlings. To eliminate any signals from autofluoresence of monolignols, WT negative control was also examined. It displayed no signal which confirms that the signals detected from GFP-tagged seedlings are solely from the fluorescence of GFP and not any autofluoresence of lignin subunits. The results clearly demonstrated that phytocyanins are localised within the secondary cell wall of mature xylem vessels.

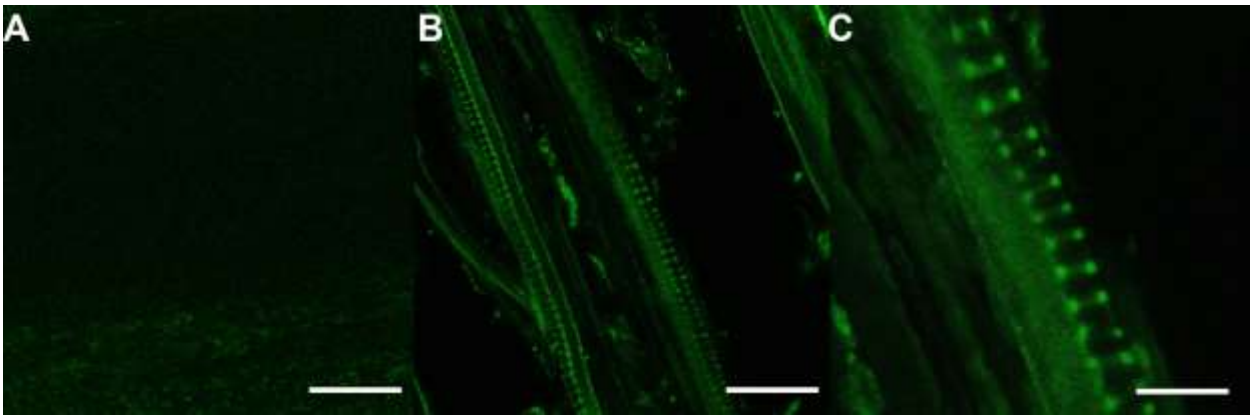

Figure 3.4.4: PHC1 localisation is confirmed by confocal microscopy. Roots of 1 week old *Arabidopsis* seedlings viewed using confocal microscopy. A: WT negative control, B: pIRX3::phc1CGFP in WT C: pIRX3::phc1CGFP in *phc1-1 phc3-1*. Scale Bars: A & C: 10 µm B: 50 µm

3.5 Characterisation of Phytocyanin Insertion Line Mutants Using Fourier transform Infrared Spectroscopy (FTIR)

An alternative to histochemical analysis is to use chemical metabolic fingerprinting (Fiehn, 2001). Fourier transform-infrared spectroscopy (FTIR) does not require sample preparation and allows rapid, simple and high throughput metabolic fingerprinting that has been demonstrated to work well with secondary cell wall mutants (Brown et al., 2005). FTIR is based on an infrared spectrum that results from transitions in quantised vibrational energy states following the bombardment of infrared light on a sample. This produces a spectrum which is essentially a metabolomic fingerprint. Metabolomic fingerprinting can complement genomic techniques to allow the determination of gene-function in plants (Griffiths and de Haseth, 2007; Dunn and Ellis, 2005). However, a metabolite profile can be very complex and difficult to interpret. Therefore, clustering analysis would help sort the data based on dimensionality reduction

(Brown et al., 2005). Examples of clustering analysis are principal component analysis and discriminant function analysis (DFA). The former is a multivariate technique to analyse data which are defined by several inter-correlated quantitative dependent variables. The aim of PCA is to extract valuable data, represent it in mutually exclusive events termed “principal components” and to portray patterns of similarities in the data as points in a map (Abdi and Williams, 2010). The latter, DFA, is as described by Stockburger (1998) to predict group membership based on internal variables. This is done to determine whether groups diverge in regards to the mean of a variable, it then to uses that variable to predict a group membership. DFA also gives insight into the relationship between groupings and the variables that are used to predict group memberships. An example would be to group graduate students who completed the programme in 5 years and those who did not. DFA can then predict if students would finish in 5 years or not based on their GRE scores and grade point averages (GPA). DFA models provide a certain prediction of whether students can finish a graduate programme in 5 years depending on their GPA and GRE scores independently or in a combinatorial fashion. Such analytical tools can provide a clustering analysis of the metabolic profile of cell walls in phytocyanins in comparison to other known cell wall mutants (PCA) and also their varying degree of relationships between known cell mutants via DFA.

The spectra of cell wall preparations from the T-DNA lines (Figure 3.5.2) showed comparable patterns typical for polysaccharides They possessed multiple peaks indicative of the plant cell wall’s intricate makeup (Figure 3.5.1). Then to assess the validity of the spectra obtained from the spectrometer, PCA was performed to determine the similarities of the technical replicates of the biological samples (Figure 3.5.2). Any variances observed caused are from technical factors i.e. sample preparation, sample loading etc. However, little or no technical variances were observed. Consequently differenced identified in the subsequent analyses are due to variations in biological samples.

Table 3.5.1: Insertion lines used in FTIR analysis

Line Name	Gene number	Allelle	Description	Origin
SRT225	At1g51680	*4cl1*	4CL mutant	Vanholme et al., 2012
SRT227	At4g34050	*ccoamt1*	CCoAMT mutant	Vanholme et al., 2012
SRT228	At2g38080	*lac4-2*	lac4 mutant (IRX12)	Berthet et al., 2011
SRT117	At5g67210 At3g50220	*irx15 irx5l*	Double DUF579 mutant	Brown et al., 2011
SRT269	At5g03170 At5g60490	*fla11 fla12*	fla 11 fla 12 double mutant	MacMillan et al., 2010
SRT236	At1g22480 At1g72230	*phc1-1* *phc3-1*	Phytocyanin double mutant	Gift from S. Turner
AP5	At1g22480	*phc1-1*	Phytocyanin mutant	
AP2	At1g72230	*phc3-2*	Phytocyanin mutant	
AP4	At1g22480	*phc1-2*	Phytocyanin mutant	
AP11	At5g07475	*phc4-1*	Phytocyanin mutant	
AP25	At2g38080	*lac4-2*	Laccase mutant	Berthet et al., 2011
AP26	At5g60020	*lac17*	Laccase mutant	Berthet et al., 2011
AP27	At2g38080 At5g60020	*lac 4-2 lac 17*	Laccase double mutant	Berthet et al., 2011
WT Col				Gift from S. Turner

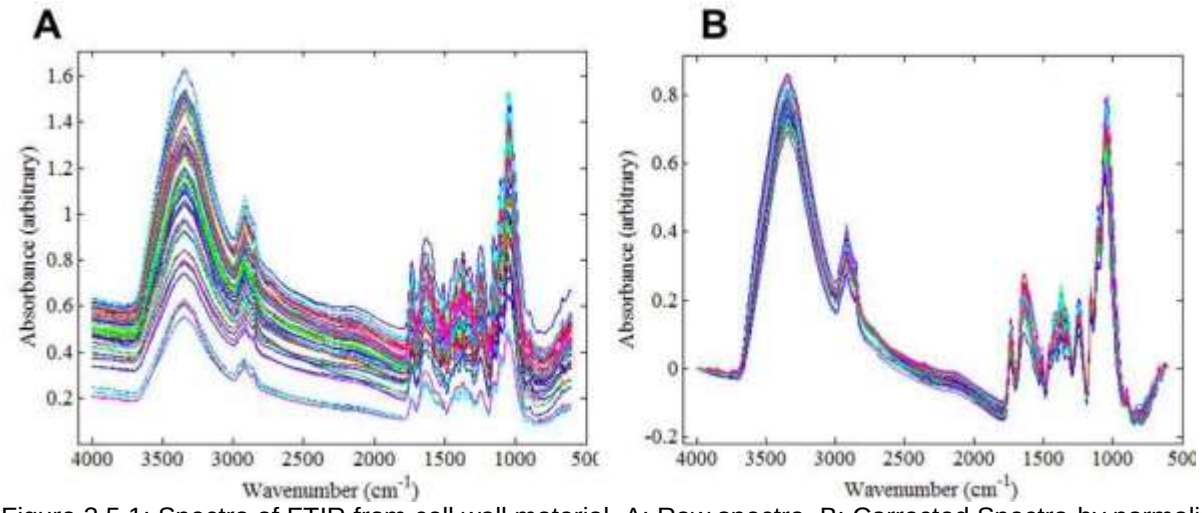

Figure 3.5.1: Spectra of FTIR from cell wall material. A: Raw spectra, B: Corrected Spectra by normalising differences in sample thickness to a total area equalling to one.

The PCA plot (Figure 3.5.3) of the samples examined showed no discernible clustering, and therefore successive DFA was performed (Figure 3.5.4). With DFA, insertion lines were more clearly separated from one another and gave clear separation between mutants and we were able to divide the mutants into several clusters. The clustering pattern was as follows: clustering of xylan deficient mutants (Cluster 1), single phytocyanin mutants with WT control (Cluster 2); single phytocyanin mutant with single laccase and double FLA mutants (Cluster 3); double phytocyanin with single laccase mutants (Cluster 4); and 4CL, CCoAMT and laccase double mutants (Cluster 5). Discriminant function 1 appears to separate the mutants depending on the degree of lignin deficiency. The phc double mutant clusters with the *lac4* and *lac17* mutants that have previously been shown to exhibit decreased lignin content. A major outlier is observed in the DFA, a known xylan deficient mutant and does not cluster with any of the samples analysed. Therefore the DFA clustered the mutants based on lignin deficiency and not on other cell wall mutants such as *IRX5 IRX5L*. FTIR analysis shows that phytocyanin genes possibly play a role in lignin biosynthesis.

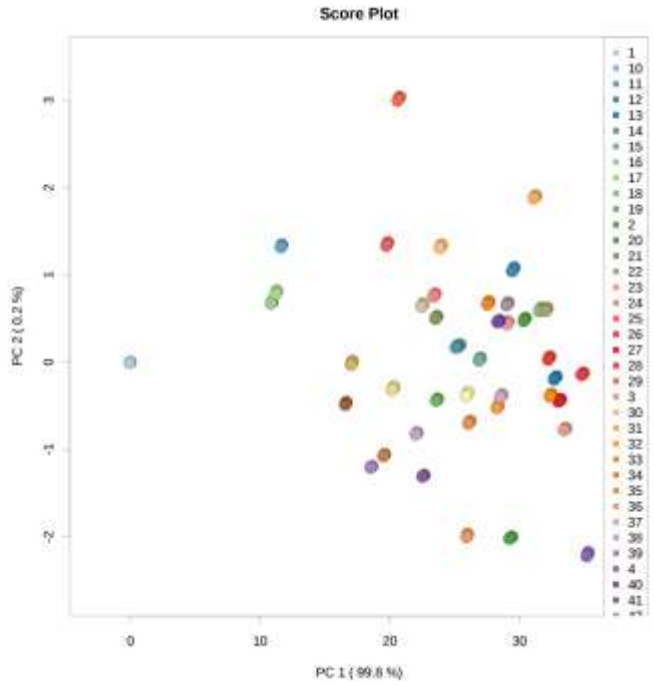

Figure 3.5.2: Principal component analysis of technical replicate. Numbers and their corresponding colours represent different biological samples. The plot verifies that no variability exists in the FT-IR analysis technique used.

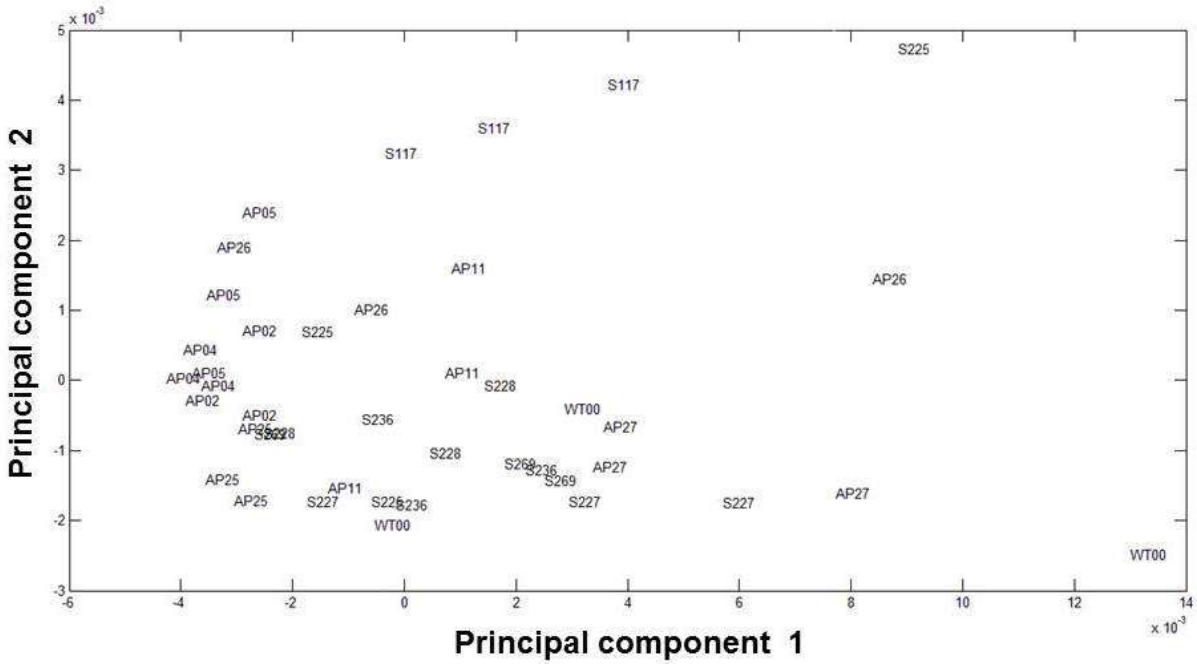

Figure 3.5.3: Principal component analysis of FTIR lines. Samples: WT00 = wild type, S117 =*IRX15 IRX15L*, S225 = *4CL1*, S227 = *CCOAMT1*, S228 = *LAC4*, S236 = *PHC1 PHC3*, S269 = *FLA11 FLA12*, AP02 = *PHC3*, AP04 = *PHC1*, AP05 = *PHC1*, AP11 = *PHC4*, AP25 = *LAC4*, AP26 = *LAC17*, AP27 = *LAC4 LAC 17*.

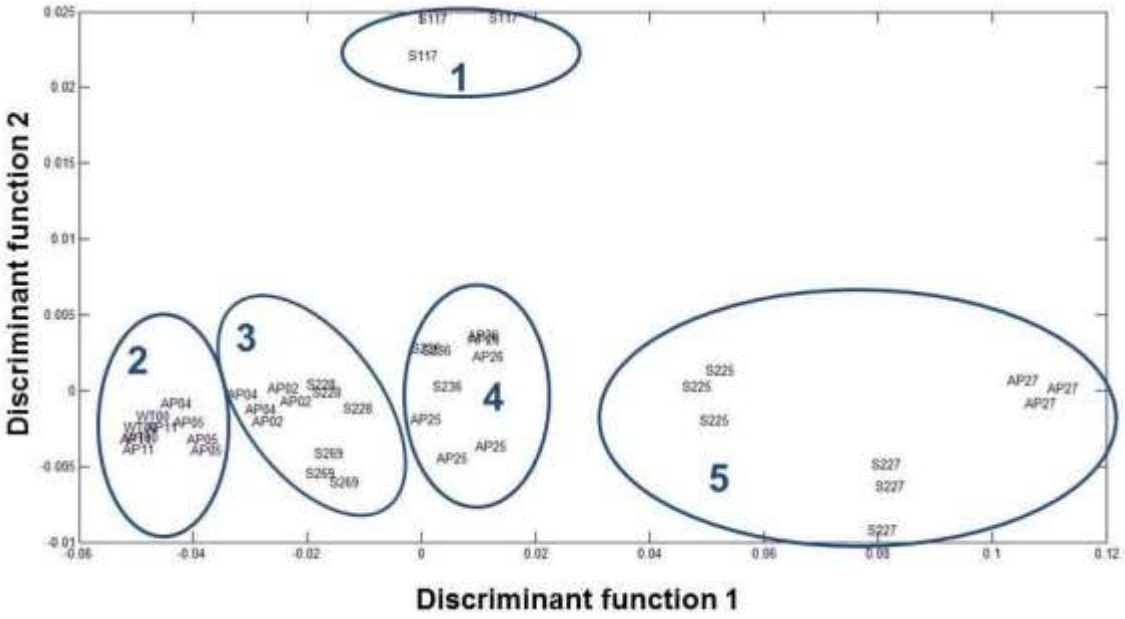

Figure 3.5.4: Discriminant function analysis of FTIR lines Samples: WT00 = wild type, S117 =*IRX15 IRX15L*, S225 = *4CL1*, S227 = *CCOAMT1*, S228 = *LAC4*, S236 = *PHC1 PHC3*, S269 = *FLA11 FLA12*, AP02 = *PHC3*, AP04 = *PHC1*, AP05 = *PHC1*, AP11 = *PHC4*, AP25 = *LAC4*, AP26 = *LAC17*, AP27 = *LAC4 LAC 17*. Circles represent clustering in results section 3.5.

Chapter 4: Discussion

4.1 Phytocyanin Expression Profiles in *Arabidopsis* Stems and the Generation of phc mutants Using T-DNA Insertions

The use of coexpression analysis is a viable tool for inferring gene functions. This is because according to Stuart et al. (2003), genes that have similar functions tend to be express similar transcription patterns. In light of this, coexpression analysis can reveal previously unknown functions if their transcription is similar to that of functionally characterised genes in a given biological process (Ruprecht and Persson, 2012). The use of coexpression in cell wall analysis has revealed that transcriptional coordination occurs during cell wall formation. For example, studies by Brown et al. (2005) revealed similar expression patterns amongst secondary cellulose synthase subunits (CesAs). More importantly, coexpression approaches were able to identify previously unknown genes involved in secondary cell wall biosynthesis. Coexpression analysis also proves to be a robust tool because candidate genes from several studies displayed similar trends in expression profiles regardless of the microarray data sets and its bait genes (Oikawa et al., 2010). Combining the fact that secondary cell wall biosynthesis is an exceedingly well-synchronised process and is exclusively restricted to certain tissues of the plant, the co-expression of certain phytocyanin genes with the secondary cell wall-specific marker gene irx3 is good circumstantial evidence that they have a role in secondary cell wall biosynthesis.

Candidate phytocyanin genes were confirmed by geneCAT and AtGenExpress to be highly coexpressed with the secondary cell wall gene irx3. Although co-expression implies that they are involved in secondary cell wall formation, the initial analysis of T-DNA mutants in single members of the phytocyanin gene family using histochemistry and whole plant morphology did not reveal any obvious phenotypical abnormalities. Based on staining of stem cross sections, xylem vessels in these mutants were identical to that of the wild-type. There was no observable decrease in lignin such as such as that seen in *irx4* xylems that causes xylem collapse (Jones et al., 2011). Single mutants displayed no clear reduction in plant height.

Given that several members of the phytocyanin gene family are expressed during stem development it is likely that functional redundancy may play some role in masking defects when only a single gene is

absent. Closely related genes may compensate for the perturbation, thereby causing the mutants to appear normal (Liu, 2012). Therefore, the approach to tackle redundancy would be to create multiple combinations of knockout mutants of phytocyanin gene families based on sequence similarity and similar expression patterns. But it should be noted that this strategy becomes daunting as the possible mutant genotype combination grows (2^n is the formula for number of combinations, where n represents number of gene members in a given family) (Krysan et al., 1999). Double mutants in the phc1 and phc3 genes were used to address the relationship between these genes. Both double mutants had the same T-DNA insertion in phc1 (*phc1*-1) but had different insertion sites at phc3 (*phc3-1 phc3*-2). Neither double mutant combination elicited a phenotype and nor did the phc3 mutant alleles as single mutants, hence leaky mutations in phc3 inserts are unlikely. However, RT-PCR data from Figure 3.2.4 showed that *phc1-1* is not a null allele, which additionally may have resulted in the lack of a mutant phenotype observed.

Furthermore, during the analysis of the phc1 transcript levels, a potential problem came to light. The T-DNA insertion in *phc3-1* was at a 5'-UTR region, so the primer used to measure transcript levels flanked the 5'-UTR region in the T-DNA insert rather than the coding region itself. This approach may not be used to accurately determine if the gene product was really being transcribed. In fact, the insertion may have even increased expression levels instead of silencing the intended gene. This event, known as "knockon" mutation is described by Krysan et al. (1999) is where T-DNA inserts may carry a constitutive promoter and drive expression of genes adjacent to its insert. This phenomenon was documented in GABI-Kat T-DNA lines that possess a 35s promoter in their right border and lead to a gain of function or overexpression in the gene downstream when GABI-KAT insert is located close to the 5'end of the gene (Uelker et al., 2008). The same situation may have occurred with the *phc3-1* mutant. The insert lay in the 5'-UTR which may have allowed the T-DNA's promoter to drive transcription instead of the endogenous promoter. Furthermore, the primers to check transcript levels flanked the 5'-UTR region instead of the exon region thereby prohibiting any detection of changes in transcription activity from the T-DNA insert accurately during RT-PCR. This error could account for the lack of mutant phenotype observed: gene silencing wasn't occurring at phc3 and the *phc1, phc3* double mutant could have ended up resembling the single mutant *phc1-1*. To resolve uncertainty regarding the possibility of phc3 knockon,

a new insert (*phc3-2*) at the exon position of phc3 was also analysed but the same phenotype was observed. Therefore, although the severity of the phc3-1 mutation remain uncertain, it is unlikely to explain lack of phenotype in *phc1,phc3* double mutants.

The lack of observable phenotype may also be due to the lack of induction by endogenous or exogenous physiological conditions. Genes have been known to function only under specific stages of development or environmental conditions. In *Arabidopsis*, specifc phytocyanins are implicated in the response to light and oxidative stress (Van Gysel et al., 1993) and in Al toxicity (Ezaki et al., 2001). It is possible that these genes are only expressed during mentioned stress conditions and the growth conditions that were used in this study did not induce any activity. RT-PCR analysis of transcript levels also revealed the *phc1-1* insert only produced a knockdown effect. This could mean that the mRNA still present would still allow normal gene function to continue (Radhamony et al., 2005). Lastly, because the largest degree of mutation using T-DNA inserts and amiRNA silencing were double and at most a triple respectively; it's possible that more mutations in the phytocyanin family are needed. Like IRX10 and IRX10L, single gene inserts elicited weak to no phenotype but the double mutants' elicted an obvious xylem collapses. Higher order mutants maybe needed considering that the family of phytocyanins contains 11 members.

4.2 *irx* Phenotype Observed in amiRNA Silenced Lines are due to Effective Gene Silencing and Off Target Effects

The attenuated xylem vessels observed from the amiRNA lines are likely due off target and not exclusively from single gene silencing effects. In the course of this study a new T-DNA insert was made available at the phc2 gene, which was initially analysed by amiRNA silencing. The insert was located at within an exon and is most likely to produce a knockout of the phc2 gene. Histochemistry of transverse sections however exhibited no phenotype equivalent to that of pIRX3::amiRNAphc2-1 line 7 in WT and lines 3, 4 and 8 in *amiRNAphc2-1 phc1-1 phc3-1* (Figure 3.3.3 A & B). The *irx* phenotype observed in the amiRNAphc2-1 in WT transformants is likely result from off-target multiple gene silencing. This was confirmed by similar phenotypes observed in pIRX3::amiRNAphc2-1 transformed in *phc1-1 phc3-1* lines. The knockdown of all three phc1 phc2 and phc3 genes resulted in xylem vessel collapses in the

secondary cell wall in *A. thaliana* stems. The *irx* phenotypes resulting from the multiple silencing of genes are consistent with a secondary cell wall defect including those observed in lignin deficient mutants of lignin deficiency (Jones et al., 2001; Berthet et al., 2011; Brown et al., 2005). This analysis adds to the previous suggestion of a role for phytocyanins in lignification function based on biochemical characteristics by Nersissian et al. (1998) who considered the copper redox moiety to be involved in oxidation of monolignols.

pIRX3::amiRNAphc2-1 lines 3, 4, and 8 in *phc1-1 phc3-1* and line 7 in WT and lines confirm that functional redundancy occurs based on the multiple gene and off-target silencing observed respectively. The functional redundancy characteristic appears to be commonly observed in studies involving lignin deficiency and its resultant collapse in xylem vessels like: *LAC4 LAC17* as described by Berthet et al. (2011) and Brown et al. (2005) and *CCR CAD* mutants (Thevenin et al., 2011) and for other cell wall polysaccharides such as glucuronoxylan mutants *IRX10 IRX10-L* (Wu et al., 2009), xylan *IRX15 IRX15-L* mutants, fasciclin-like arabinogalactan mutants *FLA11 FLA12* (MacMillan et al., 2010) and beta-xylosidases *AtBXL1* and *AtBXL4* (Goujon et al., 2003) in which only the double mutant exhibit a phenotype. The observed redundancy and the emergence of phenotypes only by multiple gene knockouts has increased as reviewed by Lloyd and Meinke (2012). Therefore, the likelihood of phytocyanins exhibiting functional redundancy as found in this study is part of an increasing trend.

4.3 PHC1-GFP Localises Into the Secondary Cell Wall

The localisation studies performed support a role for phytocyanins in secondary cell wall formation. The GFP:PHC1 fusion transformed into the *phc1 phc3* double mutant was intended for complementation studies. However, because no apparent phenotype was detected, it is unknown whether the fusion is truly able to complement the mutant. Complementation could have been verified by FTIR by comparing any metabolic changes between the WT and double mutant when GFP is added. Unfortunately, due to time constraint, this could not be performed. Another reason for PHC1-GFP tags were inserted into *phc1 phc3* was to ensure that the tagged version of the genes was not excluded by the plant due to the presence of the wild type protein being used preferentially. Insertion of GFP:PHC1 into the *phc1-1 phc3-1* mutants

that lack any endogenous PHC1 ensures that it does not interfere with PHC1-GFP trafficking in the xylem cells so that a clear signal is observed in microscopy (Wightman and Turner, 2007). Xylem vessels are particularly advantageous for this study as they are dead at maturity, so a localised fluorescence pattern observed in the vessels cannot be the result of signal from the plasma membrane or other aspect of the cells. The fluorescence observed in xylem vessels suggested that GPI anchors in phytocyanins are cleaved and are inserted into the cell wall.

Tagging of GFP at the N and C terminus and the subsequent observation that there is no significant difference in signal intensity is important. Studies by Chartrand et al. (1999) demonstrated that N-terminal or C-terminal fusions may affect posttranslational modification sites, i.e. myristylation or farnesylation sites that are required for membrane targeting.According to Tian et al. (2004), C-terminal fusions could likewise mask stem-loop structures found in 3' area of the coding sequence and in the 3' untranslated region (UTR) which are needed for the correct localization of certain mRNAs. And another important factor to consider is that fusions at these termini can cause the protein to not reach its appropriate location and may result in artifactual localisation. No significant differences from either N or C terminus tagging in PHC1 means that GFP-tagged phytocyanin localisation to the xylem vessels are reliable and thereby further improving confidence that the localisation is correct.

Despite the observation of localisation into the cell wall, GFP tagging and subsequent visualisation could not confirm whether or not phytocyanins contained a GPI anchor to tether them to the plasma membrane and remain in the extracellular matrix. This is due to the resolution of the microscopes used. Further studies to verify whether the PHC remain tethered close to the plasma membrane by the GPI anchor could be carried out using immunogold labelling and transmission electron microscopy. Given that xylem vessels undergo cell death and that the plasma membrane is not present in mature vessels the persistence of the GFP signal following cell death suggests that phytocyanins are incorporated into the wall following cleavage of the GPI anchor consistent with previous reports that phytocyanins have been purified from cell wall lacking the GPI anchor (ref).

4.4 Phytocyanins Display Similar Metabolic Characteristics as Lignin Deficient Mutants

Metabolic profile via FTIR allows rapid analysis of a large number of samples and numerous biological and technical replicates to be performed. FTIR analysis also provided information not seen from the previous phenotypic analysis of xylem tissues. FTIR analysis was able to reveal metabolic differences of phytocyanins and cluster them based on lignin deficiency. Additionally, the analysis demonstrated that phytocyanin mutants do not possess any metabolic changes similar to those brought about by altered xylan levels. This is indicated by cluster 1 of *IRX15 IRX15L* mutants remaining an outlier in the DFA (Figure 3.5.4).

In terms of lignin profiling, FTIR and subsequent discriminant functional analysis was able to delineate phytocyanins based on degree of lignin deficiency. From the data in Figure 3.5.4, the associations of phytocyanins as single mutants tend to cluster proximal to wild type and mutants that exhibit no defect in the major secondary cell wall components (cellulose lignin and xylan) such as the double FLA mutant. The phytocyanins double mutant, howver, groups with known lignin deficient mutants including *lac4* and *lac17*. The *lac4* and *lac17* single mutants were said to only display moderately decreases in lignin (Berthet et al., 2011). Therefore, if lignin levels of the PHC1 PHC3 double mutant were quantified, it would most likely appear similar to levels of LAC4 and LAC17 mutants. It is important to note as well that the known lignin mutants displayed no change in S/G subunit ratio based on Mäule staining (MacMillan et al., 2010; Berthet et al., 2011; Do et al., 2007; Lee et al., 1997). This was also observed in the phytocyanins and it can then be inferred that mutations in the phytocyanins do not affect subunit composition and ratios and are therefore more likely to affect overall lignin concentrations. The FTIR data also supported the existing functional redundancy observed from previous analysis in T-DNA inserts and amiRNA lines. As mentioned, single phytocyanins clustered near wild type but the double mutants were in the vicinity of laccases. The data is consistent with functional redundancy, but even the double mutant is not severe enough to elicit any visual phenotype.

Chapter 5: Conclusions, Limitations and Future Perspectives

5.1 Conclusion

The work in this study provided several lines of evidenc to support a role for phytocyanins in secondary cell walls. GFP tagging of PHC1 showed secondary cell wall localisation by fluorescence and confocal microscopy. Gene silencing via amiRNA resulted in effective multiple gene silencing of phytocyanins and produced an *irx* phenotype, indicating their role in xylem vessel structure and integrity. FTIR analysis revealed that phytocyanin mutants have similar metabolic profiles as lignin deficient mutants, again indicative of a function in lignification of the secondary cell wall. T-DNA insertional mutants revealed that phytocyanins display a considerable degree of functional redundancy based on the histochemistry of stem sections. Further functional characterisation of phytocyanins could provide a better understanding of lignification in secondary cell walls if functional redundancy is eliminated by generating higher-order mutants. The possibility then of manipulating phytocyanins to produce lignin structures that are less recalcitrant could lead to increased saccharification efficiency of lignocellulose sources for feasible biofuel production.

5.2 Limitations

There are various limitations involved in this study. They will be discussed based on the approaches i.e. reverse genetics, histochemical and biochemical analyses. In terms of the reverse genetics approach, the most obvious limitation is that the results indicated that phytocyanins are functionally redundant. It is only when a triple mutant were examined did any noticeable phenotype emerge however mild. Additionally, the small size of phc gene meant that finding T-DNA inserts at exons that are likely to be complete loss of function alleles was difficult. Some of the inserts (*phc3*-1 etc.) used in this study lie in the 5' untranslated region (UTR) of the gene or within introns. Intronic and UTR inserts are problematic because in the former, posttranscriptional splicing could edit out the insert allowing normal wild type proteins to be translated. In the latter, it produces leaky transcription such that translation of the protein is been knocked-down rather than knocked-out. However, the use of amiRNAs provided a suitable solution because it is allows for multiple or single target silencing and transcript-level silencing can be easily measured using RT-PCR. It would still be preferable to obtain complete knockouts in the genes of

interest. During the course of this study a TDNA insertion line within the first exon of phc2 became available. It would be interesting to combine this with *phc3-2*, which also contains an insertion in the first exon, and a complete knockout of phc1. Our studies suggest that *phc1* is leaky. Two other insertions exist in this line. One is a transposon insertion also in the same intron. This could be tested to its affect on transcript levels. There is an insertion line within an exon, but this is in the Ler background. This could be dealt with by either backcrossing or selecting multiple lines from a segregating population and would be one means of generating a line in which all three genes are complete knockouts.

The biochemical analysis performed in this study was only sufficient to show qualitative results. Lignin staining with Mäule reagent reveals lignin content and gives an indication of subunit ratio. The reliance on visual comparison means that even significant quantitative changes in plant secondary cell wall components in the phytocyanin knockdown/knockout mutants would not necessarily have been identified. Also, no quantification of the cellulose, hemicellulose and lignin polymers in cell walls was done for phytocyanin mutants. Whilst the *irx* phenotype is observed in severe lignin deficient plants such as those reported by Jones et al. (2001) and Berthet et al. (2011), *irx* phenotypes are also observed in cellulose deficient mutants (Turner and Somerville, 1997) and xylan deficient mutants such as *irx10/irx10l* with deficient xylan backbone synthesis (Brown et al., 2009; Wu et al., 2009), *irx15/irx5l* that causes xylose deficiency (Brown et al., 2011) or loss of function of genes that are responsible for the reducing end of xylans *irx7/irx7l* (Lee et al., 2012b). There is therefore a need to complement the phenotypical analysis of stem sections with quantification of polysaccharide and hydroxyphenylpropanoid levels to shed light as to why phytocyanins mutants are exhibiting such a phenotype.

In the FTIR analysis, most genotypes compared in the analysis were known lignin-deficient mutants. Whilst this was prudent on the basis of preliminary investigation and information, it resulted in an incomplete profiling. The DFA plot only determined that phytocyanin mutants were loosely clustering with certain lignin deficient mutants. A xylose deficient mutant was also examined alongside and was found to cluster with neither of the phytocyanins and was the outlier. This suggested that knockout/knockdown of phytocyanins do not affect xylose levels in secondary cell walls. However, other *irx* phenotype inducing mutants such as cellulose deficient *irx3* mutants were not included in the comparison. However, since

xylose levels remain unchanged, it is also reasonable that cellulose levels would be equivalent. What is needed is a more comprehensive survey of lignin deficient mutants because *phc1 phc3* double mutant was separated from WT in terms of lignin deficiency in df1 from the discriminant functional analysis.

5.3 Future Perspectives

This study on the functionalization and characterisation of phytocyanins is only preliminary, and much work is needed for a better and complete understanding of this family of proteins. To address experimental limitation determined in this study several suggestions will be made. Due to the functional redundancies in phytocyanins revealed by this study, a comprehensive approach to make multiple knockouts is needed. Based on coexpression data and sequence homology, PHC4 and PHC5 are the most likely candidates. In terms of metabolic analysis, adding a more comprehensive list of known cell wall mutants juxtaposed with phytocyanin mutants during FTIR will also be necessary. Once metabolic clustering of phytocyanin mutants with lignin deficient mutants has been confirmed using FTIR, its aberrant lignin structure and composition should be thoroughly analysed. NMR spectroscopy can a powerful tool for lignin structural elucidation of lignin in phytocyanin mutants as has been done in CAD and COMT-deficient plants (Ralph et al., 2001) and CCoAMT mutants (Meyermans et al., 2000). Lastly, overexpression studies similar to experiments done by Zhong et al. (2006) should be performed by generating phytocyanin overexpression lines and determining by histochemical analysis of stem sections if there is any ectopic lignification. A positive result in these lines would support the role of phytocyanins in lignifications due to their increased activity.

Testing whether or not phytocyanins are involved in lignin polymerisation similar to the mechanisms of laccases or peroxidases, dehydrogenation polymerisation (DHP) (Boerjan, Ralph, and Baucher, 2003) could be employed with recombinantly expressed phytocyanin proteins to show *in vitro* lignin polymerisation. The phytocyanin copper moiety possesses similar transition states as the copper acetate salts used by Landucci et al. (1995) to yield polylignols. If it is possible to obtain similar results to those of Landucci et al. (1995) with heterologously expressed phytocyanins, it can be deduced that phytocyanins have polymerisation roles of monolignols during secondary cell wall formation.

Functional characterisation of these heterologously expressed phytocyanin is also important in terms of its subfamily and copper moiety. It was previously mentioned that uclacyanins and stellacyanins exhibit varying redox potentials with the former being a stronger oxidising agent than the latter. The discrepancy in redox potential and its resultant capacity for electron exchange is a result of residue changes in the axial ligand of the copper moiety. This structural feature may determine the efficacy of monolignol radicalisation and may explain which phytocyanin subfamilies take part in lignification. In this study, it was phc2 knockouts that elicited the *irx* phenotype. Only PHC2 is part of the uclacyanin subfamily; the rest are stellacyanins. Therefore, it needs to be investigated whether different phytocyanin subfamilies and their respective redox potential, or a combination of uclacyanins and stellacyanins, are responsible for lignification in secondary cell walls.

Expression patterns would also add further support to a role for phytocyanins in lignification. The use of *in situ* hybridisation will allow the visualisation of expression patterns of phytocyanins in *Arabidopsis* stems (Brewer et al., 2006). If *in situ* hybridisation shows phytocyanin expression in interfascicular fibres, metaxylem cells, and secondary xylem in the WT but absence of these patterns in knockout mutants, it would confirm that phytocyanins are associated with secondary wall thickening in these tissues. Localisation expression studies can also be supplemented by laser microdissection (LM).The use of LM to harvest specific tissue regions from histological sections which are amenable to transcript profiling (Nelson et al., 2006) allows the display of cell specific expression patterns as opposed to undissected tissues in which profiles would be averaged between targeted and neighbouring tissues. This method would prove advantageous in determining phytocyanin transcript expression patterns without the background noise typical f*in situ* hybridisation methods (Brewer et al., 2006).

An in-depth analysis of the transcriptional network of lignin would also discriminate whether or not phytocyanins are activated during lignifications in secondary wall development or ectopic lignification during wounding and pathogenic attacks. If transcriptional changes are observed under overexpression or knockouts of known transcriptional switches of secondary cell wall development (e.g. MYB58/63 are transcriptional activators), then phytocyanins are most likely involved in lignification (Zhou et al., 2009).

References

Abdi, H., and Williams, L.J. (2010). Principal Component Analysis. WIREs Computational Statistics **2,** 27.

Al-Haddad, J.M., Kang, K.-Y., Mansfield, S.D., and Telewski, F.W. (2013). Chemical responses to modified lignin composition in tension wood of hybrid poplar (Populus tremula x Populus alba). Tree Physiology **33,** 365-373.

Albersheim, P., Darwill, A., Roberts, K., Sederoff, R., and Staehelin, A. (2011). Plant Cell Walls (New York City: Garland Science).

Allona, I., Quinn, M., Shoop, E., Swope, K., St Cyr, S., Carlis, J., Riedl, J., Retzel, E., Campbell, M.M., Sederoff, R., and Whetten, R.W. (1998). Analysis of xylem formation in pine by cDNA sequencing. Proceedings of the National Academy of Sciences of the United States of America **95,** 9693-9698.

Alonso, J.M. (2003). Genome-wide insertional mutagenesis of Arabidopsis thaliana (vol 301, pg 653, 2003). Science **301,** 1849-1849.

Arabidopsis Genome, I. (2000). Analysis of the genome sequence of the flowering plant Arabidopsis thaliana. Nature **408,** 796-815.

Barnett, J.R., and Bonham, V.A. (2004). Cellulose microfibril angle in the cell wall of wood fibres. Biological Reviews **79**.

Berg, J.M., Tymoczko, J.L., and Stryer, L. (2002). Biochemistry. (New York: WH Freeman).

Bertani, G. (2004). Lysogeny at mid-twentieth century: P1, P2, and other experimental, systems. Journal of Bacteriology **186,** 595-600.

Berthet, S., Demont-Caulet, N., Pollet, B., Bidzinski, P., Cezard, L., Le Bris, P., Borrega, N., Herve, J., Blondet, E., Balzergue, S., Lapierre, C., and Jouanin, L. (2011). Disruption of LACCASE4 and 17 Results in Tissue-Specific Alterations to Lignification of Arabidopsis thaliana Stems. Plant Cell **23,** 1124-1137.

Boerjan, W., Ralph, J., and Baucher, M. (2003). Lignin biosynthesis. Annual Review of Plant Biology **54,** 519-546.

Boija, E., Lundquist, A., Edwards, K., and Johansson, G. (2007). Evaluation of bilayer disks as plant cell membrane models in partition studies. Analytical Biochemistry **364,** 145-152.

Boija, E., Lundquist, A., Nilsson, M., Edwards, K., Isaksson, R., and Johansson, G. (2008). Bilayer disk capillary electrophoresis: A novel method to stud drug partitioning into membranes. Electrophoresis **29,** 3377-3383.

Bonawitz, N.D., and Chapple, C. (2010). The Genetics of Lignin Biosynthesis: Connecting Genotype to Phenotype. Annual Review of Genetics, Vol 44 **44**.

Brady, S.M., Orlando, D.A., Lee, J.Y., Wang, J.Y., Koch, J., Dinneny, J.R., Mace, D., Ohler, U., and Benfey, P.N. (2007). A high-resolution root spatiotemporal map reveals dominant expression patterns. Science **318,** 801-806.

Brewer, P.B., Heisler, M.G., Hejatko, J., Friml, J., and Benkova, E. (2006). In situ hybridization for mRNA detection in Arabidopsis tissue sections. Nature Protocols **1,** 1462-1467.

Brown, D., Wightman, R., Zhang, Z.N., Gomez, L.D., Atanassov, I., Bukowski, J.P., Tryfona, T., McQueen-Mason, S.J., Dupree, P., and Turner, S. (2011). Arabidopsis genes IRREGULAR XYLEM (IRX15) and IRX15L encode DUF579-containing proteins that are essential for normal xylan deposition in the secondary cell wall. Plant Journal **66,** 401-413.

Brown, D.M., Zeef, L.A.H., Ellis, J., Goodacre, R., and Turner, S.R. (2005). Identification of novel genes in Arabidopsis involved in secondary cell wall formation using expression profiling and reverse genetics. Plant Cell **17,** 2281-2295.

Brown, D.M., Zhang, Z., Stephens, E., Dupree, P., and Turner, S.R. (2009). Characterization of IRX10 and IRX10-like reveals an essential role in glucuronoxylan biosynthesis in Arabidopsis. Plant Journal **57,** 732-746.

Brown, D.M., Goubet, F., Vicky, W.W.A., Goodacre, R., Stephens, E., Dupree, P., and Turner, S.R. (2007). Comparison of five xylan synthesis mutants reveals new insight into the mechanisms of

xylan synthesis. Plant Journal **52,** 1154-1168.
Brown, R.M. (1996). The biosynthesis of cellulose. Journal of Macromolecular Science-Pure and Applied Chemistry **A33,** 1345-1373.
Burlat, V., Kwon, M., Davin, L.B., and Lewis, N.G. (2001). Dirigent proteins and dirigent sites in lignifying tissues. Phytochemistry **57,** 883-897.
Carroll, A., and Somerville, C. (2009). Cellulosic Biofuels. Annual Review of Plant Biology **60,** 165-182.
Chapple, C.C.S., Vogt, T., Ellis, B.E., and Somerville, C.R. (1992). An Arabidopsis mutant defective in the general phenylpropanoid pathway. The Plant Cell **4,** 12.
Chartrand, P., Meng, X.H., Singer, R.H., and Long, R.M. (1999). Structural elements required for the localization of ASH1 mRNA and of a green fluorescent protein reporter particle in vivo. Current Biology **9,** 333-336.
Chen, F., and Dixon, R.A. (2007). Lignin modification improves fermentable sugar yields for biofuel production. Nature Biotechnology **25,** 759-761.
Chen, Y.-R., and Sarkanen, S. (2003). Macromolecular lignin replication: A mechanistic working hypothesis. Phytochemistry Reviews **2,** 21.
Chen, Y.R., and Sarkanen, S. (2010). Macromolecular replication during lignin biosynthesis. Phytochemistry **71,** 453-462.
Clough, S.J., and Bent, A.F. (1998). Floral dip: a simplified method for Agrobacterium-mediated transformation of Arabidopsis thaliana. Plant Journal **16,** 735-743.
Cosgrove, D.J. (2005). Growth of the plant cell wall. Nature Reviews Molecular Cell Biology **6,** 850-861.
Davin, L.B., Wang, H.B., Crowell, A.L., Bedgar, D.L., Martin, D.M., Sarkanen, S., and Lewis, N.G. (1997). Stereoselective bimolecular phenoxy radical coupling by an auxiliary (dirigent) protein without an active center. Science **275,** 362-366.
Del Rio, J.C., Marques, G., Rencoret, J., Martinez, A.T., and Gutierrez, A. (2007). Occurrence of naturally acetylated lignin units. Journal of Agricultural and Food Chemistry **55,** 5461-5468.
del Rio, J.C., Rencoret, J., Marques, G., Gutierrez, A., Ibarra, D., Santos, J.I., Jimenez-Barbero, J., Zhang, L.M., and Martinez, A.T. (2008). Highly Acylated (Acetylated and/or p-Coumaroylated) Native Lignins from Diverse Herbaceous Plants. Journal of Agricultural and Food Chemistry **56,** 9525-9534.
Do, C.-T., Pollet, B., Thevenin, J., Sibout, R., Denoue, D., Barriere, Y., Lapierre, C., and Jouanin, L. (2007). Both caffeoyl Coenzyme A 3-O-methyltransferase 1 and caffeic acid O-methyltransferase 1 are involved in redundant functions for lignin, flavonoids and sinapoyl malate biosynthesis in Arabidopsis. Planta **226,** 1117-1129.
Drew, J.E., and Gatehouse, J.A. (1994). ISOLATION AND CHARACTERIZATION OF A PEA POD CDNA-ENCODING A PUTATIVE BLUE COPPER PROTEIN CORRELATED WITH LIGNIN DEPOSITION. Journal of Experimental Botany **45,** 1873-1884.
Dubin, M.J., Bowler, C., and Benvenuto, G. (2008). A modified Gateway cloning strategy for overexpressing tagged proteins in plants. Plant Methods **4**.
Dubos, C., Stracke, R., Grotewold, E., Weisshaar, B., Martin, C., and Lepiniec, L. (2010). MYB transcription factors in Arabidopsis. Trends in Plant Science **15,** 573-581.
Dunn, W.B., and Ellis, D.I. (2005). Metabolomics: Current analytical platforms and methodologies. Trac-Trends in Analytical Chemistry **24,** 285-294.
Eckardt, N.A. (2003). Cellulose synthesis takes the CesA train. Plant Cell **15,** 1685-1687.
Ehlting, J., Mattheus, N., Aeschliman, D.S., Li, E.Y., Hamberger, B., Cullis, I.F., Zhuang, J., Kaneda, M., Mansfield, S.D., Samuels, L., Ritland, K., Ellis, B.E., Bohlmann, J., and Douglas, C.J. (2005). Global transcript profiling of primary stems from Arabidopsis thaliana identifies candidate genes for missing links in lignin biosynthesis and transcriptional regulators of fiber differentiation. Plant Journal **42,** 618-640.
Eisen, M.B., Spellman, P.T., Brown, P.O., and Botstein, D. (1998). Cluster analysis and display of genome-wide expression patterns. Proceedings of the National Academy of Sciences of the United States of America **95,** 14863-14868.
Ezaki, B., Katsuhara, M., Kawamura, M., and Matsumoto, H. (2001). Different mechanisms of four aluminum (Al)-resistant transgenes for Al toxicity in Arabidopsis. Plant Physiology **127,** 918-927.
Fiehn, O. (2001). Combining genomics, metabolome analysis, and biochemical modelling to understand metabolic networks. Comparative and Functional Genomics **2,** 155-168.

Field, C.B., Behrenfeld, M.J., Randerson, J.T., and Falkowski, P. (1998). Primary production of the biosphere: Integrating terrestrial and oceanic components. Science **281,** 237-240.
Fraser, C.M., and Chapple, C. (2011). The Phenylpropanoid Pathway in Arabidopsis. In The Arabidopsis Book (American Society of Plant Biologists.
Friedlingstein, P., Houghton, R.A., Marland, G., Hackler, J., Boden, T.A., Conway, T.J., Canadell, J.G., Raupach, M.R., Ciais, P., and Le Quere, C. (2010). Update on CO2 emissions. Nature Geoscience **3,** 811-812.
Fry, S.C., Frankova, L., and Chormova, D. (2011). Setting the Boundaries: Primary Cell Wall Synthesis and Expansion. The Biochemist **33,** 6.
Gillmor, C.S., Lukowitz, W., Brininstool, G., Sedbrook, J.C., Hamann, T., Poindexter, P., and Somerville, C. (2005). Glycosylphosphatidylinositol-anchored proteins are required for cell wall synthesis and morphogenesis in Arabidopsis. Plant Cell **17,** 1128-1140.
Goodstein, D.M., Shu, S.Q., Howson, R., Neupane, R., Hayes, R.D., Fazo, J., Mitros, T., Dirks, W., Hellsten, U., Putnam, N., and Rokhsar, D.S. (2012). Phytozome: a comparative platform for green plant genomics. Nucleic Acids Research **40,** D1178-D1186.
Gough, J., and Chothia, C. (2004). The linked conservation of structure and function in a family of high diversity: The monomeric cupredoxins. Structure **12,** 917-925.
Goujon, T., Minic, Z., El Amrani, A., Lerouxel, O., Aletti, E., Lapierre, C., Joseleau, J.P., and Jouanin, L. (2003). AtBXL1, a novel higher plant (Arabidopsis thaliana) putative beta-xylosidase gene, is involved in secondary cell wall metabolism and plant development. Plant Journal **33,** 677-690.
Griffiths, P.R., and de Haseth, J.A. (2007). Introduction to Vibrational Spectroscopy. In Fourier Transform Infrared Spectroscopy (Hoboken, NJ: John Wiley & Sons Inc.
Hamant, O., and Traas, J. (2010). The mechanics behind plant development. New Phytologist **185,** 369-385.
Hatfield, R., and Vermerris, W. (2001). Lignin formation in plants. The dilemma of linkage specificity. Plant Physiology **126,** 1351-1357.
Hatton, D., Sablowski, R., Yung, M.H., Smith, C., Schuch, W., and Bevan, M. (1995). 2 CLASSES OF CIS SEQUENCES CONTRIBUTE TO TISSUE-SPECIFIC EXPRESSION OF A PAL2 PROMOTER IN TRANSGENIC TOBACCO. Plant Journal **7,** 859-876.
Heyer, L.J., Kruglyak, S., and Yooseph, S. (1999). Exploring expression data: Identification and analysis of coexpressed genes. Genome Research **9,** 1106-1115.
Hosel, W., and Todenhagen, R. (1980). CHARACTERIZATION OF A BETA-GLUCOSIDASE FROM GLYCINE-MAX WHICH HYDROLYSES CONIFERIN AND SYRINGIN. Phytochemistry **19,** 1349-1353.
Hosel, W., Surholt, E., and Borgmann, E. (1978). CHARACTERIZATION OF BETA-GLUCOSIDASE ISOENZYMES POSSIBLY INVOLVED IN LIGNIFICATION FROM CHICK PEA (CICER-ARIETINUM L) CELL-SUSPENSION CULTURES. European Journal of Biochemistry **84,** 487-492.
Hosmani, P.S., Kamiya, T., Danku, J., Naseer, S., Geldner, N., Guerinot, M.L., and Salt, D.E. (2013). Dirigent domain-containing protein is part of the machinery required for formation of the lignin-based Casparian strip in the root. Proceedings of the National Academy of Sciences of the United States of America **110,** 14498-14503.
Huntley, S.K., Ellis, D., Gilbert, M., Chapple, C., and Mansfield, S.D. (2003). Significant increases in pulping efficiency in C4H-F5H-transformed poplars: Improved chemical savings and reduced environmental toxins. Journal of Agricultural and Food Chemistry **51,** 6178-6183.
Johnson, K.L., Kibble, N.A.J., Bacic, A., and Schultz, C.J. (2011). A Fasciclin-Like Arabinogalactan-Protein (FLA) Mutant of Arabidopsis thaliana, fla1, Shows Defects in Shoot Regeneration. Plos One **6**.
Jones, L., Ennos, A.R., and Turner, S.R. (2001). Cloning and characterization of irregular xylem4 (irx4): a severely lignin-deficient mutant of Arabidopsis. Plant Journal **26,** 205-216.
Kaneda, M., Rensing, K.H., Wong, J.C.T., Banno, B., Mansfield, S.D., and Samuels, A.L. (2008). Tracking monolignols during wood development in lodgepole pine. Plant Physiology **147,** 1750-1760.
Kazenwadel, C., Klebensberger, J., Richter, S., Pfannstiel, J., Gerken, U., Pickel, B., Schaller, A.,

and Hauer, B. (2013). Optimized expression of the dirigent protein AtDIR6 in Pichia pastoris and impact of glycosylation on protein structure and function. Applied Microbiology and Biotechnology **97,** 7215-7227.

Kieliszewski, M.J., and Lamport, D.T.A. (1994). EXTENSIN - REPETITIVE MOTIFS, FUNCTIONAL SITES, POSTTRANSLATIONAL CODES, AND PHYLOGENY. Plant Journal **5,** 157-172.

Kim, H., Ralph, J., Yahiaoui, N., Pean, M., and Boudet, A.M. (2000). Cross-coupling of hydroxycinnamyl aldehydes into lignins. Organic Letters **2,** 2197-2200.

Kim, K.W., Moinuddin, S.G.A., Atwell, K.M., Costa, M.A., Davin, L.B., and Lewis, N.G. (2012). Opposite Stereoselectivities of Dirigent Proteins in Arabidopsis and Schizandra Species. Journal of Biological Chemistry **287,** 33957-33972.

Koornneef, M., and Meinke, D. (2010). The development of Arabidopsis as a model plant. Plant Journal **61,** 909-921.

Krysan, P.J., Young, J.C., and Sussman, M.R. (1999). T-DNA as an insertional mutagen in Arabidopsis. Plant Cell **11,** 2283-2290.

Ku, W.L., Duggal, G., Li, Y., Girvan, M., and Ott, E. (2012). Interpreting Patterns of Gene Expression: Signatures of Coregulation, the Data Processing Inequality, and Triplet Motifs. Plos One **7**.

Kubo, M., Udagawa, M., Nishikubo, N., Horiguchi, G., Yamaguchi, M., Ito, J., Mimura, T., Fukuda, H., and Demura, T. (2005). Transcription switches for protoxylem and metaxylem vessel formation. Genes & Development **19,** 1855-1860.

Lalanne, E., Honys, D., Johnson, A., Borner, G.H.H., Lilley, K.S., Dupree, P., Grossniklaus, U., and Twell, D. (2004). SETH1 and SETH2, two components of the glycosylphosphatidylinositol anchor biosynthetic pathway, are required for pollen germination and tube growth in arabidopsis. Plant Cell **16,** 229-240.

Landucci, L.L. (1995). REACTION OF P-HYDROXYCINNAMYL ALCOHOLS WITH TRANSITION-METAL SALTS .1. OLIGOLIGNOLS AND POLYIGNOLS (DHPS) FROM CONIFERYL ALCOHOL. Journal of Wood Chemistry and Technology **15,** 349-368.

Lee, C., Zhong, R., and Ye, Z.-H. (2012a). Arabidopsis Family GT43 Members are Xylan Xylosyltransferases Required for the Elongation of the Xylan Backbone. Plant and Cell Physiology **53,** 135-143.

Lee, C., Teng, Q., Zhong, R.Q., and Ye, Z.H. (2012b). Arabidopsis GUX Proteins Are Glucuronyltransferases Responsible for the Addition of Glucuronic Acid Side Chains onto Xylan. Plant and Cell Physiology **53,** 1204-1216.

Lee, D., Meyer, K., Chapple, C., and Douglas, C.J. (1997). Antisense suppression of 4-coumarate:coenzyme A ligase activity in Arabidopsis leads to altered lignin subunit composition. Plant Cell **9,** 1985-1998.

Leple, J.C., Dauwe, R., Morreel, K., Storme, V., Lapierre, C., Pollet, B., Naumann, A., Kang, K.Y., Kim, H., Ruel, K., Lefebvre, A., Joseleau, J.P., Grima-Pettenati, J., De Rycke, R., Andersson-Gunneras, S., Erban, A., Fehrle, I., Petit-Conil, M., Kopka, J., Polle, A., Messens, E., Sundberg, B., Mansfield, S.D., Ralph, J., Pilate, G., and Boerjan, W. (2007). Downregulation of cinnamoyl-coenzyme a reductase in poplar: Multiple-level phenotyping reveals effects on cell wall polymer metabolism and structure. Plant Cell **19,** 3669-3691.

Lerouxel, O., Cavalier, D.M., Liepman, A.H., and Keegstra, K. (2006). Biosynthesis of plant cell wall polysaccharides - a complex process. Current Opinion in Plant Biology **9,** 621-630.

Li, Y., Liu, D., Tu, L., Zhang, X., Wang, L., Zhu, L., Tan, J., and Deng, F. (2010). Suppression of GhAGP4 gene expression repressed the initiation and elongation of cotton fiber. Plant Cell Reports **29,** 193-202.

Liepman, A.H., Wightman, R., Geshi, N., Turner, S.R., and Scheller, H.V. (2010). Arabidopsis - a powerful model system for plant cell wall research. Plant Journal **61,** 1107-1121.

Liu, C.J. (2012). Deciphering the Enigma of Lignification: Precursor Transport, Oxidation, and the Topochemistry of Lignin Assembly. Molecular Plant **5,** 304-317.

Liu, C.J., Miao, Y.C., and Zhang, K.W. (2011). Sequestration and Transport of Lignin Monomeric Precursors. Molecules **16,** 710-727.

Liu, H., Shi, R., Wang, X., Pan, Y., Li, Z., Yang, X., Zhang, G., and Ma, Z. (2013). Characterization and Expression Analysis of a Fiber Differentially Expressed Fasciclin-like Arabinogalactan Protein Gene in Sea Island Cotton Fibers. Plos One **8**.

Lloyd, J., and Meinke, D. (2012). A Comprehensive Dataset of Genes with a Loss-of-Function Mutant Phenotype in Arabidopsis. Plant Physiology **158,** 1115-1129.
Lu, F.C., Ralph, J., Morreel, K., Messens, E., and Boerjan, W. (2004). Preparation and relevance of a cross-coupling product between sinapyl alcohol and sinapyl p-hydroxybenzoate. Organic & Biomolecular Chemistry **2,** 2888-2890.
Lukowitz, W., Mayer, U., and Jurgens, G. (1996). Cytokinesis in the Arabidopsis embryo involves the syntaxin-related KNOLLE gene product. Cell **84,** 61-71.
MacMillan, C.P., Mansfield, S.D., Stachurski, Z.H., Evans, R., and Southerton, S.G. (2010). Fasciclin-like arabinogalactan proteins: specialization for stem biomechanics and cell wall architecture in Arabidopsis and Eucalyptus. Plant Journal **62,** 689-703.
Marcinowski, S., and Grisebach, H. (1978). ENZYMOLOGY OF LIGNIFICATION - CELL-WALL-BOUND BETA-GLUCOSIDASE FOR CONIFERIN FROM SPRUCE (PICEA-ABIES) SEEDLINGS. European Journal of Biochemistry **87,** 37-44.
Mayor, S., and Riezman, H. (2004). Sorting GPI-anchored proteins. Nature Reviews Molecular Cell Biology **5,** 110-120.
McCaig, B.C., Meagher, R.B., and Dean, J.F.D. (2005). Gene structure and molecular analysis of the laccase-like multicopper oxidase (LMCO) gene family in Arabidopsis thaliana. Planta **221,** 619-636.
Mellerowicz, E.J., and Sundberg, B. (2008). Wood cell walls: biosynthesis, developmental dynamics and their implications for wood properties. Current Opinion in Plant Biology **11,** 293-300.
Meyermans, H., Morreel, K., Lapierre, C., Pollet, B., De Bruyn, A., Busson, R., Herdewijn, P., Devreese, B., Van Beeumen, J., Marita, J.M., Ralph, J., Chen, C.Y., Burggraeve, B., Van Montagu, M., Messens, E., and Boerjan, W. (2000). Modifications in lignin and accumulation of phenolic glucosides in poplar xylem upon down-regulation of caffeoyl-coenzyme A O-methyltransferase, an enzyme involved in lignin biosynthesis. Journal of Biological Chemistry **275,** 36899-36909.
Miao, Y.C., and Liu, C.J. (2010). ATP-binding cassette-like transporters are involved in the transport of lignin precursors across plasma and vacuolar membranes. Proceedings of the National Academy of Sciences of the United States of America **107,** 22728-22733.
Morreel, K., Ralph, J., Kim, H., Lu, F.C., Goeminne, G., Ralph, S., Messens, E., and Boerjan, W. (2004). Profiling of oligolignols reveals monolignol coupling conditions in lignifying poplar xylem. Plant Physiology **136,** 3537-3549.
Mutwil, M., Obro, J., Willats, W.G.T., and Persson, S. (2008). GeneCAT - novel webtools that combine BLAST and co-expression analyses. Nucleic Acids Research **36,** W320-W326.
Nelson, T., Tausta, S.L., Gandotra, N., and Liu, T. (2006). Laser microdissection of plant tissue: What you see is what you get. Annual Review of Plant Biology **57,** 181-201.
Nersissian, A.M., and Shipp, E.L. (2002). Blue copper-binding domains. Copper-Containing Proteins **60**.
Nersissian, A.M., Immoos, C., Hill, M.G., Hart, P.J., Williams, G., Herrmann, R.G., and Valentine, J.S. (1998). Uclacyanins, stellacyanins, and plantacyanins ape distinct subfamilies of phytocyanins: Plant-specific mononuclear blue copper proteins. Protein Science **7,** 1915-1929.
Oikawa, A., Joshi, H.J., Rennie, E.A., Ebert, B., Manisseri, C., Heazlewood, J.L., and Scheller, H.V. (2010). An Integrative Approach to the Identification of Arabidopsis and Rice Genes Involved in Xylan and Secondary Wall Development. Plos One **5**.
Ossowski, S., Schwab, R., and Weigel, D. (2008). Gene silencing in plants using artificial microRNAs and other small RNAs. Plant Journal **53,** 674-690.
Page, D.R., and Grossniklaus, L. (2002). The art and design of genetic screens: Arabidopsis thaliana. Nature Reviews Genetics **3,** 124-136.
Patten, A.M., Cardenas, C.L., Cochrane, F.C., Laskar, D.D., Bedgar, D.L., Davin, L.B., and Lewis, N.G. (2005). Reassessment of effects on lignification and vascular development in the irx4 Arabidopsis mutant. Phytochemistry **66,** 2092-2107.
Pena, M.J., Zhong, R., Zhou, G.-K., Richardson, E.A., O'Neill, M.A., Darvill, A.G., York, W.S., and Ye, Z.-H. (2007). Arabidopsis irregular xylem8 and irregular xylem9: Implications for the complexity of glucuronoxylan biosynthesis. Plant Cell **19,** 549-563.
Persson, S., Wei, H.R., Milne, J., Page, G.P., and Somerville, C.R. (2005). Identification of genes required for cellulose synthesis by regression analysis of public microarray data sets.

Proceedings of the National Academy of Sciences of the United States of America **102,** 8633-8638.

Persson, S., Paredez, A., Carroll, A., Palsdottir, H., Doblin, M., Poindexter, P., Khitrov, N., Auer, M., and Somerville, C.R. (2007). Genetic evidence for three unique components in primary cell-wall cellulose synthase complexes in Arabidopsis. Proceedings of the National Academy of Sciences of the United States of America **104,** 15566-15571.

Petersen, P.D., Lau, J., Ebert, B., Yang, F., Verhertbruggen, Y., Kim, J.S., Varanasi, P., Suttangkakul, A., Auer, M., Loque, D., and Scheller, H.V. (2012). Engineering of plants with improved properties as biofuels feedstocks by vessel-specific complementation of xylan biosynthesis mutants. Biotechnology for Biofuels **5**.

Pickel, B., Pfannstiel, J., Steudle, A., Lehmann, A., Gerken, U., Pleiss, J., and Schaller, A. (2012). A model of dirigent proteins derived from structural and functional similarities with allene oxide cyclase and lipocalins. Febs Journal **279,** 1980-1993.

Pickett-Heaps, J.D. (1967). Xylem wall deposition: Radioautographic investigations using lignin precursors. Protoplasma **65,** 25.

Radhamony, R.N., Prasad, A.M., and Srinivasan, R. (2005). T-DNA insertional mutagenesis in Arabidopsis: a tool for functional genomics. Electronic Journal of Biotechnology **8,** 82-106.

Raes, J., Rohde, A., Christensen, J.H., Van de Peer, Y., and Boerjan, W. (2003). Genome-wide characterization of the lignification toolbox in Arabidopsis. Plant Physiology **133,** 1051-1071.

Ralph, J. (2010). Hydroxycinnamates in lignification. Phytochemistry Reviews **9,** 65-83.

Ralph, J., Peng, J.P., Lu, F.C., Hatfield, R.D., and Helm, R.F. (1999). Are lignins optically active? Journal of Agricultural and Food Chemistry **47,** 2991-2996.

Ralph, J., Brunow, G., Harris, P.J., Dixon, R.A., Schatz, P.F., and Boerjan, W. (2008a). Lignification: are Lignins Biosynthesized via simple Combinatorial Chemistry or via Proteinaceous Control and Template Replication? Recent Advances in Polyphenol Research, Vol 1 **1,** 36-66.

Ralph, J., Kim, H., Lu, F., Grabber, J.H., Leple, J.C., Berrio-Sierra, J., Derikvand, M.M., Jouanin, L., Boerjan, W., and Lapierre, C. (2008b). Identification of the structure and origin of a thioacidolysis marker compound for ferulic acid incorporation into angiosperm lignins (and an indicator for cinnamoyl CoA reductase deficiency). Plant Journal **53,** 368-379.

Ralph, J., Lapierre, C., Marita, J.M., Kim, H., Lu, F.C., Hatfield, R.D., Ralph, S., Chapple, C., Franke, R., Hemm, M.R., Van Doorsselaere, J., Sederoff, R.R., O'Malley, D.M., Scott, J.T., MacKay, J.J., Yahiaoui, N., Boudet, A.M., Pean, M., Pilate, G., Jouanin, L., and Boerjan, W. (2001). Elucidation of new structures in lignins of CAD- and COMT-deficient plants by NMR. Phytochemistry **57,** 993-1003.

Raupach, M.R., Marland, G., Ciais, P., Le Quere, C., Canadell, J.G., Klepper, G., and Field, C.B. (2007). Global and regional drivers of accelerating CO2 emissions. Proceedings of the National Academy of Sciences of the United States of America **104,** 10288-10293.

Rohde, A., Morreel, K., Ralph, J., Goeminne, G., Hostyn, V., De Rycke, R., Kushnir, S., Van Doorsselaere, J., Joseleau, J.P., Vuylsteke, M., Van Driessche, G., Van Beeumen, J., Messens, E., and Boerjan, W. (2004). Molecular phenotyping of the pal1 and pal2 mutants of Arabidopsis thaliana reveals far-reaching consequences on phenylpropanoid, amino Acid, and carbohydrate metabolism. Plant Cell **16,** 2749-2771.

Ruprecht, C., and Persson, S. (2012). Co-expression of cell-wall related genes: new tools and insights. Frontiers in plant science **3,** 83-83.

Schellmann, S., Schnittger, A., Kirik, V., Wada, T., Okada, K., Beermann, A., Thumfahrt, J., Jurgens, G., and Hulskamp, M. (2002). TRIPTYCHON and CAPRICE mediate lateral inhibition during trichome and root hair patterning in Arabidopsis. Embo Journal **21,** 5036-5046.

Schmid, M., Davison, T.S., Henz, S.R., Pape, U.J., Demar, M., Vingron, M., Scholkopf, B., Weigel, D., and Lohmann, J.U. (2005). A gene expression map of Arabidopsis thaliana development. Nature Genetics **37,** 501-506.

Schultz, C., Gilson, P., Oxley, D., Youl, J., and Bacic, A. (1998). GPI-anchors on arabinogalactan-proteins: implications for signalling in plants. Trends in Plant Science **3,** 426-431.

Schwab, R., Ossowski, S., Riester, M., Warthmann, N., and Weigel, D. (2006). Highly specific gene silencing by artificial microRNAs in Arabidopsis. Plant Cell **18,** 1121-1133.

Seguin, A., Laible, G., Leyva, A., Dixon, R.A., and Lamb, C.J. (1997). Characterization of a gene

encoding a DNA-binding protein that interacts in vitro with vascular specific cis elements of the phenylalanine ammonia-lyase promoter. Plant Molecular Biology **35,** 281-291.

Seifert, G.J., and Roberts, K. (2007). The biology of arabinogalactan proteins. Annual Review of Plant Biology **58,** 137-161.

Sessions, A., Burke, E., Presting, G., Aux, G., McElver, J., Patton, D., Dietrich, B., Ho, P., Bacwaden, J., Ko, C., Clarke, J.D., Cotton, D., Bullis, D., Snell, J., Miguel, T., Hutchison, D., Kimmerly, B., Mitzel, T., Katagiri, F., Glazebrook, J., Law, M., and Goff, S.A. (2002). A high-throughput Arabidopsis reverse genetics system. Plant Cell **14,** 2985-2994.

Somerville, C. (2006). Cellulose synthesis in higher plants. Annual Review of Cell and Developmental Biology **22,** 53-78.

Sterjiades, R., Dean, J.F.D., Gamble, G., Himmelsbach, D.S., and Eriksson, K.E.L. (1993). EXTRACELLULAR LACCASES AND PEROXIDASES FROM SYCAMORE MAPLE (ACER-PSEUDOPLATANUS) CELL-SUSPENSION CULTURES - REACTIONS WITH MONOLIGNOLS AND LIGNIN MODEL COMPOUNDS. Planta **190,** 75-87.

Stewart, J.J., Akiyama, T., Chapple, C., Ralph, J., and Mansfield, S.D. (2009). The Effects on Lignin Structure of Overexpression of Ferulate 5-Hydroxylase in Hybrid Poplar. Plant Physiology **150,** 621-635.

Stockburger, D.W. (1998). Discriminant Function Analysis. Multivariate Statistics: Concepts Models and Applications.

Stuart, J.M., Segal, E., Koller, D., and Kim, S.K. (2003). A gene-coexpression network for global discovery of conserved genetic modules. Science **302,** 249-255.

Taiz, L., and Zeiger, E. (2002). Plant physiology. Third Edition. Plant physiology. Third Edition**,** i-xxvi, 1-690.

Taylor, N.G., Howells, R.M., Huttly, A.K., Vickers, K., and Turner, S.R. (2003). Interactions among three distinct CesA proteins essential for cellulose synthesis. Proceedings of the National Academy of Sciences of the United States of America **100,** 1450-1455.

Terashima, N., Fukushima, K., He, L.F., and Takabe, K. (1993). COMPREHENSIVE MODEL OF THE LIGNIFIED PLANT-CELL WALL. Forage Cell Wall Structure and Digestibility**,** 247-270.

Thevenin, J., Pollet, B., Letarnec, B., Saulnier, L., Gissot, L., Maia-Grondard, A., Lapierre, C., and Jouanin, L. (2011). The Simultaneous Repression of CCR and CAD, Two Enzymes of the Lignin Biosynthetic Pathway, Results in Sterility and Dwarfism in Arabidopsis thaliana. Molecular Plant **4,** 70-82.

Tian, G.W., Mohanty, A., Chary, S.N., Li, S.J., Paap, B., Drakakaki, G., Kopec, C.D., Li, J.X., Ehrhardt, D., Jackson, D., Rhee, S.Y., Raikhel, N.V., and Citovsky, V. (2004). High-throughput fluorescent tagging of full-length arabidopsis gene products in planta. Plant Physiology **135,** 25-38.

Timell, T.E. (1982). RECENT PROGRESS IN THE CHEMISTRY AND TOPOCHEMISTRY OF COMPRESSION WOOD. Wood Science and Technology **16,** 83-122.

Turner, S.R., and Somerville, C.R. (1997). Collapsed xylem phenotype of Arabidopsis identifies mutants deficient in cellulose deposition in the secondary cell wall. Plant Cell **9,** 689-701.

Uelker, B., Peiter, E., Dixon, D.P., Moffat, C., Capper, R., Bouche, N., Edwards, R., Sanders, D., Knight, H., and Knight, M.R. (2008). Getting the most out of publicly available T-DNA insertion lines. Plant Journal **56,** 665-677.

Van Acker, R., Vanholme, R., Storme, V., Mortimer, J.C., Dupree, P., and Boerjan, W. (2013). Lignin biosynthesis perturbations affect secondary cell wall composition and saccharification yield in Arabidopsis thaliana. Biotechnology for Biofuels **6**.

Vandriessche, G., Dennison, C., Sykes, A.G., and Vanbeeumen, J. (1995). HETEROGENEITY OF THE COVALENT STRUCTURE OF THE BLUE COPPER PROTEIN UMECYANIN FROM HORSERADISH ROOTS. Protein Science **4,** 209-227.

Vangysel, A., Vanmontagu, M., and Inze, D. (1993). A NEGATIVELY LIGHT-REGULATED GENE FROM ARABIDOPSIS-THALIANA ENCODES A PROTEIN SHOWING HIGH SIMILARITY TO BLUE COPPER-BINDING PROTEINS. Gene **136,** 79-85.

Vanholme, R., Morreel, K., Ralph, J., and Boerjan, W. (2008). Lignin engineering. Current Opinion in Plant Biology **11,** 278-285.

Vanholme, R., Demedts, B., Morreel, K., Ralph, J., and Boerjan, W. (2010). Lignin Biosynthesis and

Structure. Plant Physiology **153,** 895-905.
Vanholme, R., Storme, V., Vanholme, B., Sundin, L., Christensen, J.H., Goeminne, G., Halpin, C., Rohde, A., Morreel, K., and Boerjan, W. (2012). A Systems Biology View of Responses to Lignin Biosynthesis Perturbations in Arabidopsis. Plant Cell **24,** 3506-3529.
Vanholme, R., Cesarino, I., Rataj, K., Xiao, Y., Sundin, L., Goeminne, G., Kim, H., Cross, J., Morreel, K., Araujo, P., Welsh, L., Haustraete, J., McClellan, C., Vanholme, B., Ralph, J., Simpson, G.G., Halpin, C., and Boerjan, W. (2013). Caffeoyl Shikimate Esterase (CSE) Is an Enzyme in the Lignin Biosynthetic Pathway in Arabidopsis. Science **341,** 1103-1106.
Vaucheret, H., Beclin, C., Elmayan, T., Feuerbach, F., Godon, C., Morel, J.B., Mourrain, P., Palauqui, J.C., and Vernhettes, S. (1998). Transgene-induced gene silencing in plants. Plant Journal **16,** 651-659.
von Arnim, A.G., Deng, X.W., and Stacey, M.G. (1998). Cloning vectors for the expression of green fluorescent protein fusion proteins in transgenic plants. Gene **221,** 35-43.
von Heijne, G. (1998). Protein transport - Life and death of a signal peptide. Nature **396,** 111-+.
Wagner, A., Donaldson, L., Kim, H., Phillips, L., Flint, H., Steward, D., Torr, K., Koch, G., Schmitt, U., and Ralph, J. (2009). Suppression of 4-Coumarate-CoA Ligase in the Coniferous Gymnosperm Pinus radiata. Plant Physiology **149,** 370-383.
Wang, Y., Chantreau, M., Sibout, R., and Hawkins, S. (2013). Plant cell wall lignification and monolignol metabolism. Frontiers in plant science **4,** 220-220.
Wang, Y.H. (2008). How effective is T-DNA insertional mutagenesis in Arabidopsis? Journal of Biochemical Technology **1,** 10.
Weigel, D., and Glazebrook, J. (2006). Transformation of agrobacterium using electroporation. CSH protocols **2006**.
Weigel, D., Alvarez, J., Smyth, D.R., Yanofsky, M.F., and Meyerowitz, E.M. (1992). LEAFY CONTROLS FLORAL MERISTEM IDENTITY IN ARABIDOPSIS. Cell **69,** 843-859.
Whetten, R., and Sederoff, R. (1995). LIGNIN BIOSYNTHESIS. Plant Cell **7,** 1001-1013.
Wightman, R., and Turner, S.R. (2007). Severing at sites of microtubule crossover contributes to microtubule alignment in cortical arrays. Plant Journal **52,** 742-751.
Wu, A.-M., Rihouey, C., Seveno, M., Hornblad, E., Singh, S.K., Matsunaga, T., Ishii, T., Lerouge, P., and Marchant, A. (2009). The Arabidopsis IRX10 and IRX10-LIKE glycosyltransferases are critical for glucuronoxylan biosynthesis during secondary cell wall formation. Plant Journal **57,** 718-731.
Yazaki, K. (2005). Transporters of secondary metabolites. Current Opinion in Plant Biology **8,** 301-307.
Zhong, R., and Ye, Z.-H. (2009). Transcriptional regulation of lignin biosynthesis. Plant Signaling and Behavior **4,** 7.
Zhong, R.Q., Demura, T., and Ye, Z.H. (2006). SND1, a NAC domain transcription factor, is a key regulator of secondary wall synthesis in fibers of Arabidopsis. Plant Cell **18,** 3158-3170.
Zhong, R.Q., Morrison, W.H., Negrel, J., and Ye, Z.H. (1998). Dual methylation pathways in lignin biosynthesis. Plant Cell **10,** 2033-2045.
Zhong, R.Q., Lee, C.H., Zhou, J.L., McCarthy, R.L., and Ye, Z.H. (2008). A Battery of Transcription Factors Involved in the Regulation of Secondary Cell Wall Biosynthesis in Arabidopsis. Plant Cell **20,** 2763-2782.
Zhong, R.Q., Pena, M.J., Zhou, G.K., Nairn, C.J., Wood-Jones, A., Richardson, E.A., Morrison, W.H., Darvill, A.G., York, W.S., and Ye, Z.H. (2005). Arabidopsis fragile fiber8, which encodes a putative glucuronyltransferase, is essential for normal secondary wall synthesis. Plant Cell **17,** 3390-3408.
Zhou, J.L., Lee, C.H., Zhong, R.Q., and Ye, Z.H. (2009). MYB58 and MYB63 Are Transcriptional Activators of the Lignin Biosynthetic Pathway during Secondary Cell Wall Formation in Arabidopsis. Plant Cell **21,** 248-266.